STATISTICAL ANALYSIS OF MICROEARTHQUAKES OF THE SOCORRO REGION

A Dissertation
Presented to the Faculty
of the New Mexico Institute of
Mining and Technology

In Partial Fulfillment
of the Requirements for the
Degree of Doctor of Philosophy
in Geoscience

SURENDRA SINGH

June 1970

TABLE OF CONTENTS

ABSTRACT

Microearthquakes are very small-energy earthquakes. They can be considered to make up an integer-valued random process $\{N(t),\ t \geq 0\}$, where $N(t)$ is the number of microearthquakes up to the time t, t being a continuous parameter. This paper presents the statistical analysis of this microearthquake process and the conclusions derived therefrom. The data used in this study are the microearthquakes of the Socorro region, their energies and their inter-arrival times.

A probabilistic model of the seismic process is compared with the frequency-law of microearthquakes. The slope parameter in the frequency-law graph is found to be 1.15 to 1.37. No correlation is found to exist between the time of occurrence of a large microearthquake and the behavior of seismic parameters (i.e., the change in the number of shocks, the slope of the frequency-law graph and the grouping characteristics) in the temporal vicinity of the large microearthquake. Analysis of time-averages of the number of microearthquakes, their energies, and the slope of the frequency-law indicate that a large number of shocks in an energy class does not make the required length of the averaging interval for the estimation any shorter than that for an energy class with a small number of shocks.

Mean value functions for the number of shocks show that the microearthquake process is non-stationary. Cumulative energy graphs of microearthquakes seem to indicate that the accumulated energy in the focus is released, most of the times, in many small-energy shocks. Inter-arrival times of microearthquakes, as well as energies summed over intervals smaller than 15 days, are not found to be independent and show no time trend. The inter-arrival times were found to be neither exponentially nor normally distributed. About 50% of all the microearthquakes' inter-arrival times have values less than 20 hours. Analysis of the hazard function of the inter-arrival times shows that the probability of a failure for the foci in the region of Socorro remains nearly the same up to about 19 days, except for its relatively high value immediately following a shock. After about 19 days, the value of this probability increases rapidly. The microearthquake process does not follow a Poisson process.

ACKNOWLEDGMENTS

I am indebted to my advisor, Dr. A. R. Sanford, for pointing out the research problem as well as for the invaluable guidance during all phases of this study. I also wish to thank Dr. M. S. Friberg, Dr. A. J. Budding and Dr. C. R. Holmes who generously assisted me at various stages of this work.

Computing facilities were made available by the New Mexico Tech Computing Center. The research reported here was partially supported by the National Science Foundation through Grant No. 4446.

LIST OF FIGURES

LIST OF TABLES

Table | Page

INTRODUCTION

Statistical studies of earthquakes to determine the seismic conditions of various regions have concerned seismologists for a long time. The maximum size shock, periodicities in numbers and strengths of events, the slope of the frequency-law graph, correlation between a large shock and other seismological quantities, and interdependence of various parameters of the earthquake sequence, are some of the important seismic conditions of an area. This paper describes the results of a statistical investigation of the earthquake activity in the Socorro, New Mexico, region. The main topics covered under this study are as follows:

(1) The frequency-law of earthquakes is studied. A probabilistic model, based on some physical assumptions, is proposed for the interpretation of the frequency-law.

(2) An analysis is made of the temporal behavior of the activity, the slope, and the grouping parameter of earthquakes. The behavior of these three parameters is investigated for any relation to the occurrence of a large microearthquake.

(3) Time-averages of the number of earthquakes, their energy and the slope of the frequency-law, and the cumulative energy graphs of microearthquakes are studied.

(4) Inter-arrival times (intervals of time between the occurrences of two consecutive earthquakes) of earthquakes are tested for statistical independence.

(5) The distribution function of inter-arrival times is compared with the theoretical distribution functions of exponential and normal type distributions.

(6) A hazard function analysis is made for the inter-arrival times of earthquakes.

There are four main underlying purposes of the study presented in this paper. The first and fundamental purpose is to obtain a quantitative knowledge of the seismic conditions of the area. The second purpose is to investigate the feasibility of extrapolating the seismic parameters, obtained for 5 year data, into the future; for example, to get some idea about the future statistical behavior of parameters such as slope, number of shocks in a unit time-interval, grouping of shocks, approximate energy released in a unit time-interval, etc. The third purpose of this study is to explore the possibility of predicting, in time, the occurrence of large microearthquakes. This primarily involves a study of the dependence of the occurrence of a large microearthquake on the past and present values of seismic quantities of the earthquake sequence. The fourth purpose is to compare the results (or theories) of other workers with the results obtained for the Socorro region; for example, to compare the slope parameters,

reliabilities of predicting the long-term seismicity from short-term seismicity, the distribution functions of earthquakes, etc.

Pioneering work in the statistical analysis of earthquakes was done by Gutenberg and Richter (1949). They obtained a statistical relation between the cumulative number of earthquakes and their magnitudes, known as the frequency-law of earthquakes. When a straight line was fitted to the graph of this relation, the slope of the straight line was found, at least to a first approximation, to be the same for the whole world and for areas of very large dimensions. However, as data accumulated for areas of small dimensions and over small periods of time, the concept that the slope is some type of universal constant was not found to hold (Gubin, 1964; Riznichenko, 1966). Riznichenko (1958) expressed the idea that the variability of seismic conditions such as (1) the slope of the frequency-law, (2) the number of shocks and (3) the grouping characteristics of shocks may be related, in some way, to the time of occurrence of a large shock in the area.

With the exception of a few areas like California and Japan, reliable earthquake data for most regions has been available only for relatively short periods of time. Some workers, therefore, have tried to use the short-term seismic behavior of a region to extrapolate the long-term behavior. The underlying assumption made in this kind of

extrapolation is that the seismic conditions of the region do not vary erratically with time (i.e., a high statistical stationarity). A quantitative attempt to estimate the long-term seismic behavior has recently been published (Sanford and Singh, 1968) for the Socorro region.

The term "earthquake prediction", in its most general sense, can be thought of as meaning a knowledge of the seismic conditions of the region as they are going to be at a future moment. One approach to the problem is that of Lomnitz (1966), who has given an elaborate theoretical review of the statistical approach to the problem of earthquake prediction. He has discussed the feasibility of a numerical Wiener's predictor to the earthquake's time series. However, many things have to be known about the earthquakes' time series before any such approach can be of use. These approaches require a high degree of stationarity in the seismic behavior. Furthermore, the quantities to be predicted must have some kind of dependence on their present and past values. It will also be advantageous if the earthquakes are distributed according to some well-established statistical distribution. There are, likewise, many other questions about the seismic behavior of a region which need be answered in order to be able to make a reliable prediction of any of the seismic quantities.

Since June, 1960, about five hundred natural seismic events have been recorded every year in the Socorro region.

A majority of nearby shocks is located southwest of the New Mexico Tech station, beneath the local fault block mountain of the Rio Grande Graben system. The area southwest of the mountain is found to have a high density of nearby vertical faults as reported by Willard (June, 1969). Most of the large faults trend somewhat west of north. No single fault is found dominant over the others in its vertical movement. One of the swarms of shocks was located in the area mapped by Willard. Microearthquakes in the Socorro region are very small-energy events. Most of them have a vertical ground motion of less than 0.1 microns. The energy ranges up to 10^{16} ergs. On the average, about four hundred microearthquakes are annually recorded within a radius of about 20 km. of the recording station. The depth of the focus of these events ranges from 2 to 13 km. The first motions of shocks are about 75% compressional and 25% dilational. Some swarms have been found to have shocks with both compressional and dilational first motions. Microearthquakes are very irregularly distributed in time. There is a so-called background activity consisting of very small events.

We shall use the data of microearthquakes of the Socorro region for the study in this paper.

DESCRIPTION OF DATA

RECORDING

All of the earthquake statistics used in this study came from a single continuously-recording vertical component seismograph. The detector for this instrument is a Willmore electromagnetic seismometer operating at a natural period of 0.9 seconds with a damping coefficient of 0.14. The transducer rests on a solid concrete foundation 640 feet from the entrance of an approximately horizontal tunnel that is located at the base of Socorro Mountain. The depth of the transducer beneath the surface is about 300 feet. Biles (1968) has shown that at this depth and for the dominant frequencies of 5-20 c.p.s. of P and S motion in microearthquakes, the free surface does not affect the amplitudes of recorded ground motion.

The electrical signal from the transducer, after having been electronically amplified, is fed to the pen-recorder, which has a recording speed of 3.3 mm. per second. The frequency response of the whole seismograph is shown in Figure (I.1).

FOCAL DISTANCES

The focal distance of an earthquake is usually determined from the interval of time between the arrival of the

Central tunnel I

Component - Vertical,

Natural period - 0.94 seconds,

Damping coefficient - 0.14,

Recording speed - 200 mm. per minute,

Timing - Nardin Chronometer with WWV once every 24 hours directly on record,

Calibration signal - 5 mm.

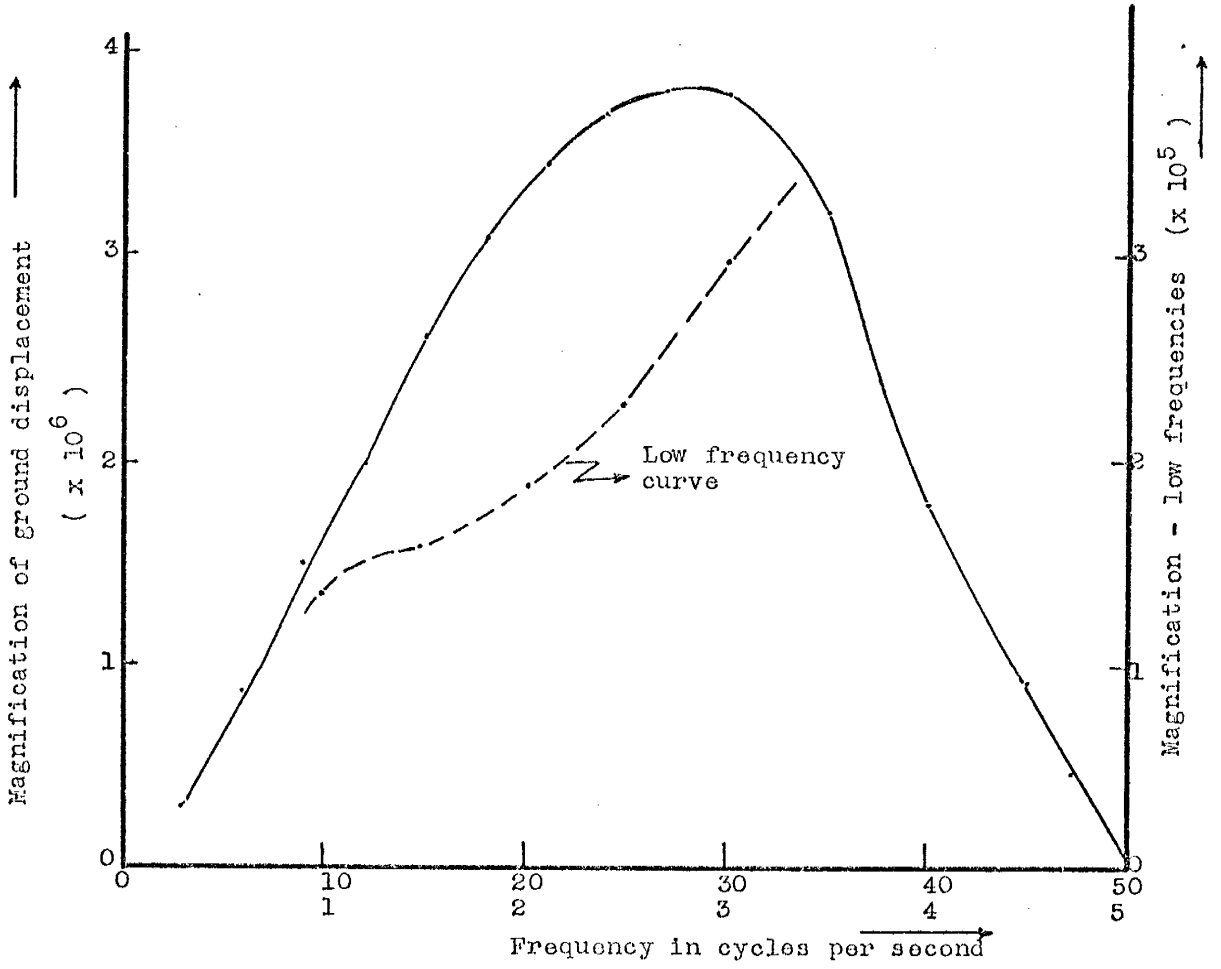

Figure I.1. Frequency-response of the seismograph.

P-phase (longitudinal elastic waves) and the S-phase (transverse elastic waves) of the earthquake. If the epicentral distance (horizontal distance between the recording station and a point on the earth's surface directly above the focus) is small, we can assume a straight ray trajectory from the focus to the recording station. Taking 0.25 and 6 km./second as the values of the Poisson ratio and the longitudinal wave-velocity, respectively, it can be shown (Richter, 1957) that the distance to the focus (in kilometers) of an earthquake is given by:

Focal distance (D) = (1.37)·6· (S-P) interval in sec.

Because the focal distances are directly proportional to the (S-P) intervals, the latter are used in this study as a measure of distance.

AREAL EXTENT OF THE EARTHQUAKE FOCI

The nature of the present work is such that only earthquakes with (S-P) intervals of less than 2.5 seconds are included in the analysis. There are many reasons for doing so. First of all, microearthquakes are very small energy events, many of which would not be recorded at distances greater than 20 km. Even if some of the larger microearthquakes are recorded, the absorption in the medium and the geometrical spreading will distort the amplitude information.

These factors can be very serious for microearthquakes as weak as those in the Socorro region. Second, the data were limited in areal extent to make sure that the data came from one single seismically homogeneous block of the crust. If the region considered is too large, there is a possibility that the data will be a mixture from areas having different seismic behavior. Finally, the events from this area (less than 2.5 sec. of S-P interval) make up more than 80% of all the microearthquakes observed by our instrument.

CLASSIFICATION OF DATA

Spatial Distribution of Microearthquakes

Microearthquakes of the Socorro region are not uniformly distributed about the recording station. A major number of shocks seems to originate in a rather small region on the southwest flank of Socorro Mountain (Sanford and Long, 1965; Sanford and Holmes, 1962). When the number of shocks are plotted against their (S-P) intervals, most of the shocks are centered about two peaks corresponding to (S-P) intervals equal to 1.8 and 0.9 seconds (Sanford and Singh, 1968). It seems likely that the two peaks represent activity from only two regions. It is, therefore, assumed that the shocks, coming from the regions corresponding to (S-P) intervals of 1.8 (1.8 ± 0.15; 0.15 to allow for the reading errors on the seismogram) and 0.9 (0.9 ± 0.15) seconds, belong to two isolated

independent focal zones. The main implication of this assumption is that these two focal zones behave, on a small scale of space and time (say 5 years), as two independent physical systems, and that the data from them is not affected by what happens outside any one of these focal zones. A particular focal zone most probably consists of many small fractures behaving in a similar mechanical fashion. Some scattering, therefore, of quantities associated with such data can be expected. However, quantities such as (S-P) interval, relative amplitudes of P- and S-phase (the other particular phases like S_xP and S_xS and their intervals) should remain relatively fixed for a particular focal zone. These are the main factors used to separate the data belonging to a particular focal zone from the rest of the data.

Data Identification

Throughout the whole study, five kinds of data are used. To identify each kind of data in a neat and compact way, they are given specific designations. These designations will be used, whenever necessary, instead of describing the nature of the particular kind of data each time.

On the basis of their (S-P) interval, and character, the microearthquakes in the region are divided into three main classes. The first class consists of all the shocks with (S-P) interval equal to 1.8 ± 0.15 seconds, recorded

from January, 1963, to December, 1967. This group, which contains 839 shocks, will be known as DATA1.

The second class consists of all the shocks with (S-P) interval equal to 0.9 ± 0.15 seconds, recorded from January, 1963, to December, 1967. This group, which contains 642 shocks, will be called DATA2.

The third class consists of all the shocks with (S-P) interval ranging from 0.2 to 2.5 seconds, recorded from July, 1961, to March, 1967. This data class, which contains 4266 shocks, is called DATA3.

Two additional groups of data are used. The first of these is called DATA4 which is the same as DATA1 but over a shorter period of observation. Its observation period is the years 1965, 1966 and 1967. This group contains 491 shocks. The second group is called DATA5 which is the same as DATA2 but over a shorter period of observation, from January, 1963, to the first week of April, 1967. DATA5 contains 560 shocks.

AMPLITUDES

General

The amplitude used in this study is the peak-to-peak amplitude of the largest oscillation in the first few cycles of the S-phase, sometimes simply called the amplitude of an earthquake. The observed amplitudes in mm.

are normalized with respect to a nominal calibration signal of 5 mm. This is done to eliminate the errors due to the change in the sensitivity of the recording instrument. Only microearthquakes with normalized amplitudes equal to or greater than 10 mm. are used in this study.

Saturated Amplitudes

The maximum amplitude on the chart is not always a correct representation of the maximum ground velocity. For the instrument under consideration, the problems which distort the amplitude on the chart can be summarized as follows:

(a) Saturation Due to Pen Guard Dimensions. The amplitudes are limited by the dimensions of a pen guard inside of which the pen oscillates. Thus, the earthquakes can not be recorded correctly if their amplitudes are greater than 60 mm. peak-to-peak.

(b) Curvature of Pen Trace. The recording pen has a finite length (about 75 mm.) and whenever the pen makes a large oscillation, the trace of the pen has considerable curvature. However, for many purposes, this error is not significant and measurements can be made with a straight edge scale.

(c) Amplifier Distortion. The signal input to the amplifier and the amplitude of the pen motion are linearly related up to peak-to-peak amplitudes of about 40 mm. (in

the frequency range of 5 to 20 c.p.s.). Beyond this amplitude, the sensitivity (mm./mV.) decreases. At amplitudes beyond 60 mm., it is difficult to make a correction for this factor.

Estimation of True Amplitudes

For the purpose of computing energies and magnitudes of large shocks, we need to estimate the values of the true amplitudes of these events. Because the elastic limit of the rock deformation, the confining pressure and other physical factors around the focus remain the same over a considerable period of time, it is physically reasonable to assume that the amplitude of a shock is directly proportional to its duration (the time interval from the start of the event to the point at which the signal falls to the level of the background noise). We, therefore, use the value of the duration of a large shock to estimate its true amplitude. In the following, such amplitude-duration relations are discussed for DATA1 and DATA2.

The amplitude-duration curves for the two earthquake sources having (S-P) = 1.8 ± 0.15 and 0.9 ± 0.15 seconds are given in Figures (I.2) to (I.4). Apparently, for the source with an (S-P) interval of 0.9 ± 0.15 seconds, this relation did not change much during the period of observation from 1963 - 1967. However, there was a large scattering in the amplitude-duration curve for the source with an

(S-P) interval of 1.8 ± 0.15 seconds. To minimize the possible computational error due to this scattering, the amplitude-durations were computed on a yearly basis.

Assuming that the observed amplitude-duration relations can be extrapolated to higher amplitudes, the true amplitudes of the stronger shocks can be estimated with the help of the curves in Figures (I.2) to (I.4). A multiplication factor is given with each figure. This factor, when multiplied by the duration, gives an estimate of the true amplitude of the stronger shocks.

INTER-ARRIVAL TIMES

The time interval between the occurrences of two consecutive shocks is defined to be the inter-arrival or inter-occurrence time. For 3 shocks, we will have 2 values of inter-arrival times, for 4 shocks, we will have 3 inter-arrival times, etc.

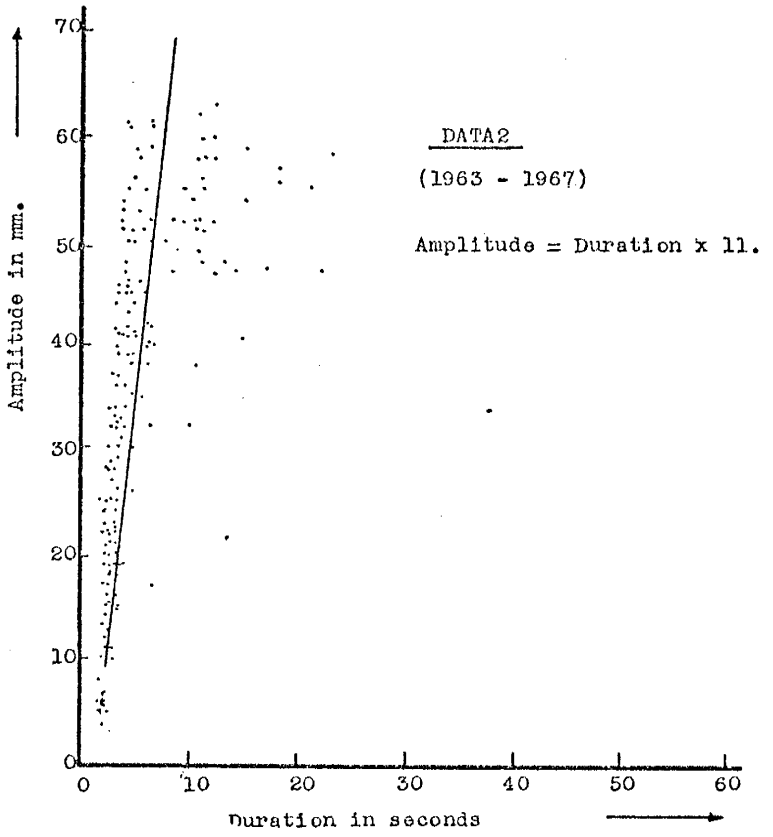

Figure I.2. Amplitude-duration relation for DATA2.

DATA1

(1964, 1967)

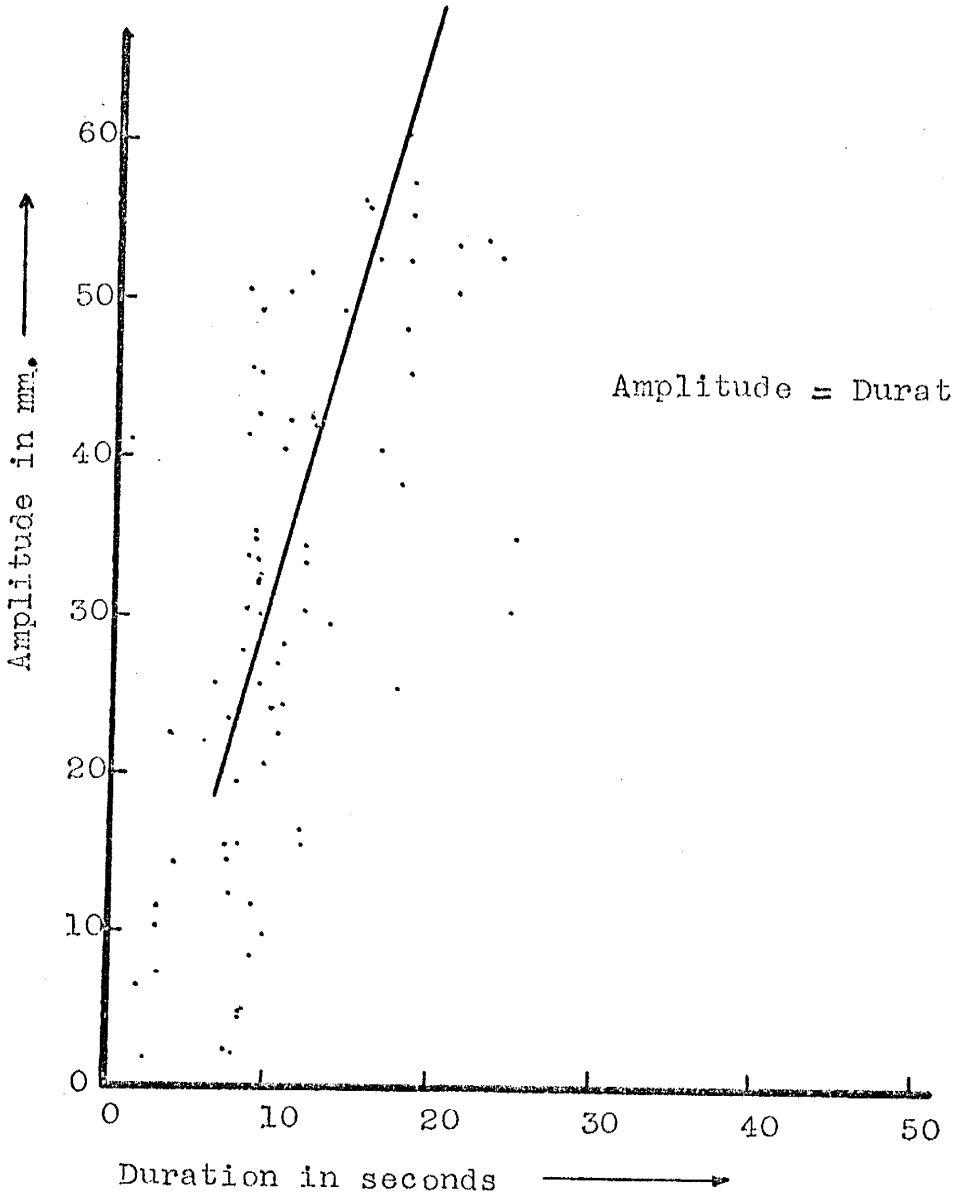

Amplitude = Duration x 3.5 .

Figure I.3. Amplitude-duration relation for DATA1.

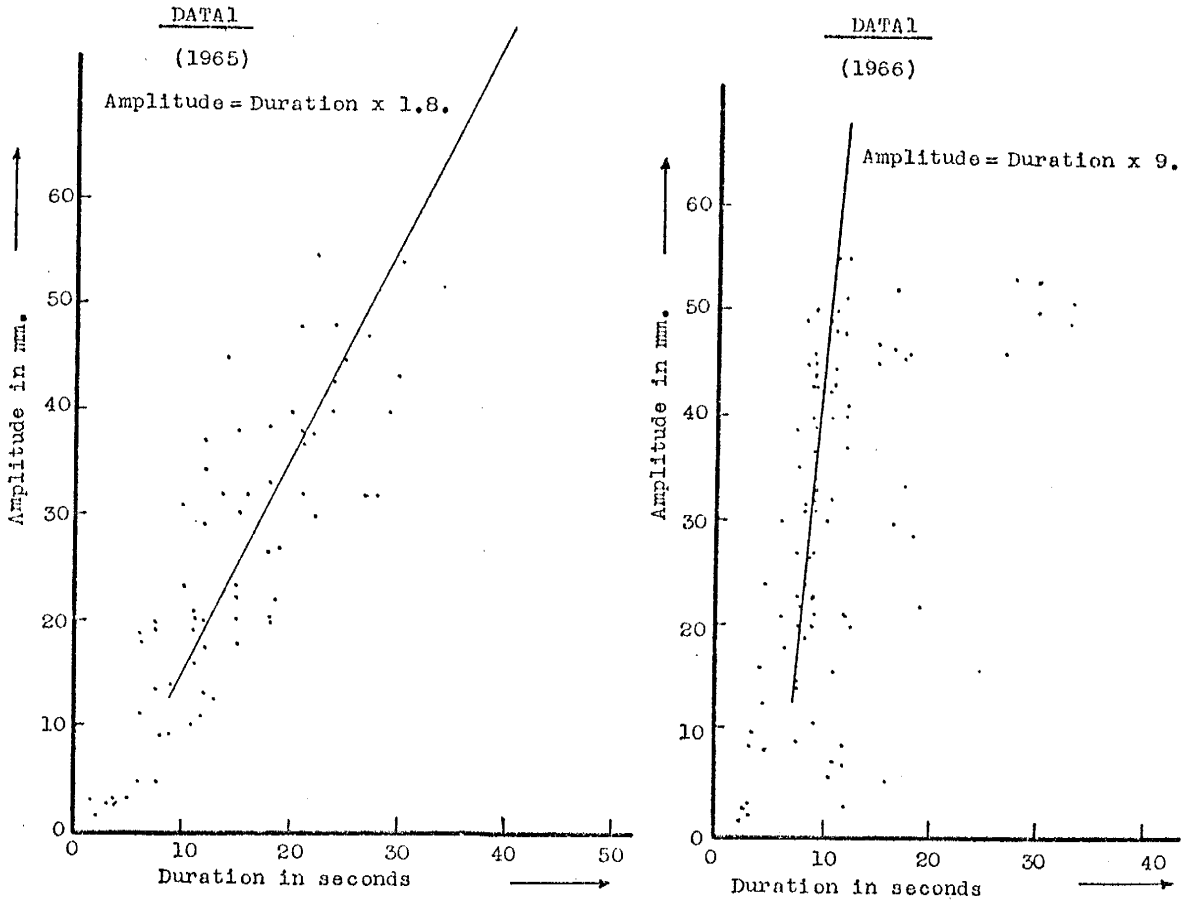

Figure I.4. Amplitude-duration relation for DATA1.

SECTION I

FREQUENCY AND ENERGY RELATIONSHIP OF EARTHQUAKES

INTRODUCTION

General

Earthquakes, in general, have a wide range of energy release. Earthquakes with small energy release are observed to occur more frequently than those with relatively large energy release. The relation between the common logarithm of the number of earthquakes and their magnitude (a quantity directly proportional to the common logarithm of the energy) is, in the literature of geophysics, known by the name of "the frequency-law of earthquakes". It has been observed that frequency-law of earthquakes can be represented by a straight line except for the portion toward the higher energy end where the straight line bends rapidly toward the energy axis.

In this section, we will investigate the nature of this empirical frequency-law using a physical probabilistic model. The frequency-law for the data on microearthquakes in the Socorro region is analyzed in the light of the proposed model and the numerical values of the parameters associated with the frequency-law are explained in terms of the quantities used in the model.

Previous Work

The frequency-law, in general, can be expressed in the form (Gutenberg and Richter, 1949)

$$\log N = A' - \gamma \cdot M' \ , \qquad (1.1)$$

where N is the member of earthquakes of magnitude M'; A' and γ are, respectively, the intercept and the slope of the linear relation (1.1).

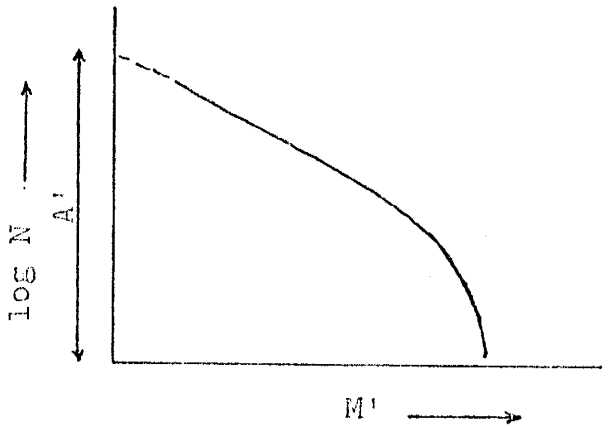

Figure 1.1. Frequency-law of earthquakes.

The relation (1.1) can also be put in the form

$$N(M') = 10^{A'} \cdot 10^{-\gamma \cdot M'} = B \cdot 10^{-\gamma \cdot M'} \ , \qquad (1.2)$$

or

$$N(M') \cdot dM' = B \cdot 10^{-\gamma M'} \cdot dM' \ . \qquad (1.3)$$

$N(M') \cdot dM'$ is the number of earthquakes in the magnitude range M' to M' + dM'. However, if some of the magnitude ranges do not have some earthquakes associated with them or the number of earthquakes in some magnitude classes is small, there will be a large scattering of points in graphs of the type shown in Figure (1.1). Consequently, it will be

difficult to satisfactorily fit a straight line to the data. To overcome this problem, the following relation is generally used instead of equation (1.1):

$$\log N_{\Sigma}(M') = A - \gamma \cdot M' \ , \qquad (1.4)$$

where

$$A = \log (B/\gamma \cdot \ln 10) \ , \qquad (1.5)$$

and $N_{\Sigma}(M')$ is the cumulative number of earthquakes with the magnitude M' or greater. The quantity $N_{\Sigma}(M')$ is given by

$$N_{\Sigma}(M') = B \cdot \int_{M'}^{\infty} 10^{-\gamma \cdot M'} \cdot dM' = \frac{B}{\gamma \cdot \ln 10} \cdot 10^{-\gamma \cdot M'} . \qquad (1.6)$$

The equation (1.4) is known as "cumulative frequency-law" of earthquakes. The slope of the linear relation in equation (1.4) is the same as slope of equation (1.1); however, the constant terms in the two equations are different. The constant term A is known as the activity at an arbitrarily chosen value of M'.

The energy is related to the magnitude as shown below (Richter, 1957):

$$\log E = c_1 + c_2 \cdot M' \ , \qquad (1.7)$$

where c_1 and c_2 are constants. Sometimes the relation

$$\log E = c_3 \cdot M' \qquad (1.8)$$

is also used by some workers (Riznichenko, 1965).

The slope γ in (1.4) is by far the most important quantity. It determines the way in which earthquakes are

distributed with respect to their magnitudes. It is a measure of the ratio of small shocks to larger shocks. Gutenberg (1949) computed the frequency-law for earthquakes and he found that the value of the slope was 0.9 ± 0.2 for shallow shocks; 1.2 ± 0.2 for intermediate and deep shocks. The value of slope for earthquakes of Southern California was found to be 0.88 ± 0.03.

Surprisingly enough, relations similar to (1.1) are observed in the case of fracturing of rocks in mines (Vinogradov, 1963) and in laboratory fracture experiments on rocks and other materials (Mogi, 1962). In addition, the value is approximately equal to 1 for coal samples and on the order of 0.7-0.08 for samples of granite and diabase (Vinogradov, 1959).

It is very natural for one to wonder as to why the value of the slope of the straight line is about 1, under such varied conditions of size, location, material properties, and a wide range of energies. Riznichenko (1965) has tried to explain this behavior by applying the principle of minimum potential energy to the block of ground under consideration. He considers two extreme situations: (1) when the total potential elastic energy is released and (2) when only a small part of the stored potential elastic energy is released. According to him the theoretical values of the slopes for the two cases are 1.0 and 0.5, respectively.

Similar attempts have been made by other workers to explain the linear nature of the frequency-law of earthquakes.

Housner (1955) and Mogi (1962) have suggested probabilistic models to explain the frequency-law under some idealistic assumptions. Many of these assumptions are dropped in the model put forward, later on, in this study.

Fracture Source for Microearthquakes

No single theory of generating earthquakes is found to answer satisfactorily all the questions a geophysicist may have about the mechanism of an earthquake. However, a certain theory or model may be more satisfactory than others in a particular case. For example, consider microearthquakes in the Socorro region which have maximum depths of foci of about 15 km.. Some of the shocks have (S-P) intervals as short as 0.3 secs. which means focal depths of 2.4 km or less. Because the deep microearthquakes have the same characteristics as the shallow shocks, it is likely that the mechanism for both is the same. Therefore, the most likely mechanism appears to be brittle shear fracture or movement along pre-existing shear fractures. Old fractures under load will release energy by propagating further and/or by slipping suddenly when the shear stress across the fault surface exceeds the frictional resistance to sliding.

THEORY

General

It has been widely believed by seismologists that most earthquakes are caused by brittle shear fracture in the

rth's crust and upper mantle. According to Mogi (1962), terogeneity of the material and the spatial distribution the stress are the main factors in deciding the ratio of e smaller to larger earthquakes. If a uniform field of ress is applied to a heterogeneous rock sample, numerous ncentrations of stress appear, and fracture is likely to t in at these points. However, these local fractures do always grow to very large lengths because they are stop- d by various irregularities due to the heterogeneous na- re of the medium and the stress field. Consequently, ere are many small size fractures and few large ones. On e other hand, if a uniform stress field is applied to a nogeneous material, small fractures occur very seldom. ee the fracturing process sets in in such a medium, there nothing to stop a fracture and it grows to full scale of e sample.

The same kind of situation arises if the stress varies tially in a medium. A substance can be homogeneous and a varying stress on it will produce many smaller frac- es and few large ones. In this case, the halting of tial fractures is caused by an irregular distribution of stress in the medium.

Thus, heterogeneity is the most important factor in de- mining the distribution of fractures. As far as energy eased from a fracture is concerned, this will be directly ated to the dimension of the fracture. However, the di- sion of a fracture is not the only factor which determines

the energy release. The strength of the medium, frictional coefficient of the two surfaces of the fracture, and the stress intensity are some of the other important factors that decide the energy of a shock. If we consider fractures in a small segment of the earth's crust such that all the above factors can be assumed to be, on the average, constant, then the energy released at the focus will be a function of the dimension of the fracture only. The model proposed here uses this assumption to express the energy at the focus as a function of the dimension of the fracture concerned.

Description of the Model

The following main assumptions are used in the construction of our model:

(a) Microearthquakes are caused by a sudden slippage along and extension of fracture planes. Most of the fractures have formed some time in the past, with a definite size distribution dictated by the heterogeneity of the crust and/or the applied tectonic stresses. This size distribution is maintained through the seismic history of the region.

(b) All the fractures are two-dimensional fractures and the extension of the fracture is in the manner shown in Figure (1.2).

(c) The energy of a shock is linearly related to the area of the fracture on which it occurs.

(d) The area of a particular fracture, at any instant of its growth, can be considered to be a random variable.

According to assumptions (a) and (c), the present distribution of earthquakes with respect to energy release will be the same as the present distribution of fractures with respect to fracture area and the latter will be the same as the original distribution of fractures in the segment of crust under consideration.

The basic problem is to find a relation between number of earthquakes and their energies that is based on a probabilistic model of fracture distribution.

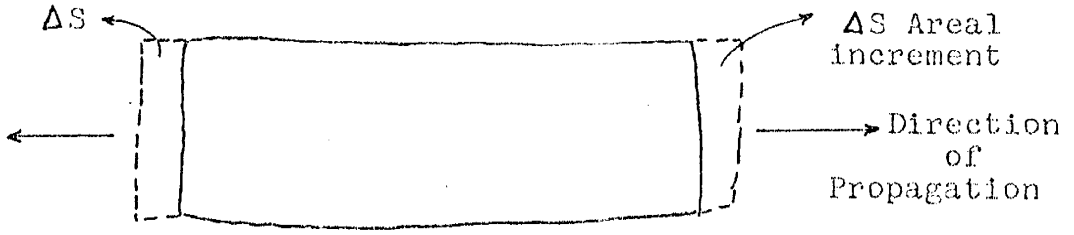

Figure 1.2. The propagating fracture.

If N(S) denotes the number of fractures having area S or greater, then N(S+dS) will be the number of fractures having area (S+dS) or greater and

$$\frac{dN(S)}{dS} = \lim_{\Delta S \to 0} \frac{N(S+dS) - N(S)}{dS} , \qquad (1.9)$$

and $$dN(S) = - \left[N(S) - N(S+dS) \right] .$$

If the observations are taken over a large region and a large time period, there will probably be some earthquakes

or every (S,S+dS) interval and the limit in (1.9) will exist. rom this assumption the probability that a dislocation will ot proceed farther than (S+dS), when its original value was , can be expressed as

$$\text{the no. of fractures between S \& S+dS)/(the no. of fractures t S)} = -\frac{dN(S)}{N(S)} = -d\left[\ln N(S)\right]. \tag{1.10}$$

It is physically reasonable to assume that in the process of extension of fractures, large fractures will have elatively large areal increments as compared to those of mall fractures, or

$$\Delta S \propto S, \tag{1.11}$$

here ΔS is the incremental area, S is the original area of he fracture (at some stage of its growth) just before it increased its area by ΔS. The relation (1.11) shows that the real increment increases with increasing area, or in other ords, the probability of a large fracture becoming larger a certain amount is greater than that of the small one enarging by the same amount. We can now formulate such a distribution of fractures. According to such a distribution, he probability that a dislocation of area S will stop its rowth between S and S+dS can be written as,

$$P(\text{a fracture will stop between S \& S+dS}) = \frac{C_1(k)\cdot dS}{S^{1n}}, \tag{1.12}$$

where $C_1(k)$ is a constant function of the heterogeneity k, of the medium. C_1 and m are positive constants.

Comparing (1.10) and (1.12),

$$\frac{C_1(k)\cdot dS}{S^m} = - d\left[\ln N(S)\right] . \qquad (1.13)$$

As pointed out before, our aim in this model is to derive a relation between the number of earthquakes and their energy. We, therefore, next establish a relation by which the energy of an earthquake can be expressed as a function of the area of the fracture and vice versa.

According to the assumption (c),

$$E_f \propto S, \qquad (1.14)$$

where E_f is the energy released at the focus.

Due to the asymmetry of the focal radiation and the anisotropy of the medium, the energy released at the focus may not radiate uniformly in all directions. Also some of the energy radiated toward the detecting station is absorbed by the medium. However, for a fixed location of the detecting station and the focus, it can be said that

$$E_o \propto E_f , \qquad (1.15)$$

where E_o is the estimate of the total seismic energy released at the focus, as observed at the earth's surface.

Comparing (1.14) and (1.15),

$$S \propto E_o \quad . \tag{1.16}$$

The observed energy at the surface can be converted into an energy index M such that

$$E_o = C_2 \cdot 10^{C_3 M} \quad , \tag{1.17}$$

where M is the logarithm of the S-phase amplitude and C_2, C_3 are positive constants.

Substituting (1.17) into (1.16),

$$S = C_4(C_2 \cdot 10^{C_3 M}) = C_5 \cdot 10^{C_3 M} \quad , \tag{1.18}$$

where C_5 is a positive constant.

Case I: When m = 1.

Equation (1.13) becomes

$$-d\left[\ln N(S)\right] = d\left[\ln S^{C_1}\right] \quad ,$$

or

$$N(S) = C_6 \cdot S^{-C_1} \quad . \tag{1.19}$$

Replacing S by (1.18),

$$N(M) = C_6 \cdot \left[C_5 \cdot 10^{C_3 M} \right]^{-C_1(\kappa)}$$

$$N(M) = C_7 \cdot 10^{-C_8(\kappa) \cdot M} \quad , \tag{1.20}$$

C_7 and C_8 are positive constants. Upon comparing (1.20) with (1.2) we notice that this is the well-known frequency-law in its exponential form.

Case II: When $m \neq 1$, equation (1.13) becomes

$$\frac{C_1(k)\cdot dS}{S^m} = -\,d\left[\ln N(S)\right],$$

or $$-d\left[\ln N(S)\right] = C_1(k)\cdot d\left[\frac{S^{1-m}}{1-m}\right],$$

or $$N(S) = C_9 \cdot \exp\left[\frac{-C_1(k)\cdot S^{1-m}}{1-m}\right], \qquad (1.21)$$

where C_9 is a positive constant.

Again substituting for S from (1.18), (1.21) becomes

$$N(M) = C_9\cdot\exp\left[\frac{-C_1(k)}{1-m}\left\{C_5\cdot 10^{C_3M}\right\}^{1-m}\right], \qquad (1.22)$$

or $$N(M) = C_9\cdot\exp\left[\frac{-C_{10}(k,m)}{1-m}\cdot 10^{C_3M(1-m)}\right], \qquad (1.23)$$

where C_{10} is a positive constant.

Taking the logarithm of both sides of (1.23),

$$\ln N(M) = C_{11} - C_{12}(k,m)\cdot 10^{C_3M(1-m)}, \qquad (1.24a)$$

$m < 1$ and C_{12} is positive,

$$\ln N(M) = C_{11} + C_{12}(k,m)\cdot 10^{-C_3M(m-1)}, \qquad (1.24b)$$

$m > 1$.

Consider (1.23) for $m<1$. At $M=0$, $N(0) = C_9\cdot\exp\left[\frac{-C_{10}}{1-m}\right]$ $= C_9\cdot(\text{quantity}<1)$. Hence, C_9 is a number greater than 1,

ince N(O) is the number of fractures at an M of the order f O or greater which cannot be less than 1. Consequently, C_{11} which is the logarithm of C_9 is a positive constant. hen it follows that however big a value we chose for M in 1.24b), ln N(M) never goes to O. This would not represent our real data conditions and hence this solution is rejected and with it, the assumption that m>1.

Then, the solution should be, with m<1 and C_{11}, C_{12} positive,

$$\ln N(M) = C_{11} - C_{12}(k,m)\cdot 10^{C_3 M(1-m)} \quad . \qquad (1.24a)$$

Let us take $(1-m) \simeq +0$.

$$\ln N(M) = C_{11} - C_{12}(k,m)\cdot \exp\left[\ln 10\cdot C_3\cdot M(1-m)\right]$$

$$\ln N(M) = C_{11} - C_{12}(k,m)\cdot e^{M\cdot C_{13}} \qquad (1.25)$$

where $0 < C_{13} << 1$. Hence,

$$\ln N(M) = C_{11} - C_{12}\left[1+(C_{13}\cdot M)+\frac{(C_{13}\cdot M)^2}{2!}+ - - -\right]$$

$$\ln N(M) = (C_{11} - C_{12}) - (C_{12}\cdot C_{13})\cdot M - - -$$

$$\ln N(M) = C_{14}(k,m) - C_{15}(k,m)\cdot M \quad , \qquad (1.26)$$

rejecting small higher order terms.

Comparing (1.26) with (1.1), we conclude that for m≃1 and small values of M, (1.24a) is the straight line frequency-law.

However, when the condition m≃1 is not satisfied, the frequency-law is to be represented by the relation (1.24a). The previous two cases were derived simply to show that (1.24a) will represent a straight line for a specific value of m.

FREQUENCY-LAW FOR SOCORRO MICROEARTHQUAKES

Results

The energy index M is computed according to the formula

$$M = \log\left[(\text{amp}\cdot 5/\text{cal})\cdot 10^3\right], \qquad (1.27)$$

where amp is the maximum S-phase amplitude on the seismogram and cal is the amplitude of the calibration signal on the seismogram.

Table (1.1) lists the logarithm of the cumulative number of microearthquakes for various values of M. These values are plotted in Figures (1.3), (1.4), (1.5) for DATA1, DATA2, and DATA3, respectively. A duration-amplitude relation could not be found for every (S-P) interval for all the years of data and, therefore, all the events of DATA3 that had normalized amplitudes greater than 80 mm are represented by a single point at M = 4.9.

Discussion of Results

Discussion of Figures (1.3) - (1.5)

The first (a-b) part of these curves is nearly horizontal.

Table 1.1. Logarithm of the Cumulative Number of Shocks N_{Σ} and the Energy Index M.

$\log N_{\Sigma}$

DATA1	DATA2	DATA3	M
2.92	2.81	3.63	3.0
2.92	2.81	3.63	3.1
2.92	2.81	3.62	3.2
2.92	2.81	3.61	3.3
2.91	2.81	3.60	3.4
2.91	2.80	3.58	3.5
2.90	2.79	3.54	3.6
2.88	2.78	3.51	3.7
2.86	2.76	3.46	3.8
2.84	2.74	3.42	3.9
2.81	2.73	3.34	4.0
2.75	2.66	3.28	4.1
2.71	2.60	3.20	4.2
2.65	2.54	3.09	4.3
2.57	2.45	2.98	4.4
2.49	2.36	2.87	4.5
2.39	2.26	2.72	4.6
2.20	2.08	2.63	4.7
2.05	1.92	2.54	4.8
1.97	1.79	2.11	4.9
1.74	1.69		5.0
1.49	1.57		5.1
1.36	1.36		5.2
1.18	1.11		5.3
1.08	1.04		5.4
0.85	0.70		5.5
0.48	0.60		5.6
0.30	0.30		5.7

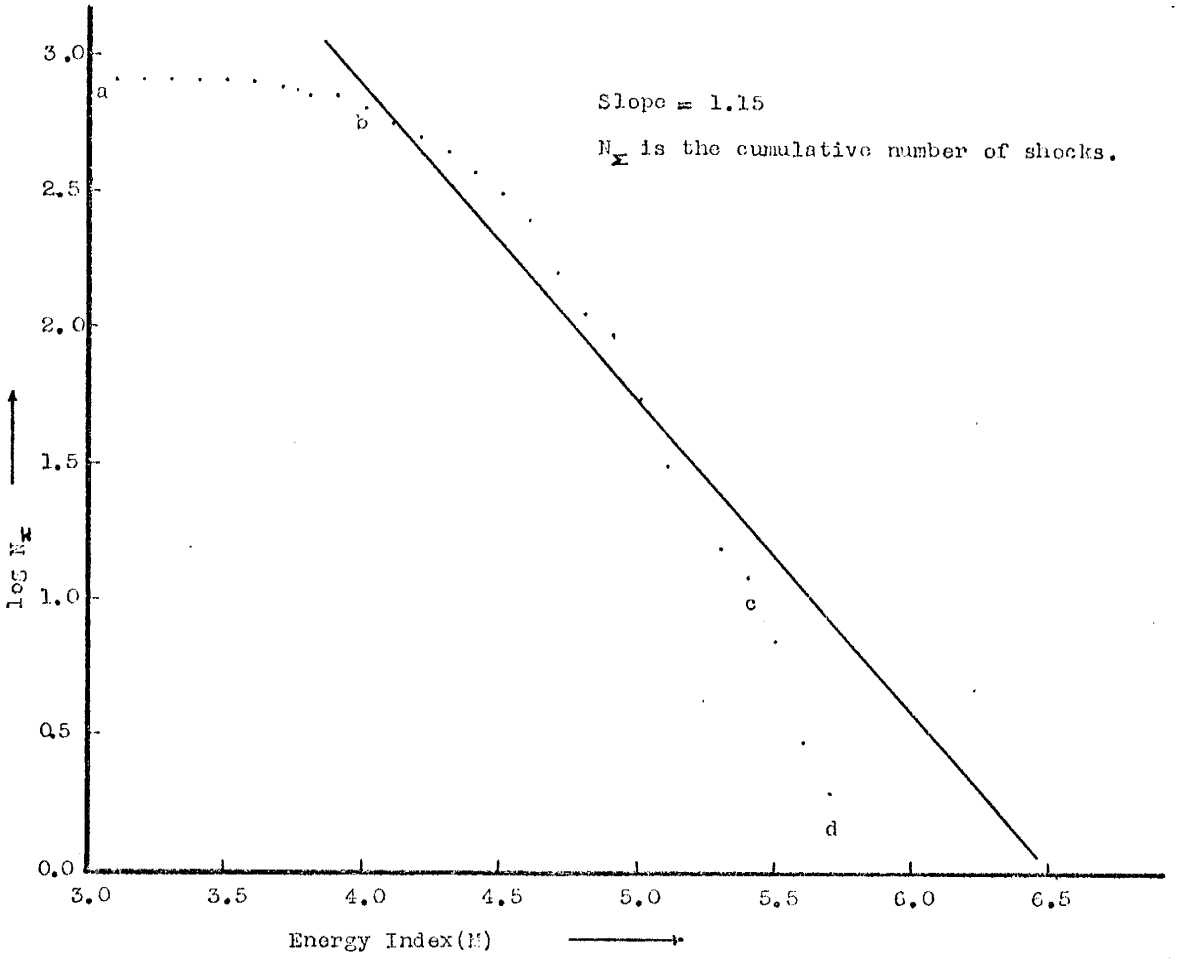

Figure 1.3. Frequency-law for DATA1.

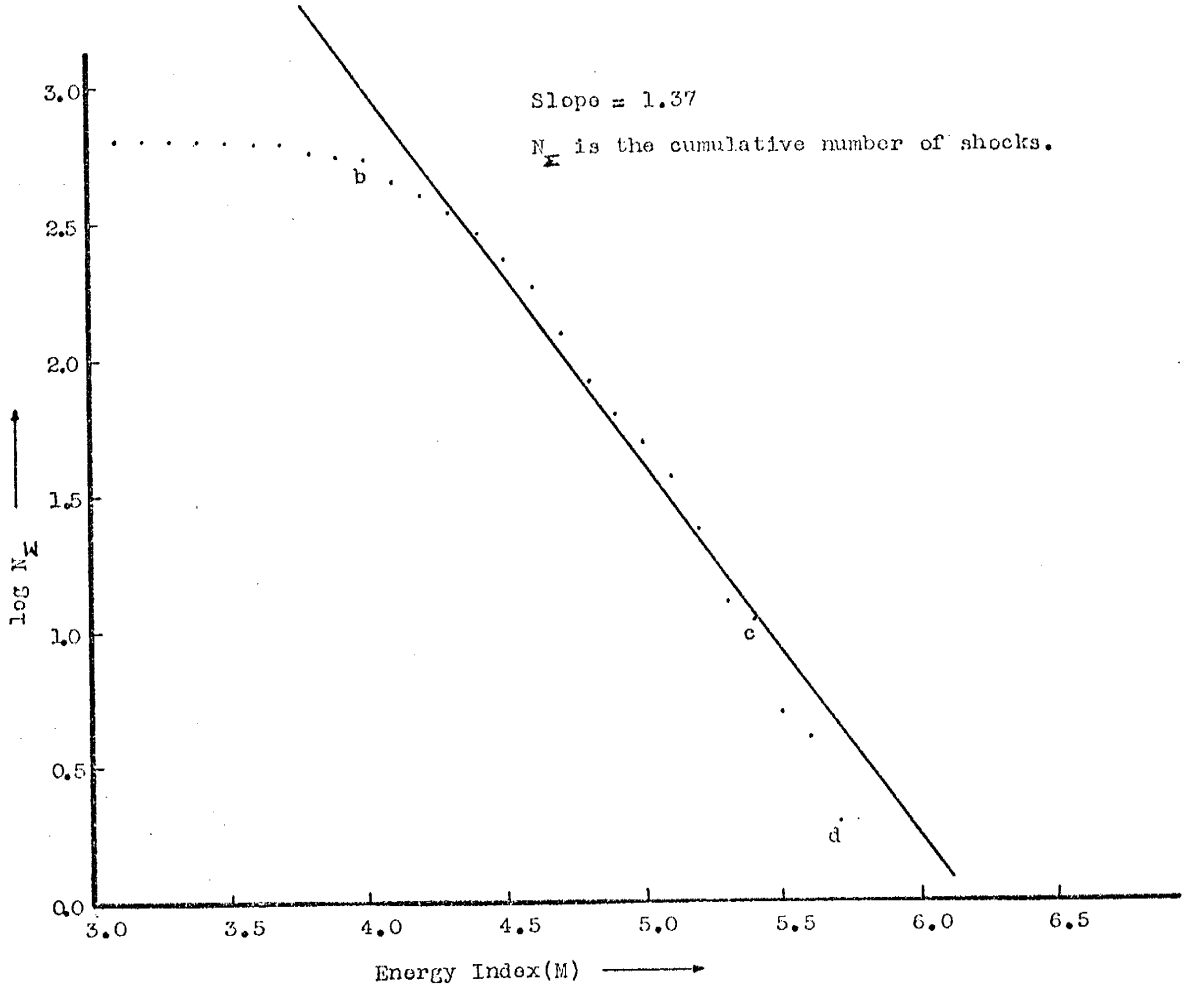

Figure 1.4. Frequency-law for DATA2.

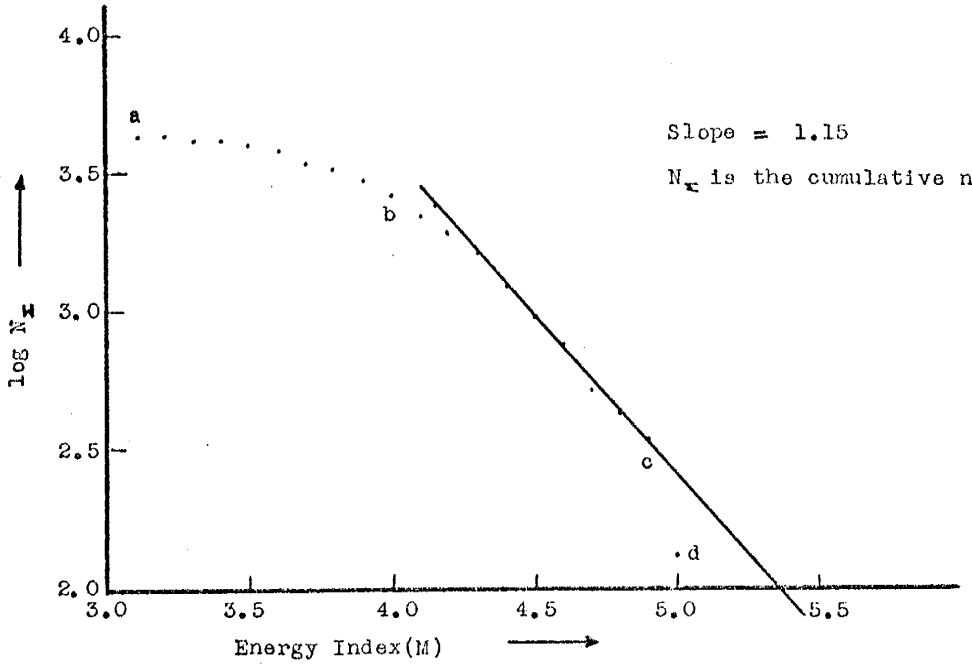

Figure 1.5. Frequency-law for DATA3.

The identification of small shocks, especially the isolated ones, is difficult at low recording sensitivities. This is very likely the reason why the portion of the frequency-law graph corresponding to trace amplitudes of 1 mm to about 10 mm is, more or less, parallel to the M-axis.

We define the activity A of each region, as the value of the common logarithm of the cumulative number of shocks having M=4.0 or greater, which corresponds to a normalized trace amplitude of 10 mm or greater. The activity in the case of the seismic zones corresponding to DATA1, DATA2, and DATA3 is

$$A_{DATA1} = 2.81, \quad A_{DATA2} = 2.73, \quad A_{DATA3} = 3.42.$$

The part (b-c) of Figures (1.3) through (1.5) can be represented by a straight line. The straight line is drawn by eye from M=4.0 to 5.4 for DATA1 and DATA2, whereas the straight line for DATA3 in Figure (1.5) is drawn from M=4.0 to 4.9. The range M=4.0 to 5.4 corresponds to 10-250 mm of amplitude and a major number of shocks falls in this range.

The slope γ of the linear (b-c) part is 1.15 for DATA1, 1.37 for DATA2 and 1.15 for DATA3. On the basis of this part of the curves, the cumulative number of shocks for DATA1 and DATA2 increases by a factor of 14 and 23, respectively, for each unit decrease in M. These values of γ compare well with those obtained by other workers (Brazee and Stover, 1969).

The part (c-d) of Figures (1.3) and (1.4) deflects nward toward the abscissa. Unfortunately, only 3 points ine this part of the curve, and it is difficult to deter- e the shape of the curve. However, the approximate nts at which the curve intercepts abscissa are of inter- . According to the curves, M=5.8, which corresponds to a othetical seismogram amplitude of 630 mm, is the maximum ength a microearthquake could likely have in the areas over the period represented by DATA1 and DATA2. This imum amplitude is equivalent to about 0.7 microns of ound displacement, at a system magnification of 0.9×10^6 6 cycles per second.

e value of m in (1.24a) for microearthquakes

The frequency-law graphs of DATA1 and DATA2 were fitted the general frequency-law relation in equation (1.24a), ploying a least square error criterion.

The value of m for the portion from M=4.0 to 4.9 was und to be 0.993 for both DATA1 and DATA2. A value of m ughly equal to 1 checks the correctness of the theoretical nclusion (1.26) that predicts m should be roughly equal to for straight line portions of the observed graphs.

However, when the least square fit was made to the whole rve from M=4.0 to 5.7, the values of m were found to be 21 for for DATA1 and 0.27 for DATA2, Mogi (1962) and ousner (1955) have derived the straight line type frequency- w by assuming m=1, as discussed under Case I of THEORY.

comparing the values of m for microearthquakes, it is
ear that assuming m=1 explains only a part of the
equency-law. Therefore, it seems that the frequency-law
lation of the type (1.24a) is more in tune with the ob-
rved data than a simple straight line relation (1.1) or
.20).

SECTION II

TEMPORAL VARIATION OF SEISMIC PARAMETERS

INTRODUCTION

Many of the large earthquakes are known to have foreshocks and aftershocks associated with them. Therefore, it has been a belief of many seismologists (Riznichenko, 1958; Katok, 1966) that an earthquake sequence behaves in the temporal vicinity of a relatively large earthquake in a way that differs from its so-called normal behavior. The normal behavior here can be roughly defined as the one before the foreshocks start or after the aftershocks die out; or in other words, the behavior of the part of the earthquake sequence unaffected by the large event. In this section, the temporal variations of three seismological parameters, activity-A, slope-γ, and grouping-R are discussed.

A. P. Katok (1966) and Yu. V. Riznichenko (1958) have discussed the results of this kind of parametric analysis for some earthquakes in the U. S. S. R.. Riznichenko (1958), in his discussion of behavior of A, γ , R, and the product ArR in the Peter-the-First Range, states that all large earthquakes with a single exception occurred at a time when the values of R in that region were increasing. This, according to him, indicates that the large earthquakes occur when the seismic conditions become "feverish". In another paper, Riznichenko (1966) further asserts, on the basis of observations from the

ratory tests on rocks and other materials and mine bursts, the seismic activity A increases before a major burst, slope γ of the earthquake frequency-law decreases, and grouping R increases.

However, the results for the Socorro region are found to quite different from the above-mentioned studies. Analysis the temporal variation of these three parameters for the roearthquakes of the Socorro region show that there is no sistent correspondence between a large shock and the val- s of A, γ , R. Thus the prediction of large microearth- kes on the basis of A, γ , and R behavior seems very unlikely.

THEORY

Activity A and Slope γ

Parameters A and γ are obtained from the earthquake quency-law

$$\log N_{\Sigma} = A - \gamma . M .$$

s the slope of the linear relation between the logarithm the cumulative number N_{Σ} and the energy index M (as defined ler SECTION I). The value of A at an arbitrary value of = M_o is defined the activity-A of the region. M_o is gener- ly the lowest value observable in the area, and thus A is e logarithm of the total number of earthquakes detected.

Grouping R

The parameter R describes the grouping characteristics of earthquakes in time. The parameter R for a unit time interval is defined here as follows:

$$R = \sqrt{\frac{(N_1^2 - \bar{N}^2) + (N_2^2 - \bar{N}^2) + \text{- - -}}{N}} \quad , \qquad (2.2)$$

where N is the total number of earthquakes in a unit time interval, $\bar{N}$ is the average number of earthquakes in each subinterval of equal duration, and N_i is the number of earthquakes in the i^{th} subinterval.

Suppose there are K subintervals in the unit time interval. Then,

$$K \cdot \bar{N} = N, \text{ and}$$

$$R = \sqrt{\frac{\sum_K N_i^2 - \sum_K \bar{N}^2}{K \cdot \bar{N}}} = \sqrt{\frac{\sum_K N_i^2 + K \cdot \bar{N}^2 - 2K \cdot \bar{N}^2}{K \cdot \bar{N}}}$$

$$R = \sqrt{\frac{\sum_K N_i^2 - \sum_K \bar{N}^2 - 2\bar{N}(N_1 + N_2 + \text{- - -} + N_K)}{K \cdot \bar{N}}}$$

$$R = \sqrt{\frac{\sum_K (N_i - \bar{N})^2}{K \cdot \bar{N}}} = \frac{\sigma_N}{\sqrt{\bar{N}}} \quad , \qquad (2.3)$$

where σ_N is the standard deviation of N earthquakes distributed in K subintervals. The equation (2.3) shows R is a non-negative number. The value of R is large for a given number of earthquakes if the standard deviation is large, or, in other words, if the number of earthquakes in individual

subintervals deviates from the mean $\bar{N}$, by a large amount which makes $\sigma_{\bar{N}}$ large and therefore, R large.

To give an example, assume that the earthquake sequence is a sample function of a Poisson process. In that case,

$$\sigma_{\bar{N}} = \sqrt{\bar{N}} \quad \text{and} \quad R = \frac{\sqrt{\bar{N}}}{\sqrt{\bar{N}}} = 1.$$

Since a Poisson process has independent inter-arrival times, the value of R=1 represents a distribution of earthquakes in K subintervals where events are independent of each other. However, R=1 would not always imply that the process is a Poisson process.

The value of R>1 indicates a high degree of grouping. Similarly, R<1 will indicate a low degree of grouping; less than expected on a chance basis. The value of R=0 implies no grouping at all. This is possible only when $\sigma_{\bar{N}}=0$ and thus each subinterval contains exactly the same number of earthquakes.

In order to understand the significance of the parameter R, let us compute and examine its values for K=10 and N=3 and 5. Taking N=3 first, the distinctly different number of ways in which 3 earthquakes can be distributed in 10 subintervals, can be given as,

(1) 3, 0, 0, 0, 0, 0, 0, 0, 0, 0

(2) 2, 1, 0, 0, 0, 0, 0, 0, 0, 0 $\quad \bar{N} = 0.3$

(3) 1, 1, 1, 0, 0, 0, 0, 0, 0, 0

$$\sigma^2_{3(1)} = \frac{(3-0.3)^2 + 9(0-0.3)^2}{10} = \frac{7.29 + 0.81}{10} = 0.81$$

$$R_{3(1)} = \sqrt{\frac{0.81}{0.3}} = \sqrt{2.7} \simeq 1.6$$

$$\sigma^2_{3(2)} = \frac{(2-0.3)^2 + (1-0.3)^2 + 8(0.3)^2}{10} = \frac{4.10}{10} = 0.41$$

$$R_{3(2)} = \sqrt{\frac{0.41}{0.3}} \simeq \sqrt{1.4} \simeq 1.2$$

$$\sigma^2_{3(3)} = \sqrt{\frac{3(1-0.3)^2 + 7(0.3)^2}{10}} = \sqrt{\frac{1.83}{10}} = 0.183$$

$$R_{3(3)} = \sqrt{\frac{0.183}{0.3}} = \sqrt{0.61} \simeq 0.8 \quad .$$

Taking N=5, there are the following different ways to arrange 5 eqrthquakes into 10 subintervals,

(1) 5, 0, 0, 0, 0, 0, 0, 0, 0, 0

(2) 4, 1, 0, 0, 0, 0, 0, 0, 0, 0

(3) 3, 2, 0, 0, 0, 0, 0, 0, 0, 0

(4) 3, 1, 1, 0, 0, 0, 0, 0, 0, 0 $\quad \bar{N} = 0.5$

(5) 2, 2, 1, 0, 0, 0, 0, 0, 0, 0

(6) 2, 1, 1, 1, 0, 0, 0, 0, 0, 0

(7) 1, 1, 1, 1, 1, 0, 0, 0, 0, 0

We compute R for the most grouped, (1), and the least grouped, (7), combinations.

$$\sigma^2_{5(1)} = \frac{(5-0.5)^2 + 9(0-0.5)^2}{10} = \frac{22.50}{10} = 2.25$$

$$R_{5(1)} = \sqrt{\frac{2.25}{0.5}} = \sqrt{4.5} \simeq 2.1$$

$$\sigma^2_{5(7)} = \frac{5(1-0.5)^2 + 5 \times 0.25}{10} = \frac{2.5}{10} = 0.25$$

$$R_5(7) = \sqrt{\frac{0.25}{0.5}} = \sqrt{0.5} \simeq 0.7 .$$

For K=10, N=3, R values are 1.6, 1.2, and 0.8. These are the only possible values that R can have for N=3. Changing K would not change the number of possible values unless K gets lower than the value of N. For K=10, N=5, there are 7 possible values and R ranges from 0.7 to 2.25.

For N=3, R values do not change much from 1. In other words, no matter how one chooses to distribute 3 earthquakes in 10 subintervals, he will get a value of R within a narrow range of 0.8 - 1.6. For N=5, different distributions of earthquakes in subintervals give significantly different values of R. Therefore, we will consider the R values only for N=5 or greater.

METHOD OF ANALYSIS

The basic data used for analysis of temporal variations in A, γ, and R was DATA1, DATA2, and DATA3. The 5 year period covered by these data sets was broken into smaller intervals of one month each. For each month, the values of the activity A, the slope γ, and the grouping R were computed.

The linear portion of the frequency-law curve from M=4.0 to M=4.9 was used to determine the slope γ (see SECTION I). This M-range spans the S-phase amplitude range from 10 mm. to 80 mm.. Because many months have a small number of earthquakes the values of γ are very susceptible to error. The value of γ

for all monthly intervals was calculated using the following relation.

$$\gamma = \left[\frac{\log N_{4.0}-\log N_{4.9}}{4.9-4.0} + \frac{\log N_{4.3}-\log N_{4.9}}{4.9-4.3} + \frac{\log N_{4.6}-\log N_{4.9}}{4.9-4.6}\right], \quad (2.5)$$

where $N_{4.0}$ is the cumulative number of earthquakes at M=4.0, - - - etc.. This gives us γ as the arithmetic mean of the slope at three points.

To compute the parameter R for an interval of one month, the relation,

$$R = \sqrt{\frac{(N_1-\bar{N})^2 + (N_2-\bar{N})^2 + \text{ - - - } + (N_K-\bar{N})^2}{\bar{N}.(K-1)}} \quad (2.6)$$

was employed.

The choice of a value for the number of subintervals K, depends primarily upon the number of earthquakes in the interval. It also depends on the grouping characteristics of the earthquake sequence. For example, take a 30 day interval with three subintervals of 10 day duration. If the grouping behaves in such a way that the first 5 day interval has many earthquakes and the next 5 day interval has no earthquakes, then taking the whole 10 day period might show no grouping at all. However, if we take K=6, this grouping will show up. For some particular periods of Socorro earthquake activity, R values for each month were computed using K=3, 6, 10, 15. From these computations, the best results were obtained by subdividing one month intervals into 10 subintervals.

RESULTS

The data DATA1 and DATA2 were used to compute the A, γ, R parameters for a 60 month interval, starting from January, 1963. Results for DATA1 are given in Tables (2.1) to (2.3) for 1 month, 2 month and 3 month intervals, respectively, and those for DATA2 in Tables (2.4) to (2.6).

For both the data sets, the specifications for the computations are as follows:

(a) One month interval: number of intervals = 60, K = 10.

(b) Two month interval: number of intervals = 30, K = 10.

(c) Three month interval: number of intervals = 20, K = 15.

Classes of energy index M: 24, from 4.0 to 6.3 with 0.1 increment.

Slope (γ) estimate: Arithmetic mean of 3 values corresponding to straight lines from the point at M=4.9 to 4.0, M=4.9 to 4.3 and M=4.9 to 4.6.

Grouping Parameter R: $\frac{\sigma_{\bar{N}}}{\sqrt{\bar{N}}}$, where $\bar{N}$ is the mean number of earthquakes in each subinterval of 3 days for month intervals and 6 days for 2 and 3 month intervals. $\sigma_{\bar{N}}$ is the estimate of the standard deviation.

DATA3 was also used to calculate A, γ and R (Table 2.7) using the same specifications as above, except the time period was 69 months and only one month intervals with K=10 were used.

The first column in Tables (2.1) to (2.7) lists the activity (A) for a particular interval, the second column gives

the slope (γ), the third column is the grouping parameter (R), the fourth column has the value of σ_N, the fifth column is the value of $\bar{N}$, and the last column lists the product of A, γ, and R. Results of Tables (2.1) to (2.7) are plotted in Figures (2.1) to (2.7), respectively. The values corresponding to the intervals which have less than 5 earthquakes are not shown in the figures.

Before the results are discussed, one important aspect of the nature of the earthquakes in the Socorro region needs clarification. The term 'big event' has been used previously without defining it. A 'big event' is defined here as a microearthquake having a S-phase peak-to-peak amplitude equal to or greater than 100 mm. on the seismogram when the recording system has a magnification of 0.9×10^6 at 6 cycles per second. Assuming the S-phase is dominated by 6 c.p.s. oscillations, a 100 mm. amplitude on the record corresponds to 0.11 microns of ground motion.

Tables (2.8) and (2.9) list all the shocks with amplitudes greater than 70 mm. These tables also list qualitative value of A, γ, R and the product $A \cdot \gamma \cdot R$, at the time these shocks occurred. For example, the first event in Table (2.8) has a medium A, high γ, low R and medium $A \cdot \gamma \cdot R$, as seen from Figure (2.4). A value is called medium if it is midway between the maximum and minimum of a particular curve, medium-high if between the medium and maximum, medium-low if between the medium and the minimum, high if close to the maximum and low if close to minimum.

Table 2.1. Values of A, γ , R for Successive Month Intervals for DATA1.

No.	Activity A	Slope γ	Grouping R	σ_N	$\bar{N}$	AγR
1	1.23	1.73	2.63	3.43	1.70	5.61
2	1.15	1.78	1.33	1.58	1.40	2.72
3	0.60	1.09	0.81	0.52	0.40	0.53
4	1.08	1.98	1.91	2.10	1.20	4.09
5	1.28	2.36	2.17	3.00	1.90	6.55
6	0.70	0.98	0.74	0.53	0.50	0.51
7	1.20	1.16	2.47	3.13	1.60	3.47
8	1.30	1.88	2.72	3.86	2.00	6.66
9	0.00	0.00	1.00	0.32	0.10	0.00
10	0.48	0.97	1.73	0.95	0.30	0.80
11	0.00	0.00	0.00	0.00	0.00	0.00
12	1.45	1.93	1.63	2.74	2.80	4.57
13	0.48	0.34	0.88	0.48	0.30	0.14
14	1.15	1.28	2.39	2.84	1.40	3.51
15	1.23	1.60	1.30	1.70	1.70	2.57
16	0.70	0.52	1.00	0.71	0.50	0.36
17	1.18	1.54	2.00	2.46	1.50	3.63
18	1.90	1.44	1.26	1.14	0.80	1.64
19	1.11	1.44	1.09	1.25	1.30	1.76
20	1.15	1.80	1.95	2.32	1.40	4.04
21	1.18	1.63	1.19	1.51	1.60	2.28
22	1.00	1.37	1.41	1.41	1.00	1.93
23	0.85	1.18	2.25	1.89	0.70	2.24
24	0.60	0.72	1.37	0.97	0.50	0.60
25	0.00	0.00	0.88	0.48	0.30	0.00
26	1.18	1.29	2.93	3.83	1.70	4.44
27	1.30	0.34	1.76	2.49	2.00	0.79
28	1.54	0.62	5.19	10.27	3.90	4.99
29	1.40	1.33	2.51	3.98	2.50	4.66
30	0.85	0.91	1.73	1.55	0.80	1.33
31	0.30	0.11	0.88	0.48	0.30	0.03
32	0.30	0.11	1.41	0.63	0.20	0.04
33	0.60	0.56	1.10	0.70	0.40	0.37
34	0.48	0.18	0.88	0.48	0.30	0.07
35	0.00	0.00	1.00	0.32	0.10	0.00
36	0.95	0.30	1.60	1.52	0.90	0.46
37	1.15	1.28	1.94	2.46	1.60	2.84
38	0.30	0.61	0.94	0.42	0.20	0.17
39	0.30	0.00	1.41	0.63	0.20	0.00
40	1.38	1.11	1.28	2.07	2.60	1.96
41	1.00	0.52	1.41	1.41	1.00	0.74
42	1.18	0.50	2.04	2.51	1.50	1.19
43	0.78	0.78	1.13	0.95	0.70	0.68
44	1.34	0.51	1.44	2.15	2.20	0.99
45	1.41	0.21	2.05	3.31	2.60	0.59

Table 2.1 Cont'd.

.	Activity A	Slope γ	Grouping R	$\sigma_{\bar{N}}$	$\bar{N}$	$A\gamma R$
5	1.04	0.17	1.93	2.02	1.10	0.33
7	0.70	0.34	1.20	0.85	0.50	0.28
8	0.00	0.00	0.00	0.00	0.00	0.00
9	0.78	0.37	0.90	0.70	0.60	0.26
0	0.70	0.65	1.00	0.71	0.50	0.45
1	0.85	0.58	1.26	1.06	0.70	0.62
2	0.90	1.58	1.15	1.03	0.80	1.64
3	1.30	2.06	2.51	3.56	2.00	6.75
4	1.71	2.20	1.98	4.62	5.40	7.47
5	1.15	1.29	1.20	1.43	1.40	1.78
6	0.48	0.44	1.23	0.67	0.30	0.26
7	0.30	0.11	0.94	0.42	0.20	0.03
8	0.00	0.00	1.00	0.32	0.10	0.00
9	0.48	0.68	1.23	0.67	0.30	0.39
0	0.00	0.00	1.00	0.32	0.10	0.00

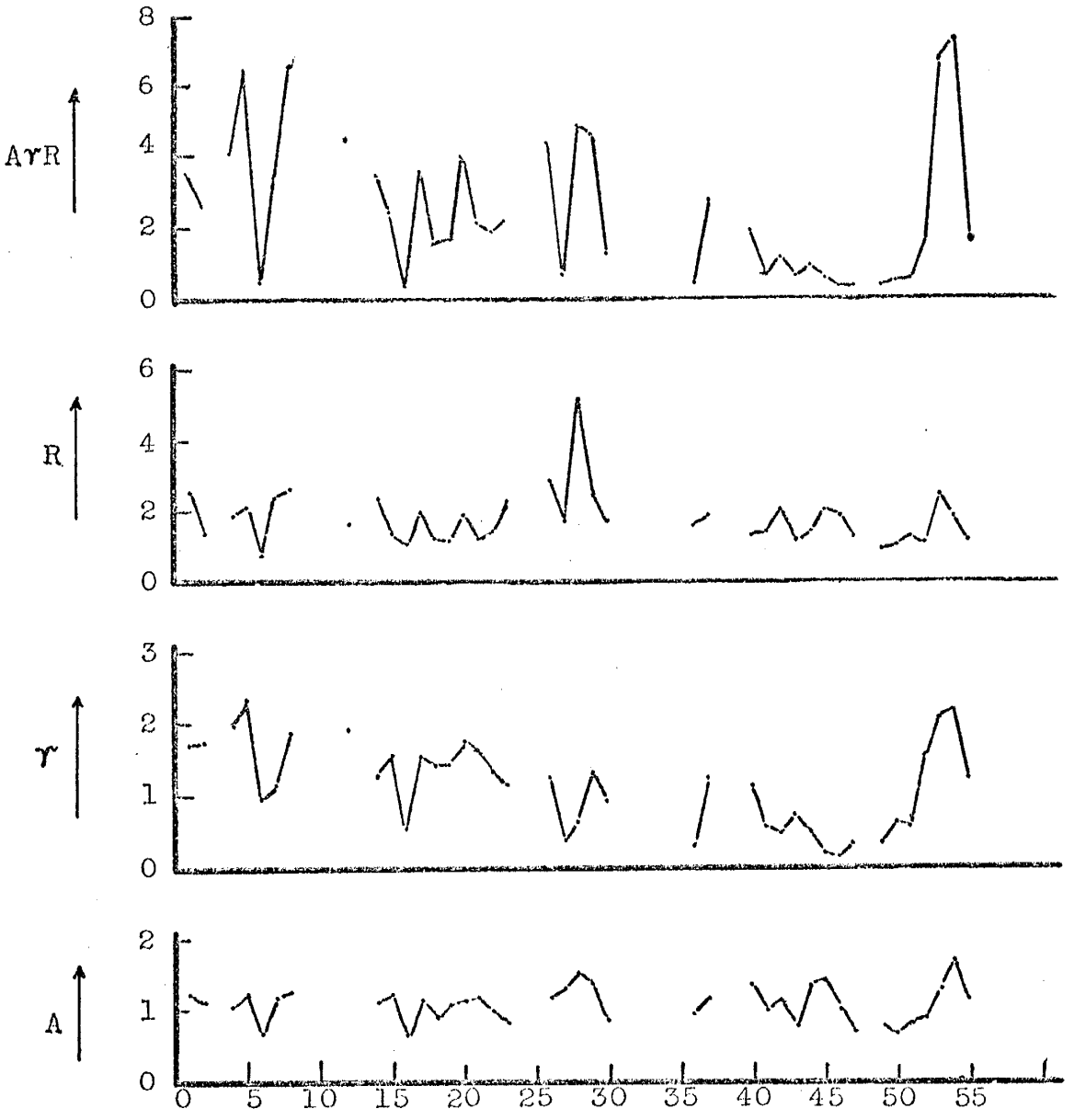

Figure 2.1. A, r , R curves for one month intervals, for DATA1.

able 2.2. Values of A,γ, R for Successive Two Month Intervals for DATA1.

o.	Activity A	Slope γ	Grouping R	$\sigma_{\bar{N}}$	$\bar{N}$	AγR
	1.49	2.37	2.46	4.33	3.10	8.71
	1.20	2.26	1.79	2.27	1.60	4.87
	1.38	2.53	2.74	4.25	2.40	9.57
	1.56	1.47	2.34	4.45	3.60	5.37
	0.60	1.02	1.52	0.97	0.40	0.93
	1.45	1.93	2.28	3.82	2.80	6.38
	1.23	1.36	2.82	3.68	1.70	4.72
	1.34	1.84	1.55	2.30	2.20	3.82
	1.36	2.11	1.94	2.95	2.30	5.57
0	1.43	2.26	1.57	2.58	2.70	5.07
1	1.40	2.13	1.13	1.84	2.60	3.38
2	1.04	1.59	1.91	2.10	1.20	3.18
3	1.20	1.32	3.49	4.94	2.00	5.54
4	1.74	0.50	4.14	10.07	5.90	3.57
5	1.51	1.24	2.26	4.11	3.30	4.22
6	0.60	0.39	1.20	0.85	0.50	0.28
7	0.85	0.70	0.98	0.82	0.70	0.58
8	1.00	0.32	1.49	1.49	1.00	0.47
9	1.20	1.11	1.98	2.66	1.80	2.65
0	1.41	1.08	1.84	3.08	2.80	2.81
1	1.40	0.51	1.43	2.27	2.50	1.01
2	1.45	0.57	1.88	3.21	2.90	1.56
3	1.57	0.20	1.68	3.23	3.70	0.51
4	0.70	0.34	1.20	0.85	0.50	0.28
5	1.04	0.75	0.70	0.74	1.10	0.54
6	1.18	1.77	1.03	1.27	1.50	2.15
7	1.85	2.16	2.80	7.62	7.40	11.20
8	1.23	1.59	1.20	1.57	1.70	2.34
9	0.48	0.68	0.88	0.48	0.30	0.28
0	0.60	0.72	1.10	0.70	0.40	0.48

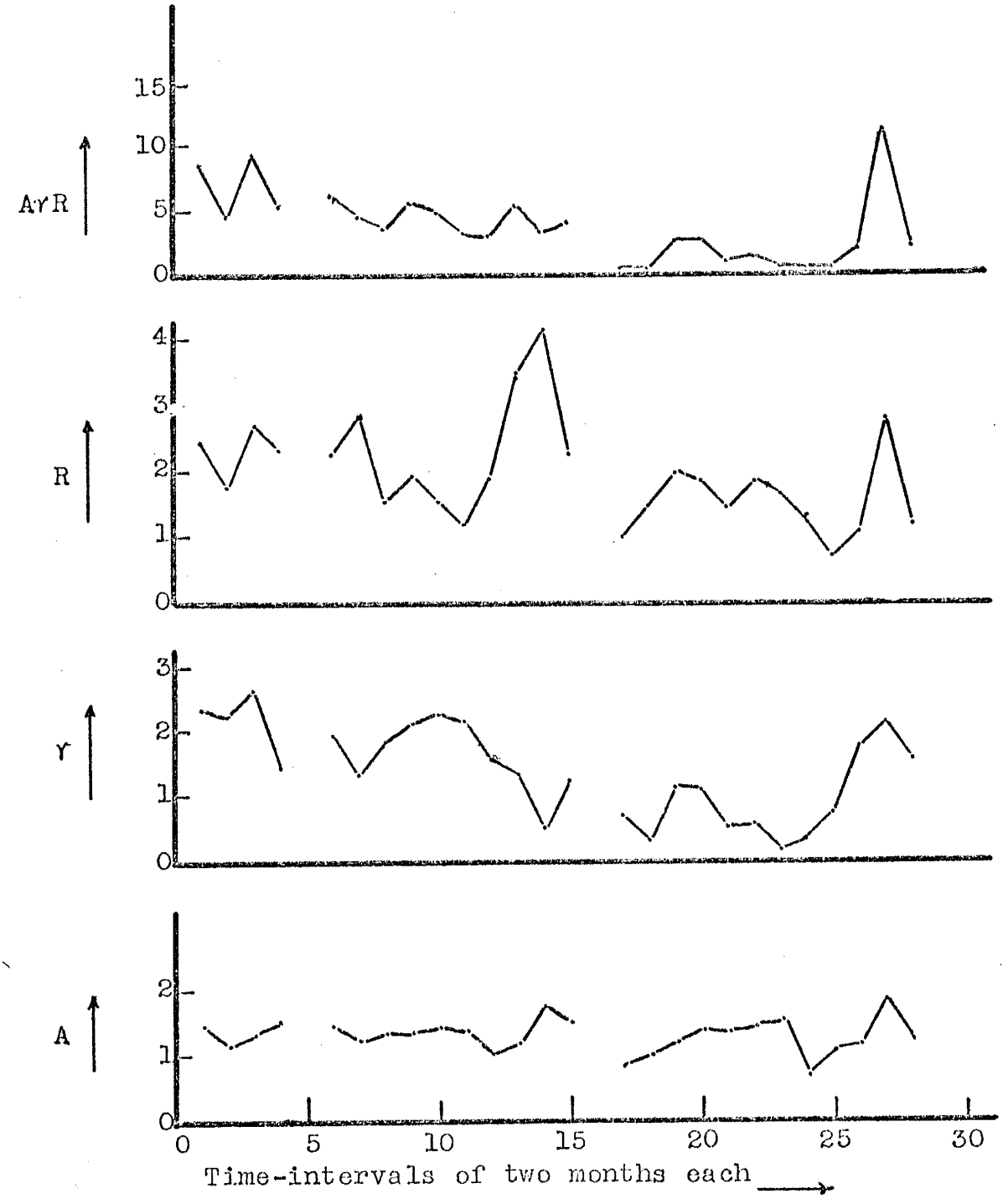

Figure 2.2. A, γ, R curves for two month intervals, for DATA1.

Table 2.3. Values of A, γ , R for Successive Three Month Intervals for DATA1.

No.	Activity A	Slope γ	Grouping R	$\sigma_{\bar{N}}$	$\bar{N}$	AγR
1	1.54	2.57	2.40	3.68	2.33	9.53
2	1.56	2.30	2.43	3.78	2.40	8.71
3	1.57	1.48	2.51	3.94	2.47	5.81
4	1.49	1.61	2.31	3.33	2.07	5.56
5	1.53	1.83	2.25	3.39	2.27	6.31
6	1.45	2.25	1.83	2.50	1.87	5.96
7	1.62	2.61	1.40	2.39	2.87	5.97
8	1.32	2.11	1.55	1.88	1.47	4.34
9	1.56	0.59	2.86	4.69	2.67	2.63
10	1.83	0.83	3.90	8.55	4.80	5.94
11	0.90	0.77	1.06	0.83	0.60	0.74
12	1.11	0.40	1.39	1.30	0.87	0.62
13	1.26	0.82	1.98	2.29	1.33	2.04
14	1.69	0.85	1.41	2.61	3.40	2.04
15	1.73	0.36	1.75	3.35	3.67	1.09
16	1.20	0.23	1.65	1.71	1.07	0.46
17	1.26	0.89	0.98	1.08	1.20	1.10
18	1.90	2.30	2.88	6.75	5.47	12.62
19	1.28	1.76	1.27	1.44	1.27	2.87
20	0.70	1.05	1.06	0.62	0.33	0.78

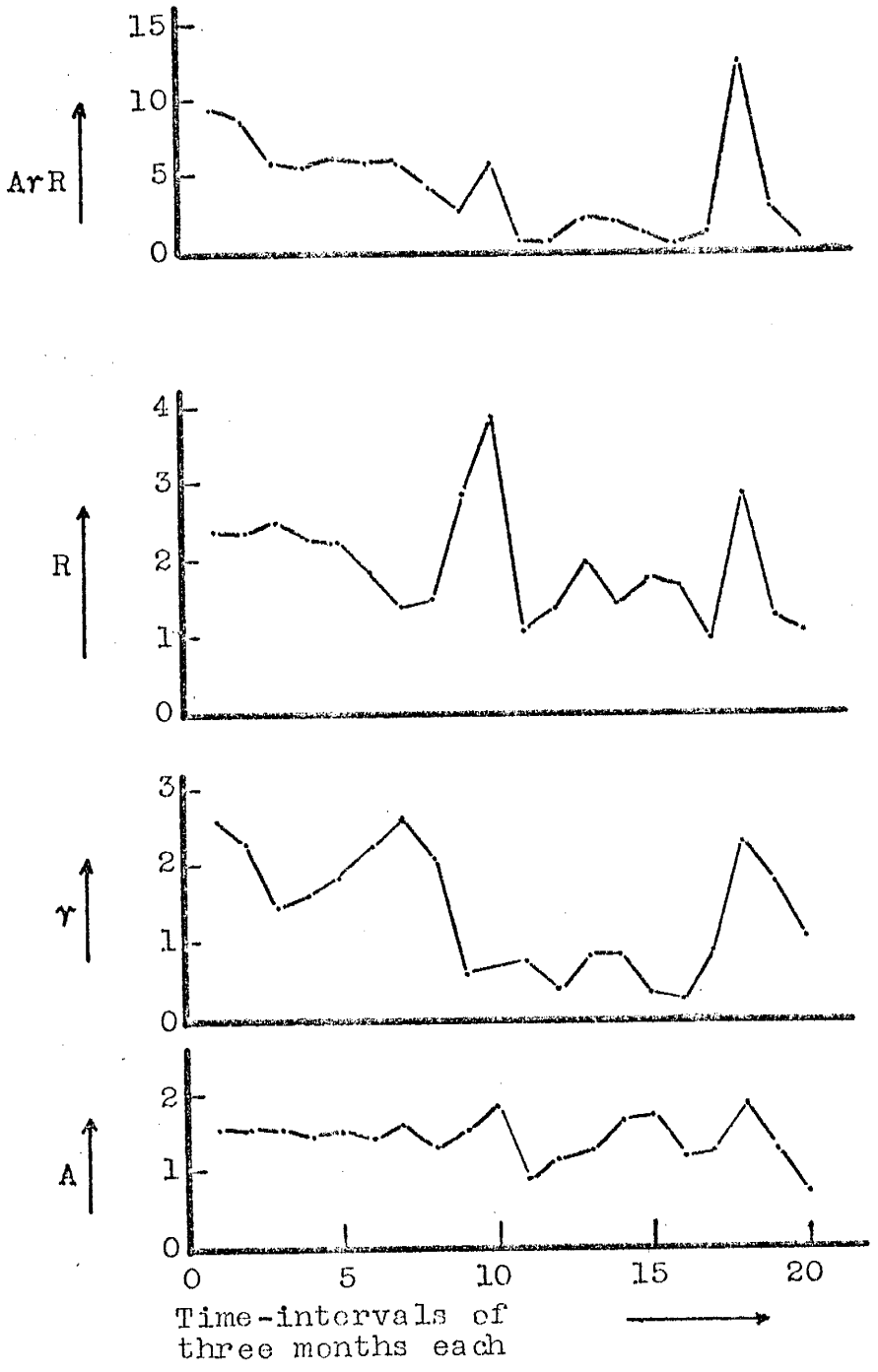

Figure 2.3. A, γ , R curves for three month intervals, for DATA1.

Table 2.4. Values of A, γ , R for Successive Month Intervals for DATA2.

No.	Activity A	Slope γ	Grouping R	σ_N	$\bar{N}$	AγR
1	1.36	1.92	1.35	2.06	2.30	3.54
2	0.78	1.21	1.38	1.07	0.60	1.30
3	1.04	0.85	1.14	1.20	1.10	1.01
4	1.11	1.38	2.15	2.45	1.30	3.29
5	0.85	1.28	1.49	1.25	0.70	1.61
6	1.00	1.51	1.69	1.70	1.00	2.56
7	0.30	0.28	0.94	0.42	0.20	0.07
8	0.00	0.00	1.00	0.32	0.10	0.00
9	0.60	0.39	1.10	0.70	0.40	0.26
10	0.85	0.91	2.25	1.89	0.70	1.73
11	0.85	1.23	1.13	0.95	0.70	1.18
12	0.70	0.86	1.00	0.71	0.50	0.60
13	0.60	0.56	0.81	0.52	0.40	0.27
14	0.95	1.60	1.60	1.52	0.90	2.45
15	0.85	1.08	1.87	1.57	0.70	1.70
16	1.58	1.89	3.47	6.78	3.80	10.35
17	0.95	1.08	1.26	1.20	0.90	1.29
18	0.78	1.01	1.24	0.97	0.60	0.98
19	0.78	0.55	1.38	1.07	0.60	0.59
20	0.70	0.59	1.79	1.27	0.50	0.74
21	1.76	0.84	3.66	8.83	5.80	5.44
22	1.11	1.62	1.09	1.25	1.30	1.98
23	0.48	0.34	0.88	0.48	0.30	0.14
24	0.85	1.28	1.49	1.25	0.70	1.61
25	0.30	0.11	0.94	0.42	0.20	0.03
26	1.08	1.62	0.83	0.92	1.20	1.45
27	1.15	1.41	1.39	1.65	1.40	2.25
28	0.30	0.61	0.94	0.42	0.20	0.17
29	0.48	0.07	1.10	0.70	0.40	0.03
30	0.00	0.00	1.00	0.32	0.10	0.00
31	0.78	0.46	1.08	0.84	0.60	0.38
32	1.00	1.09	1.22	1.29	1.10	1.34
33	1.04	0.72	1.38	1.45	1.10	1.03
34	0.85	1.04	1.49	1.25	0.70	1.31
35	0.90	0.67	1.02	0.92	0.80	0.62
36	0.00	0.00	1.00	0.32	0.10	0.00
37	1.23	2.03	3.11	4.06	1.70	7.77
38	0.30	0.28	0.94	0.42	0.20	0.07
39	0.90	0.72	1.16	1.10	0.90	0.75
40	0.85	0.48	1.26	1.06	0.70	0.51
41	0.95	0.99	1.52	1.45	0.90	1.43
42	0.90	0.60	1.37	1.23	0.80	0.74
43	0.70	0.52	1.20	0.85	0.50	0.44
44	1.00	0.97	1.05	1.05	1.00	1.01
45	0.60	0.82	1.52	0.97	0.40	0.75

Table 2.4 Cont'd.

No.	Activity A	Slope γ	Grouping R	σ_N	$\bar{N}$	$A\gamma R$
46	0.30	0.11	1.41	0.63	0.20	0.04
47	0.85	0.75	0.80	0.67	0.70	0.50
48	0.85	0.58	1.26	1.06	0.70	0.61
49	0.70	1.26	1.52	1.08	0.50	1.34
50	1.04	1.31	1.59	1.75	1.20	2.17
51	0.78	0.89	0.90	0.70	0.60	0.62
52	1.18	1.35	1.68	2.07	1.50	2.68
53	1.15	0.59	2.36	2.80	1.40	1.60
54	0.60	0.49	1.52	0.97	0.40	0.44
55	1.04	1.63	1.14	1.20	1.10	1.94
56	0.00	0.00	1.00	0.32	0.10	0.00
57	1.00	1.33	2.49	2.49	1.00	3.32
58	0.70	0.52	0.74	0.53	0.50	0.27
59	0.90	0.50	1.56	1.40	0.80	0.70
60	1.00	1.23	1.49	1.49	1.00	1.82

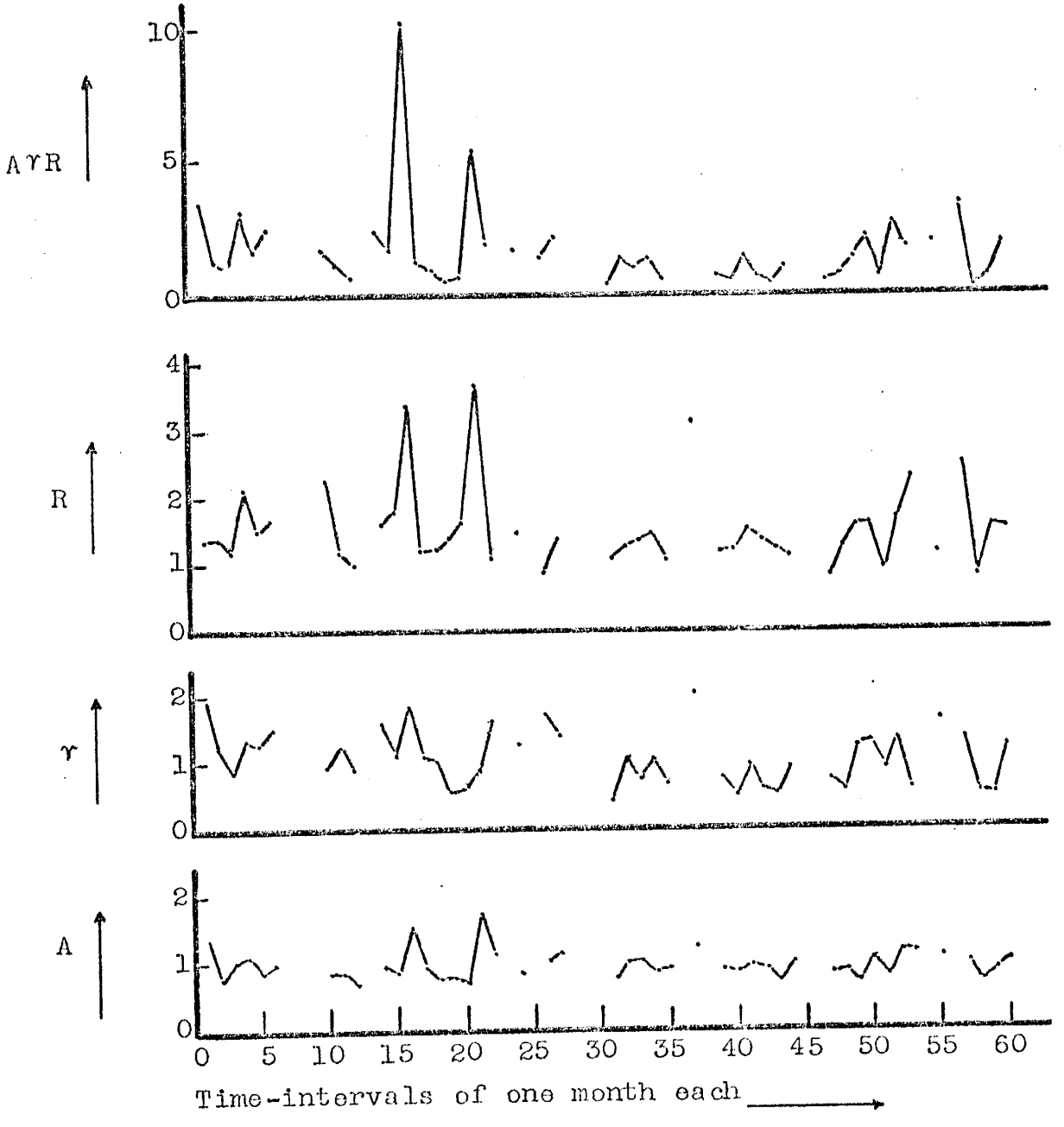

Figure 2.4. A, γ , R curves for one month intervals, for DATA2.

Table 2.5. Values of A, γ, R for Successive Two Month Intervals for DATA2.

No.	Activity A	Slope γ	Grouping R	σ_N	$\bar{N}$	AγR
1	1.46	1.64	1.55	2.64	2.90	3.72
2	1.38	1.03	1.52	2.37	2.40	2.17
3	1.23	2.01	2.04	2.67	1.70	5.07
4	0.48	0.44	0.88	0.48	0.30	0.18
5	1.04	1.14	1.76	1.85	1.10	2.09
6	1.08	1.68	1.12	1.23	1.20	2.03
7	1.11	1.86	1.24	1.42	1.30	2.57
8	1.65	2.05	4.63	9.83	4.50	15.70
9	1.18	1.66	1.23	1.51	1.50	2.40
10	1.04	0.86	1.38	1.45	1.10	1.23
11	1.85	0.94	3.40	9.07	7.10	5.89
12	1.00	1.40	1.24	1.25	1.00	1.74
13	1.15	1.67	1.20	1.43	1.40	2.31
14	1.20	1.58	1.75	2.22	1.60	3.34
15	0.60	0.21	1.00	0.71	0.50	0.12
16	1.20	0.83	0.88	1.16	1.70	0.89
17	1.26	1.33	1.30	1.75	1.80	2.17
18	0.95	0.74	1.35	1.29	0.90	0.96
19	1.28	1.53	2.89	3.98	1.90	5.66
20	1.18	1.24	1.06	1.35	1.60	1.55
21	1.23	0.90	1.25	1.64	1.70	1.39
22	1.18	1.22	1.03	1.27	1.50	1.48
23	0.78	0.89	1.38	1.07	0.60	0.95
24	1.15	0.95	0.90	1.07	1.40	0.99
25	1.20	1.29	1.73	2.26	1.70	2.70
26	1.32	1.77	1.79	2.60	2.10	4.19
27	1.26	0.70	2.64	3.55	1.80	2.33
28	1.08	1.65	1.47	1.62	1.20	2.62
29	1.18	1.02	1.93	2.37	1.50	2.32
30	1.26	1.43	1.25	1.69	1.80	2.26

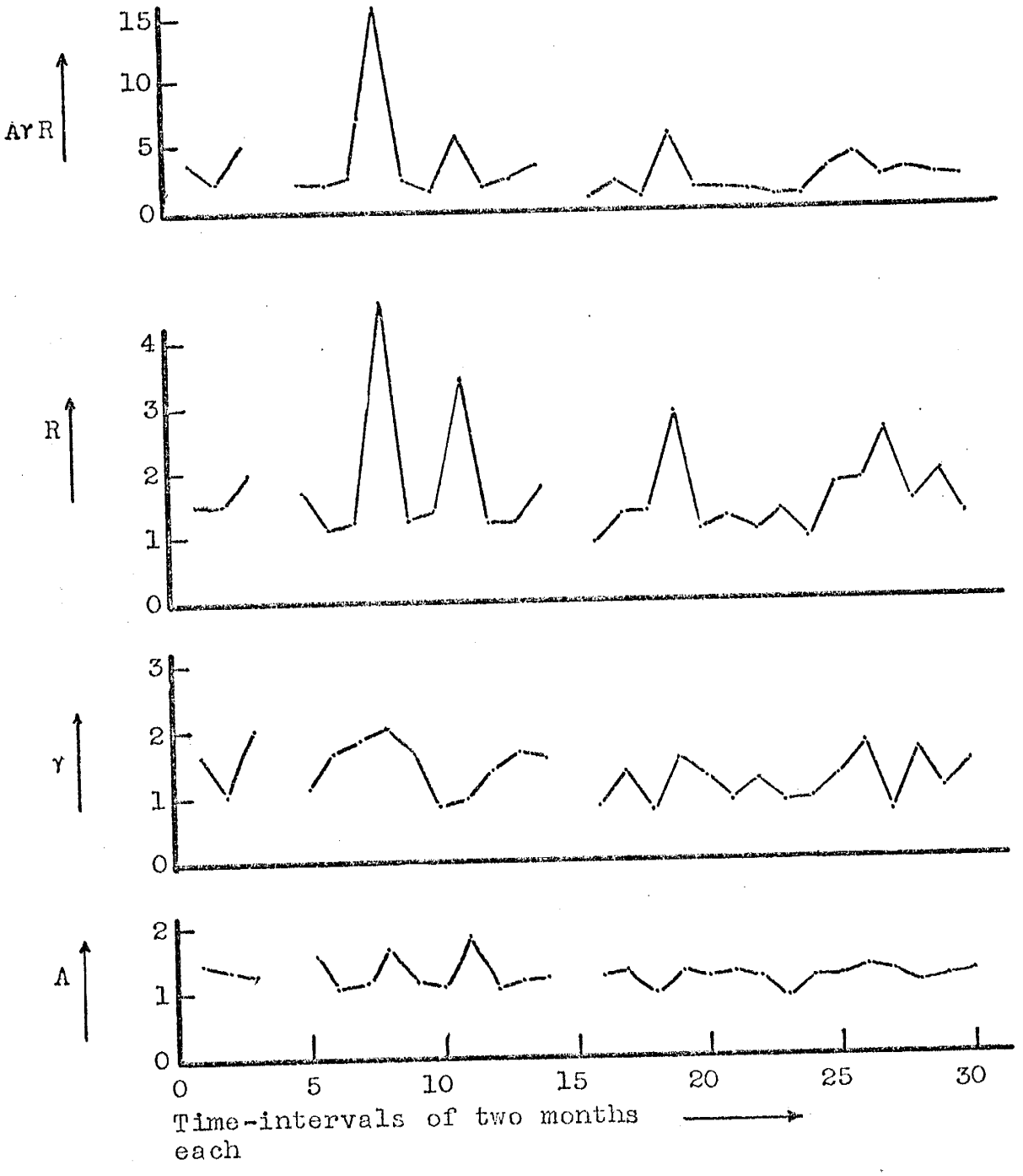

Figure 2.5. A, γ , R curves for two month intervals, for DATA2.

Table 2.6. Values of A, γ , R for Successive Three Month Intervals for DATA2.

No.	Activity A	Slope γ	Grouping R	$\sigma_{\bar{N}}$	$\bar{N}$	AγR
1	1.60	1.27	1.38	2.26	2.67	2.81
2	1.48	2.37	1.98	2.80	2.00	6.93
3	0.85	0.70	0.93	0.64	0.47	0.55
4	1.28	1.25	1.51	1.71	1.27	2.42
5	1.30	2.17	1.41	1.63	1.33	3.99
6	1.72	1.82	4.26	8.02	3.53	13.36
7	1.84	0.91	3.76	8.07	4.60	6.28
8	1.36	1.53	1.29	1.60	1.53	2.69
9	1.45	1.88	1.43	1.96	1.87	3.89
10	0.78	0.73	0.93	0.64	0.47	0.53
11	1.43	1.03	1.03	1.41	1.87	1.51
12	1.20	0.92	1.34	1.39	1.07	1.48
13	1.43	1.71	2.39	3.27	1.87	5.86
14	1.38	1.08	1.22	1.55	1.60	1.82
15	1.28	1.10	1.13	1.28	1.27	1.60
16	1.20	0.98	1.06	1.10	1.07	1.25
17	1.34	1.47	1.58	1.96	1.53	3.11
18	1.52	0.88	2.31	3.43	2.20	3.09
19	1.34	2.12	1.86	2.26	1.47	5.31
20	1.36	1.23	1.17	1.46	1.53	1.97

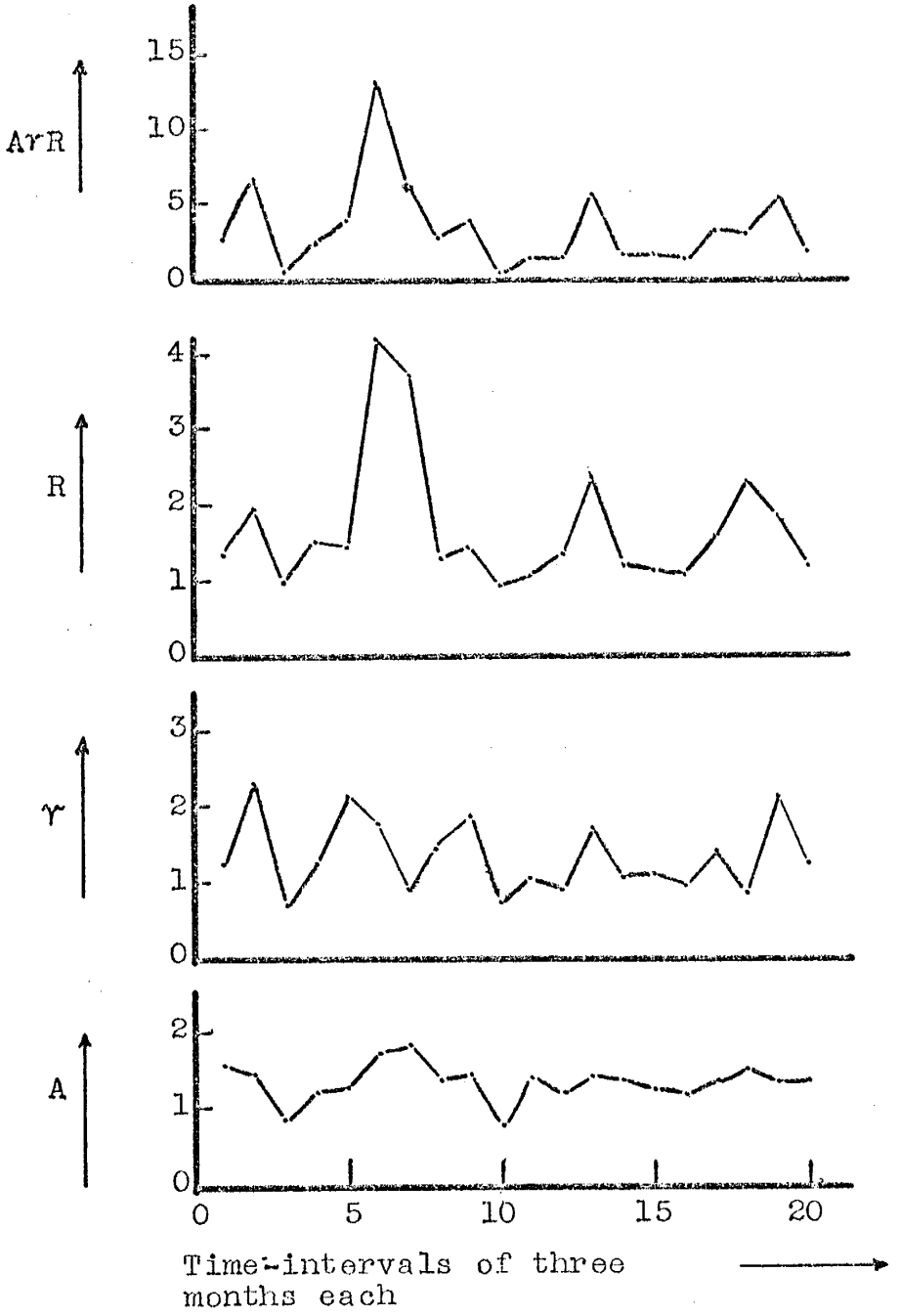

Figure 2.6. A, γ , R curves for three month intervals for DATA2.

Table 2.7. Values of A, γ, R for Successive Month Intervals for DATA3.

No.	Activity A	Slope γ	Grouping R	$\sigma_{\bar{N}}$	$\bar{N}$	AγR
1	1.48	1.13	0.77	1.33	3.00	1.28
2	1.23	0.96	1.15	1.49	1.70	1.35
3	1.66	0.93	1.93	4.14	4.60	2.98
4	2.01	1.18	2.02	6.44	10.20	4.79
5	1.88	0.80	2.00	5.48	7.50	3.01
6	1.23	0.68	1.49	1.95	1.70	1.24
7	1.60	0.63	1.70	3.40	4.00	1.71
8	1.58	1.92	1.30	2.53	3.80	3.94
9	1.73	2.70	1.55	3.60	5.40	7.23
10	1.58	1.92	1.28	2.49	3.80	3.87
11	1.78	2.79	1.40	3.43	6.00	6.94
12	1.67	0.32	1.55	3.37	4.70	0.83
13	1.77	0.32	1.73	4.20	5.90	0.97
14	1.52	0.57	2.80	5.08	3.30	2.41
15	1.45	0.90	1.35	2.25	2.80	1.75
16	1.30	0.58	1.63	2.31	2.00	1.22
17	1.61	0.71	2.50	5.07	4.10	2.87
18	1.99	0.66	1.43	4.45	9.70	1.87
19	1.76	0.77	1.59	3.82	5.80	2.14
20	1.56	0.88	1.22	2.32	3.60	1.67
21	1.54	0.85	1.24	2.32	3.50	1.62
22	1.66	0.89	1.71	3.66	4.60	2.52
23	1.74	2.42	2.53	5.93	5.50	10.65
24	1.36	2.13	1.08	1.64	2.30	3.12
25	1.67	1.46	2.39	5.19	4.70	5.85
26	1.62	2.68	2.71	5.55	4.20	11.80
27	1.54	0.51	1.80	3.37	3.50	1.42
28	1.23	0.99	2.34	3.06	1.70	2.84
29	1.26	0.80	2.04	2.74	1.80	2.05
30	1.58	0.82	1.53	2.97	3.80	1.97
31	1.30	1.73	2.11	2.98	2.00	4.74
32	1.58	1.22	2.11	4.10	3.80	4.04
33	1.62	2.52	1.69	3.46	4.20	6.89
34	1.82	1.83	3.63	9.32	6.60	12.06
35	1.58	0.50	2.01	3.91	3.80	1.58
36	1.71	0.74	2.18	4.93	5.10	2.77
37	1.57	1.04	1.15	2.21	3.70	1.87
38	1.67	1.29	0.82	1.77	4.70	1.75
39	2.00	0.57	3.43	10.89	10.10	3.90
40	1.70	0.78	1.10	2.45	5.00	1.45
41	1.23	1.59	1.54	2.00	1.70	3.01
42	1.34	2.07	1.58	2.35	2.20	4.40
43	0.90	0.60	1.03	0.92	0.80	0.55
44	1.54	1.94	1.82	3.41	3.50	5.46
45	1.63	0.69	1.70	3.53	4.30	1.91

Table 2.7 Cont'd.

No.	Activity A	Slope γ	Grouping R	$\sigma_{\bar{N}}$	$\bar{N}$	$A\gamma R$
6	1.70	0.70	3.41	7.63	5.00	4.05
7	1.53	1.13	1.81	3.34	3.40	3.12
8	1.71	0.69	2.19	4.95	5.10	2.58
9	1.28	1.20	1.51	2.08	1.90	2.30
0	1.23	0.89	1.81	2.36	1.70	1.97
1	1.40	0.35	1.61	2.55	2.50	0.78
2	1.32	0.66	1.24	1.79	2.10	1.07
3	1.28	1.51	2.06	2.85	1.90	3.97
4	1.45	0.87	1.89	3.16	2.80	2.38
5	1.70	1.36	1.98	4.42	5.00	4.58
6	1.23	0.75	1.31	1.70	1.70	1.19
7	1.18	0.70	0.96	1.18	1.50	0.79
8	1.60	2.00	1.05	2.11	4.00	3.37
9	1.52	0.83	1.68	3.06	3.30	2.13
0	1.49	2.11	2.06	3.63	3.10	6.50
1	1.49	2.31	1.57	2.77	3.10	5.41
2	1.64	2.15	1.51	3.17	4.40	5.32
3	1.64	1.79	1.95	4.09	4.40	5.74
4	1.41	1.81	1.38	2.22	2.60	3.52
5	1.28	1.99	0.80	1.10	1.90	2.03
6	1.20	1.67	0.67	0.84	1.60	1.34
7	1.08	2.11	1.71	1.87	1.20	3.89
8	1.41	1.64	1.18	1.90	2.60	2.72
9	1.45	2.08	1.64	2.74	2.80	4.94

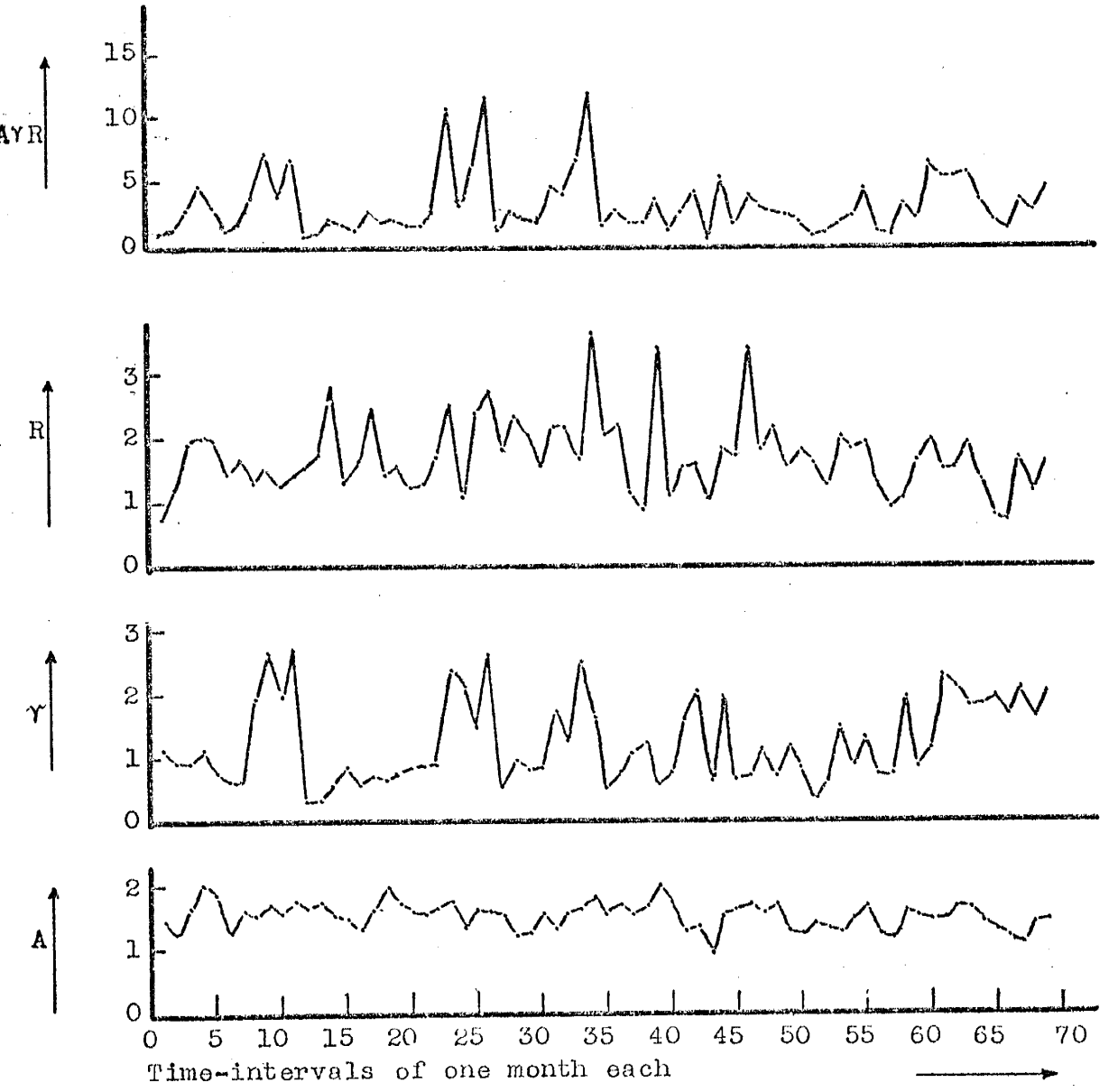

Figure 2.7. A, γ, R curves for one month intervals, for DATA3.

ole 2.8. Behavior of A, Y , R and AYR Curves at the Time of Occurrence of Shocks with Amplitudes Greater than 70 mm.; for DATA1.

nth .	Date	Time	Amp. in mm.	A	Y	R	AYR
	022663	14-30-12	80	M	H	L	M
	030263	14-52-27	70				
	042163	21-12-04	105	M	H	M	M-H
	051863	01-20-39	137	M-H	Mx	M	H
	052263	10-18-00	84				
	070363	12-08-04	210	M-H	M	M-H	M-H
	070363	12-12-08	147				
	081263	20-41-02	137	H	H	M-H	H
	081263	21-26-16	126				
	081463	01-45-42	105				
0	100263	09-02-00	105	L			
2	122063	06-37-00	84	H	H	M-L	M-H
4	020464	11-58-00	120	M	M-H	M-H	M
	020464	12-11-33	87				
9	062964	00-18-23	74	M	M-H	M-L	M-L
	062964	00-29-09	105				
1	090164	00-54-00	84	M-H	H	L	M-L
7	030965	06-06-07	80	M-H	L	M	L
	030965	12-04-52	144				
	031965	02-02-00	74				
8	041065	00-01-00	86	H	M-L	Mx	H
	041065	17-09-00	86				
	041065	18-11-41	74				
	041665	28-08-58	110				
9	042265	19-43-00	74	H	M-H	M-H	H
0	052265	17-09-12	80	M	M	M	M-L
6	121165	10-42-00	140	M	L	M-L	L
	121165	11-00-00	140				

Table 2.8 Cont'd.

onth o.	Date	Time	Amp. in mm.	A	γ	R	AγR
7	122165	20-33-32	144	M-H	M-H	M	M
9	031466	13-18-00	333	L			
1	042266	02-36-00	246	M	M-L	M-L	L
	050266	17-05-00	648				
2	052866	18-40-00	405	M-H	L	M	L
	060966	17-52-00	297				
	061066	22-14-00	297				
3	062666	11-29-00	270	M-L	M-L	L	L
	071166	09-40-00	99				
4	071666	15-56-00	108	M-H	M-L	M-L	L
	072166	00-55-00	94				
	072466	18-05-00	135				
	080266	01-11-00	94				
	080266	22-56-00	94				
	080466	22-14-00	108				
	081166	00-04-00	135				
	081466	05-29-00	81				
5	081566	07-31-00	243	M-H	L	M	L
	081566	07-42-00	243				
	081766	11-14-00	135				
	081766	21-20-00	75				
	082466	21-23-00	108				
	082566	00-13-00	99				
	082566	06-00-00	108				
	082666	12-56-00	81				
	082666	13-14-00	81				
	082866	00-06-00	81				
	082866	17-52-00	75				
	083066	22-05-00	81				
	090166	20-32-00	81				
	090266	01-52-00	85				
	090366	03-44-00	81				
	090666	07-34-00	270				
	090666	22-48-00	81				
6	092866	16-57-00	95	M	L	M	L
	100766	02-11-00	150				
	100766	02-17-00	95				
	100866	12-22-00	170				
	100966	03-30-00	172				
	100966	03-52-00	99				

Table 2.8 Cont'd.

Month No.	Date	Time	Amp. in mm.	A	γ	R	AγR
47	101966	14-26-00	153	L	L	M-L	L
	102466	05-14-00	85				
	110866	12-13-00	75				
49	121366	05-57-00	81	L	L	L	L
	122466	12-51-00	95				
54	051567	16-40-00	72	Mx	H	H	Mx

Notes: H = High
M = Medium
L = Low
Mx = Maximum

le 2.9. Behavior of A, γ, R and AγR Curves at the Time of ccurrence of Shocks with Amplitudes Greater than 70 mm.; for DATA2.

th	Date	Time	Amp. in mm.	A	γ	R	AγR
	010663	22-59-19	165	H	H	M	M-H
	031363	13-11-11	363	M	M	M-L	L
	031363	22-54-03	132				
	031463	13-46-54	132				
	042563	20-34-39	132	M-H	M-H	M-H	M-H
	052263	16-45-00	116	M	M-H	M	M-L
	052263	17-57-00	99				
	060663	01-04-00	132	M	M-H	M-H	M
	060663	03-22-00	121				
	100763	01-32-51	264	M-L	M	M-H	M-L
	100763	03-08-46	132				
	102463	13-12-37	94				
	112463	07-37-20	209	M-L	M-H	M-L	M-L
	033064	17-18-00	99	H	H	H	Mx
	041764	07-42-00	121				
	051264	14-40-00	110	M	M	M-L	M-L
	060764	18-56-00	121	M-L	M	M-L	L
	082464	19-47-16	165	Mx	M-L	Mx	H
	083164	20-54-00	110				
	091464	20-28-00	121				
	091464	20-55-55	594				
	091564	01-16-00	110				
	091564	13-02-00	80				
	091564	16-02-00	121				
	091664	10-23-26	132				
	091664	11-06-00	121				
	091664	11-10-00	121				
	091664	11-17-35	440				
	091664	11-19-00	121				
	091664	15-18-00	88				
	091864	21-00-00	132				
	092064	03-03-00	121				

Table 2.9 Cont'd.

Month No.	Date	Time	Amp. in mm.	A	γ	R	AγR
22	100164	19-11-00	198	M-H	H	M-L	M
27	030265	19-54-00	125	M-H	M-H	M-L	M
31	070165	00-18-00	132	M	L	M-L	L
32	073165	00-42-45	198	M	M	M-L	M-L
34	100265	01-35-00	132	M	M	M	M-L
35	110165	17-28-00	154	M	M-L	M-L	L
37	010966	18-53-00	99	M-H	Mx	H	H
41	041766	21-31-00	121	M	M	M	M-L
	051266	16-31-00	121				
42	051766	15-14-00	143	M	L	M	L
44	072266	20-00-00	146	M	M	M-L	M-L
	081166	04-59-00	115				
45	081566	06-54-00	154	L			
49	121766	22-25-00	115	L	M-H	M	M-L
50	013067	16-07-00	121	M	M-H	M	M-L
	013067	20-07-00	198				
52	031467	20-32-00	115	M-H	M-H	M-H	M
53	041267	00-34-49	231	M-H	L	H	M-L
	041267	00-40-00	115				
	050367	19-32-00	99				
	050367	19-35-00	180				
57	081967	00-44-09	253	M	M-H	H	M-H
58	092267	07-24-00	132	L	L	L	L
60	111967	08-06-56	165	M	M-H	M	M-L
	111967	08-46-56	88				

Notes: H = High
M = Medium
L = Low
Mx = Maximum

DISCUSSION OF RESULTS

General Behavior of A, γ , R

Though the range of the value of A depends upon the engths of the interval of time and the data type, A in the resent analysis never goes beyond 2.01 or 103 shocks which appens for DATA3 and for the interval's length of one month. he value of A fluctuates between 0 and a maximum for each et of computations in Tables (2.1) to (2.7).

The value of γ lies between 0 and 2.79 and oscillates n this range for different data sets and different time- ntervals. The effect of the length of the interval on γ ill be discussed in the next section. The value of γ indi- ates the behavior of the stress release for a particular nterval of time and this behavior is not stationary as videnced by the variation in γ over different intervals of ime.

The value of R, most of the time, is larger than 1, in- icating a grouping of shocks more than expected from a ran- om set of observations. The value of R changes from one nterval of time to another.

Similarities between A, γ , R Curves of Figure (2.1)

It was seen that the interpretations derived for DATA1 re also valid for DATA2. Hence the curves of DATA1 only are iscussed and the discussion of DATA2 is omitted from the ollowing.

(1) A and γ-curves have similar character for some periods of time, for example, near point #5, 6, 16 and 54. However, periods of time near points like #28, 43 and 45 do not show this similarity.

(2) A and R curves show a greater degree of similarity than A and γ-curves. The points #15,21 are some of the exceptions.

(3) γ and R-curves compare less favorably than others.

(4) The A·γ·R curve accentuates the strong similarities between A, γ, R curves and suppresses the peaks which are not consistent in all three curves. There is no consistent similarity between A, γ, R and A·γ·R curves.

The Relation of A, γ, R Curves and the Occurrence of Big Events in Figure (2.1)

(1) The monthly intervals, represented by the points #4 and 10 contain big events (amp. - 105 mm.), but the value of A is medium at the 4^{th} and very low at the 10^{th} point (not plotted since A is less than 0.69). Hence big events are not necessarily accompanied by a large value of A (see Table 2.8 for details).

(2) The point #54 contains only 1 sizable event (amp. - 72 mm.). However, the largest values of A and A·γ·R curves occur during this month. Large values of A, therefore, sometimes occur in the absence of large events.

(3) The point #36 has 2 big events (amp. - 140, 140 mm.) on the same day and has a medium A, low γ and medium R.

(4) The point #44 has 4 big events and has a low-medium , low-medium γ and medium-high A.

(5) The point #45 has 6 big events and still has a edium-high A, low γ and medium R.

(6) The 46th point has 3 big events and has a medium A, ow γ , and medium R.

(7) The 43rd point has 2 big events (amp. - 270, 99 mm.) nd has a low A, high γ and low R.

(8) The point #28 has 1 big event (amp. - 110 mm.) and as a high A, medium-low γ and maximum R.

(9) Peaks and troughs of A.γ.R-curves also do not show ny consistent correlation with the big events.

Hence, high (or low) values of A, γ , R or A.γ.R have no consistent correlation with the occurrences of big events.

Discussion of Figures (2.2) and (2.3) of DATA1

Both the figures show no consistent similarity between A, γ and R curves. However, as before, there is relatively more similarity between A and R curves than that between other curves, but no consistent correlation between a big event (or events) and the peak (or trough) of these curves.

Discussion of Figure (2.7) of DATA3

There is much less similarity between the curves for DATA3 than that between the curves of DATA1 and DATA2. This is most probably due to the fact that DATA3 contains earthquakes from many different focal regions whose mechanisms

fer considerably in their behavior. As the values of the litudes of the stronger events are not known for DATA3, statement concerning the correlation between the peaks the big event can not be made on the basis of Figure (2.7).

CONCLUSIONS

On the basis of Tables (2.8) and (2.9) and Figures (2.1) - 7), the following conclusions can be drawn for microearthkes in the Socorro region:

(1) A lack of similarity between A and γ curves indites that the number of microearthquakes in an interval of me does not have any consistent relation with the slope of e frequency-law.

(2) A good degree of in-phase similarity between A and curves means that whenever there is a large number of rthquakes, they tend to occur in swarms. The term 'swarm' the case of microearthquakes can be taken to mean a groupg of events within a short period, e.g., 3 days to 6 days.

(3) There is no consistent correlation between γ and R rves. We recall here that a large value of R means a ouping of events, a large value of γ means that most of e energy is released in numerous small shocks and a small lue of γ means that most of the energy is released in many rge shocks. A lack of correlation shows, then, that large icroearthquakes (small γ) are as likely to come in swarms arge R) as the small ones (large γ).

(4) A large microearthquake (or a group of them) is not necessarily associated with a large value of A. In other words, a large event may occur without any foreshocks or aftershocks.

(5) A large number of microearthquakes also does not guarantee the occurrence of a large event (or events) with them.

(6) The grouping of events also is not found to have any bearing on the occurrence of large microearthquakes.

(7) The computation of the $A \cdot \gamma \cdot R$ curve was to check whether there is any correlation between the increase (or decrease) of the $A \cdot \gamma \cdot R$ value and a large event. Figures (2.1) - (2.7) show that there is no such correlation.

(8) The correlation between a large event and a combination of high A, high R and low γ (given the number of shocks in an interval, $\gamma_1 > \gamma_2$ if γ_1 is the value when the number of shocks of strengths less than some arbitrary medium value E_m is N_1 and γ_2 is the value when this number is N_2, N_1 being greater than N_2) is not consistent either. That is, a large number of relatively large events with a high degree of grouping also does not always mean a high probability of the occurrence of a big event.

SECTION III

TIME-AVERAGES OF THE NUMBER OF EARTHQUAKES AND THEIR ENERGIES

Time-averages of the number and energies of earthquakes have been studied. The time-averages were computed in two ways. The first kind of average was taken over unit intervals into which the period of the data set is broken. The second kind of average was taken by averaging over T_1, T_2,- - -, T_n, where $T_i > T_{i-1}$ and $T_2 - T_1 = T_3 - T_2$ - - -, etc., and T_n covers the whole range of the data period.

AVERAGES OF NUMBER OF SHOCKS IN SUCCESSIVE EQUAL INTERVALS OF TIME

Procedure

Consider the earthquake sequence to be a random process in time. The number of earthquakes in a unit time is termed to be the intensity function $\nu(t)$ of the process where t refers to the position of the unit time interval in the time-domain. In order to be able to speak about the process, let us assume that almost all the sample functions of the process are equivalent functions of time. There is only one sample function known to us. Then, at the time t, the intensity function of the process,

$\nu(t)$ = the number of shocks in the unit time-interval centered at t of the earthquake sequence. (3.1)

The unit interval of time is 15 days long in the present nalysis. For the sake of simplicity, we compute, then, the umber of earthquakes per day for the particular interval and his value represents $\nu(t)$ in the results.

Results

Table (3.1) lists the results for a period of 1740 days, eginning July 1, 1963. The data used was DATA3. The data as divided into 3 amplitude categories of 5 - 15 mm., 15 - 30 mm., and 30 - 40 mm.. The fact that an (S-P) interval as large as 2.5 seconds contains events from more than one focal zone that are likely to have different seismic parameters, and that the detection and the amplitude of an event decays with the distance does not influence the value $\nu(t)$ for the simple reason that the above factors do not change with time. The kind of dependence that $\nu(t)$ had on the aforesaid factors at the time $t = t_1$ also holds for $t = t_2$ for t_1, t_2 belonging to T where T is the total period of the data set.

Conclusions

(1) From the curves in Figure (3.1), we see that, most of the times, whenever there is a rise for the 15 - 30 mm.

lass, there is a rise for the 5 - 15 mm. and 30 - 40 mm. lasses, also. This means that earthquakes are likely to ccur in all amplitude classes. However, the increase (or ecrease) may not be equal in all ranges and that is why the lope changes with time in the frequency-law analysis, as was hown in SECTION II.

(2) The microearthquake sequence has a time-varying ean and a time-varying mean-square value. Hence the earth-uake sequence is a non-stationary process.

(3) The results show that the larger the value of the ean of a $\nu(t)$-curve, the larger is the mean-square error.

(4) The over-all average values of the curves are 0.55, .47 and 1.5 for the 15 - 30 mm., 30 - 40 mm. and 5 - 15 mm. anges, respectively. This means, for the data analyzed, that there are about 75 shocks a month in the 5 - 40 mm. range of the amplitude.

ble 3.1. Mean Number of Microearthquakes per Day for 15 Days Successive Intervals, for DATA3.

.	5 - 15 mm.	15 - 30 mm.	30 - 40 mm.
	3.40	0.67	0.07
	0.67	0.73	0.20
	1.80	0.73	0.20
	0.40	0.33	0.27
	2.00	0.20	0.47
	2.27	0.67	0.73
	5.80	1.53	1.60
	2.40	0.80	1.53
	2.73	1.47	1.07
0	1.93	1.00	0.80
1	0.87	0.87	0.27
2	0.20	0.00	0.00
3	1.27	0.53	0.20
4	2.13	0.93	0.60
5	1.60	0.40	0.07
6	1.93	0.60	0.67
7	1.80	0.67	0.47
8	2.00	0.93	0.87
9	2.27	1.00	0.13
0	1.67	0.67	0.47
1	1.33	0.67	0.67
2	2.07	1.07	0.93
3	2.00	0.60	0.60
4	1.73	0.33	0.73
5	2.47	0.47	0.60
6	3.53	1.00	1.07
7	3.00	0.40	0.33
8	1.93	0.20	0.20
9	2.27	0.13	0.27
0	2.87	0.73	0.40
1	2.00	0.60	0.40
2	1.33	0.20	0.20
3	1.07	0.40	0.33
4	1.53	0.80	0.47
5	1.87	1.13	1.07
6	3.13	1.27	1.93
7	2.47	1.07	0.53
8	1.80	0.53	0.60
9	1.20	0.80	0.33
0	1.53	0.47	0.53
1	1.00	0.60	0.47
2	1.73	0.13	0.47
3	1.53	0.73	0.67
4	2.67	0.40	0.53
5	1.13	0.33	0.20

Table 3.1 Cont'd.

No.	5 - 15 mm.	15 - 30 mm.	30 - 40 mm.
46	2.33	0.53	1.93
47	1.80	0.27	0.40
48	1.47	0.33	0.27
49	2.27	1.00	0.20
50	1.53	0.27	0.33
51	1.20	0.20	0.53
52	2.13	0.87	0.40
53	0.60	0.47	0.13
54	1.33	0.80	0.60
55	0.67	0.00	0.80
56	0.73	0.13	0.07
57	0.40	0.07	0.07
58	0.93	0.20	0.27
59	1.67	0.53	0.13
60	2.60	0.73	0.40
61	1.47	0.60	0.40
62	0.87	0.27	0.07
63	1.20	0.47	0.67
64	0.53	0.33	0.60
65	0.93	0.67	0.60
66	1.53	0.53	0.47
67	3.60	1.00	1.27
68	1.53	0.00	0.20
69	2.47	0.87	0.07
70	2.27	0.33	0.47
71	1.07	0.33	0.20
72	2.33	1.40	1.33
73	1.20	0.40	0.27
74	0.87	0.47	0.53
75	1.20	0.73	0.27
76	0.07	0.87	0.87
77	0.87	0.47	1.20
78	3.67	1.47	1.40
79	3.07	0.40	0.67
80	1.67	0.67	0.33
81	1.80	0.33	0.33
82	0.73	0.00	0.00
83	1.87	0.40	0.40
84	0.20	0.20	0.20
85	0.53	0.13	0.00
86	0.53	0.13	0.00
87	0.60	0.53	0.20
88	0.93	0.47	0.73
89	0.80	0.47	0.67
90	0.13	0.47	0.73

Table 3.1 Cont'd.

No.	5 - 15 mm.	15 - 30 mm.	30 - 40 mm.
91	0.53	0.53	0.53
92	1.13	0.47	0.60
93	1.13	0.53	0.60
94	0.80	0.20	0.27
95	9.47	2.00	0.80
96	5.00	1.60	0.60
97	1.67	0.13	0.07
98	1.00	0.07	0.00
99	0.87	0.33	0.07
100	1.60	0.40	0.13
101	1.53	0.27	0.27
102	2.20	0.47	0.40
103	1.93	0.60	0.07
104	0.33	0.00	0.27
105	0.60	0.27	0.13
106	1.13	0.27	0.27
107	0.67	0.13	0.27
108	1.13	0.33	0.47
109	1.53	0.87	0.40
110	0.60	0.67	0.73
111	0.00	0.20	0.33
112	0.20	0.27	0.67
113	0.20	0.07	0.40
114	0.87	0.40	0.33
115	0.87	0.47	0.53
116	1.93	0.73	0.13

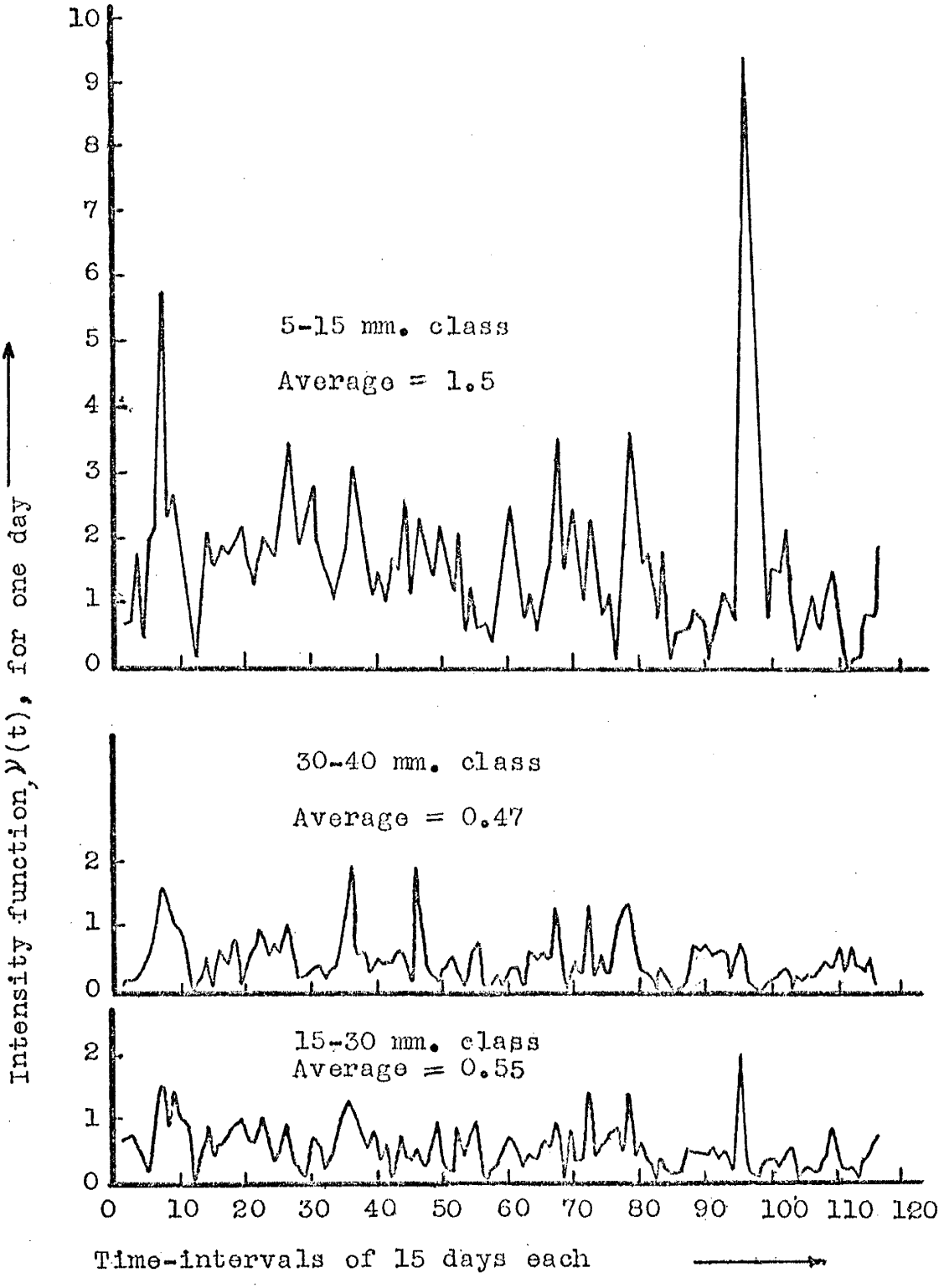

Figure 3.1. Mean number of earthquakes per day for 15 days successive intervals for DATA3.

NUMBER OF SHOCKS AVERAGED OVER SUCCESSIVELY INCREASING PERIODS

Results

Tables (3.2) and (3.3) give the results of the time-averages of the number of microearthquakes per 10 days for 6 amplitude ranges. The averaging period is increased in steps of about 60 days. Thus, the 30^{th} value represents an average over the whole 5 year period. Figures (3.2) and (3.3) show the graphs of the results listed in Tables (3.2) and (3.3) for DATA1 and DATA2, respectively.

Table (3.2) also lists the values of the percentage errors with respect to the means of the curves of the amplitude ranges $\geqslant 1$ mm., 30 - 40 mm., and $\geqslant$ 40 mm.. Similarly, the values of the percentage errors for the amplitude ranges 30 - 40 mm., and $\geqslant$ 40 mm. are given for DATA2 in Table (3.3). The graphs of these percentage errors are given in Figure (3.4).

Conclusions

(1) Consider the curves of Figures (3.2) and (3.3) after the 10^{th} interval. These curves show that the larger the value of the mean of a curve, the larger is the value of the square-error ψ_i^2, i.e., $\sum_{j=11}^{30} \left[y_i(j) - \text{mean } (1) \right]^2$, where ψ_i^2 is the square-error for the i^{th} curve.

(2) A visual inspection of the curves of Figures (3.2), (3.3) and the error-curves of Figure (3.4) shows that the

onvergence of the curves with a high mean value is no faster han the convergence of those with a relatively low mean alue. As explained in the APPENDIX, this is due to the fact hat curves with a high mean value have a large variance as ompared to the variance of those with a low mean value.

(3) We see that the percentage errors for DATA1, never o beyond 12.42 after the first 60 days. Therefore, the mean umber of shocks (≥ 1 mm.) can safely be estimated, within bout 10% error, by taking any interval of time more than 2 onths. However, the errors fluctuate erratically between 0 nd 12.42 up to the 15^{th} interval and afterwards the range f fluctuations becomes narrow.

(4) For DATA1, there are about 11 microearthquakes per onth with an amplitude greater than 10 mm. There are about shocks with an amplitude greater than 40 mm.

For DATA2, there are about 3 shocks with amplitudes greater than 40 mm. and about 9 with amplitudes greater than 10 mm. per month.

Table 3.2. Mean Number of Earthquakes over Successively Increasing Periods, for DATA1.

No.	1-10 mm.	10-20 mm.	20-30 mm.	30-40 mm.	⩾40 mm.	⩾1 mm.	% error ⩾ 1 mm.	% error 30-40 mm.	% error ⩾ 40 mm.
1	0.34	1.89	1.03	0.69	1.55	5.50			
2	0.34	1.02	0.59	0.68	1.62	4.25			
3	0.34	0.79	0.68	0.62	1.87	4.30			
4	0.85	1.14	0.85	0.68	1.82	5.34	12.42		
5	0.73	1.03	0.73	0.58	1.69	4.76			
6	0.67	1.20	0.67	0.55	1.42	4.51		5.70	5.20
7	0.62	1.22	0.69	0.49	1.44	4.46		5.70	6.60
8	0.64	1.14	0.75	0.52	1.27	4.32		0.00	5.90
9	1.01	1.23	0.75	0.48	1.27	4.74		7.70	5.90
10	1.03	1.21	0.78	0.51	1.26	4.79		2.00	6.60
11	1.12	1.25	0.76	0.56	1.27	4.96		7.70	5.90
12	1.17	1.24	0.73	0.54	1.24	4.92		3.80	6.10
13	1.17	1.16	0.69	0.54	1.20	4.76		3.80	11.10
14	1.15	1.20	0.70	0.59	1.48	5.12		13.40	9.60
15	1.15	1.28	0.73	0.57	1.53	5.26	10.70	9.60	13.30
16	1.13	1.21	0.69	0.54	1.42	4.99	5.00	3.80	5.20
17	1.09	1.17	0.67	0.54	1.35	4.82	1.40	3.80	0.00
18	1.02	1.14	0.65	0.51	1.29	4.61	2.90	2.00	4.40
19	1.00	1.11	0.65	0.51	1.29	4.56	4.00	2.00	4.40
20	1.03	1.14	0.67	0.51	1.24	4.59	3.30	2.00	8.10
21	1.01	1.17	0.68	0.52	1.22	4.60	3.10	0.00	9.60
22	0.97	1.15	0.67	0.54	1.28	4.61	2.90	3.80	5.10
23	0.95	1.14	0.69	0.53	1.40	4.71	0.80	2.00	3.70
24	0.94	1.11	0.68	0.52	1.40	4.65	2.10	0.00	3.79
25	0.89	1.05	0.66	0.50	1.34	4.44	6.50	3.80	0.70

Table 3.2 Cont'd.

No.	1-10 mm.	10-20 mm.	20-30 mm.	30-40 mm.	⩾40 mm.	⩾1 mm.	% error ⩾1 mm.	% error 30-40 mm.	% error ⩾40 mm.
26	0.90	1.04	0.66	0.49	1.33	4.42	6.90	5.70	1.50
27	1.12	1.17	0.69	0.54	1.43	4.95	4.20	3.80	5.90
28	1.09	1.17	0.71	0.54	1.41	4.92	3.50	3.80	4.40
29	1.05	1.13	0.68	0.52	1.36	4.74	0.20	0.00	0.70
30	1.05	1.10	0.66	0.51	1.33	4.65	2.10	2.00	1.50

Notes: Mean for error calculation is taken 4.75 for ⩾1 mm. class.

Mean for error calculation is taken 0.52 for 30-40 mm. class.

Mean for error calculation is taken 1.35 for ⩾40 mm. class.

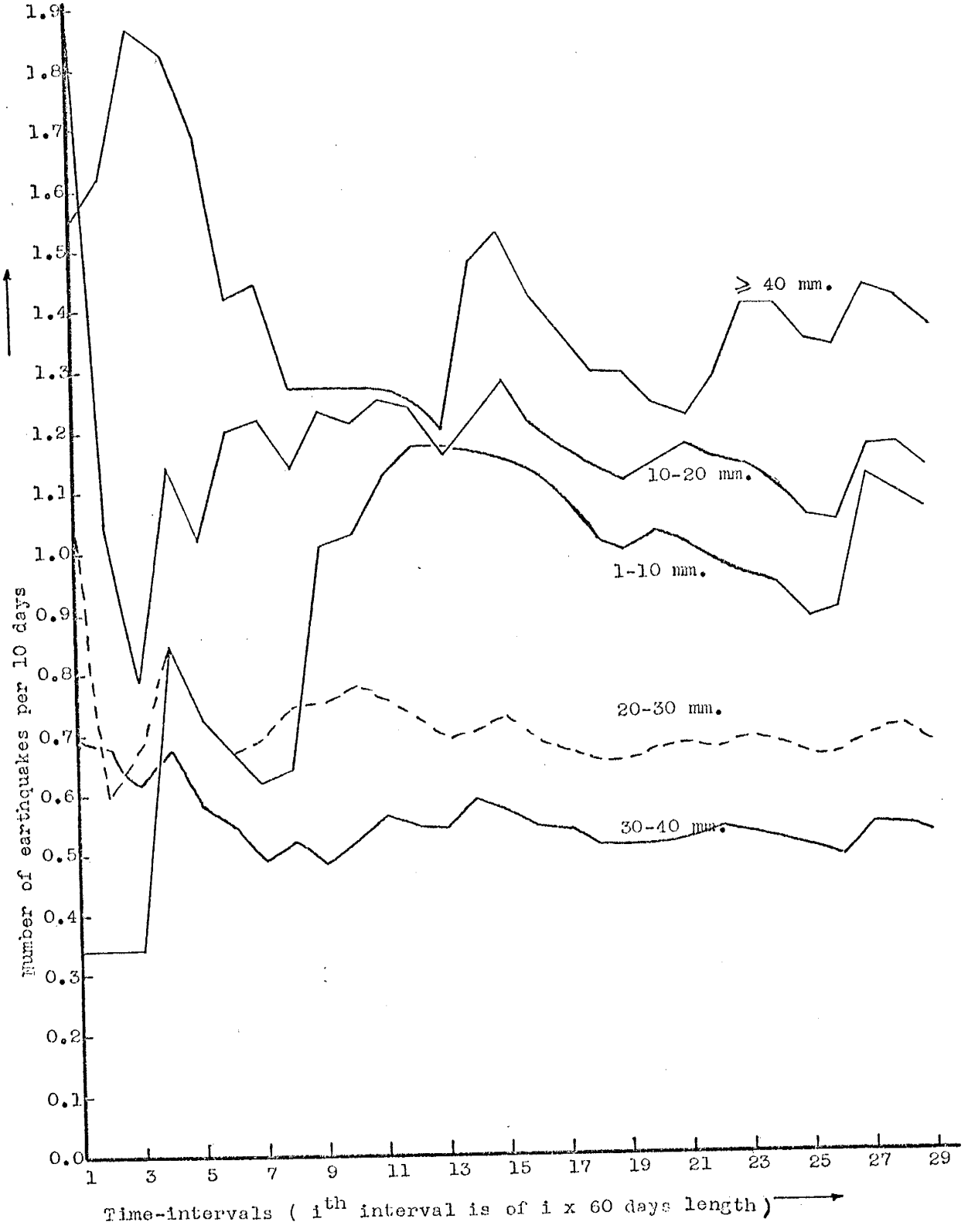

Figure 3.2. Mean number of earthquakes per 10 days over successively increasing periods, for DATA1.

Table 3.3. Mean Number of Earthquakes over Successively Increasing Periods, for DATA2.

No.	1-10 mm.	10-20 mm.	20-30 mm.	30-40 mm.	⩾40 mm.	⩾1 mm.	% error ⩾1 mm.	% error 30-40 mm.	% error ⩾40 mm.
1	0.96	1.92	1.73	0.38	1.53	6.52			
2	0.69	1.74	0.95	0.34	1.56	5.28			
3	0.62	1.37	0.68	0.51	1.42	4.60			
4	0.51	1.13	0.61	0.51	1.18	3.94			
5	0.44	0.91	0.47	0.40	1.04	3.26			
6	0.36	0.86	0.41	0.39	1.00	3.02		2.50	5.20
7	0.33	0.79	0.45	0.36	1.01	2.94		10.00	6.30
8	0.40	1.03	0.61	0.46	1.14	3.64		15.00	20.00
9	0.48	1.01	0.63	0.43	1.08	3.63		7.50	13.70
10	0.47	0.98	0.67	0.40	0.98	3.50		0.00	3.10
11	0.74	1.24	0.86	0.41	1.31	4.56		2.50	35.80
12	0.77	1.17	0.84	0.40	1.24	4.42		0.00	30.50
13	0.75	1.11	0.83	0.41	1.18	4.28		2.50	24.20
14	0.71	1.06	0.77	0.44	1.20	4.18		10.00	26.30
15	0.69	1.02	0.75	0.42	1.17	4.05		5.00	23.10
16	0.68	1.03	0.72	0.39	1.11	3.93		2.50	16.80
17	0.66	1.07	0.71	0.41	1.07	3.92		2.50	12.60
18	0.65	1.06	0.70	0.41	1.03	3.85		2.50	8.40
19	0.61	1.02	0.68	0.44	1.02	3.77		10.00	7.30
20	0.61	1.02	0.66	0.43	0.98	3.77		7.50	3.10
21	0.62	1.03	0.66	0.42	0.98	3.71		5.00	3.10
22	0.66	1.03	0.64	0.41	0.97	3.71		2.50	2.10
23	0.65	1.00	0.61	0.40	0.95	3.61		0.00	0.00
24	0.63	1.00	0.64	0.39	0.92	3.52		2.50	3.10
25	0.61	0.98	0.61	0.39	0.95	3.58		2.50	0.00

Table 3.3 Contd.

No.	1-10 mm.	10-20 mm.	20-30 mm.	30-40 mm.	≥40 mm.	≥1 mm.	% error ≥ 1 mm.	% error 30-40 mm.	% error ≥40 mm.
26	0.60	1.02	0.60	0.38	0.94	3.54		5.00	1.00
27	0.62	1.03	0.60	0.38	0.95	3.58		5.00	0.00
28	0.61	1.02	0.59	0.38	0.94	3.54		5.00	1.00
29	0.60	1.02	0.57	0.40	0.93	3.52		0.00	2.10
30	0.60	1.02	0.56	0.39	0.93	3.50		2.50	2.10

Notes: Mean for error calculation is taken 0.4 for 30-40 mm. class.

Mean for error calculation is taken 0.95 for ≥ 40 mm. class.

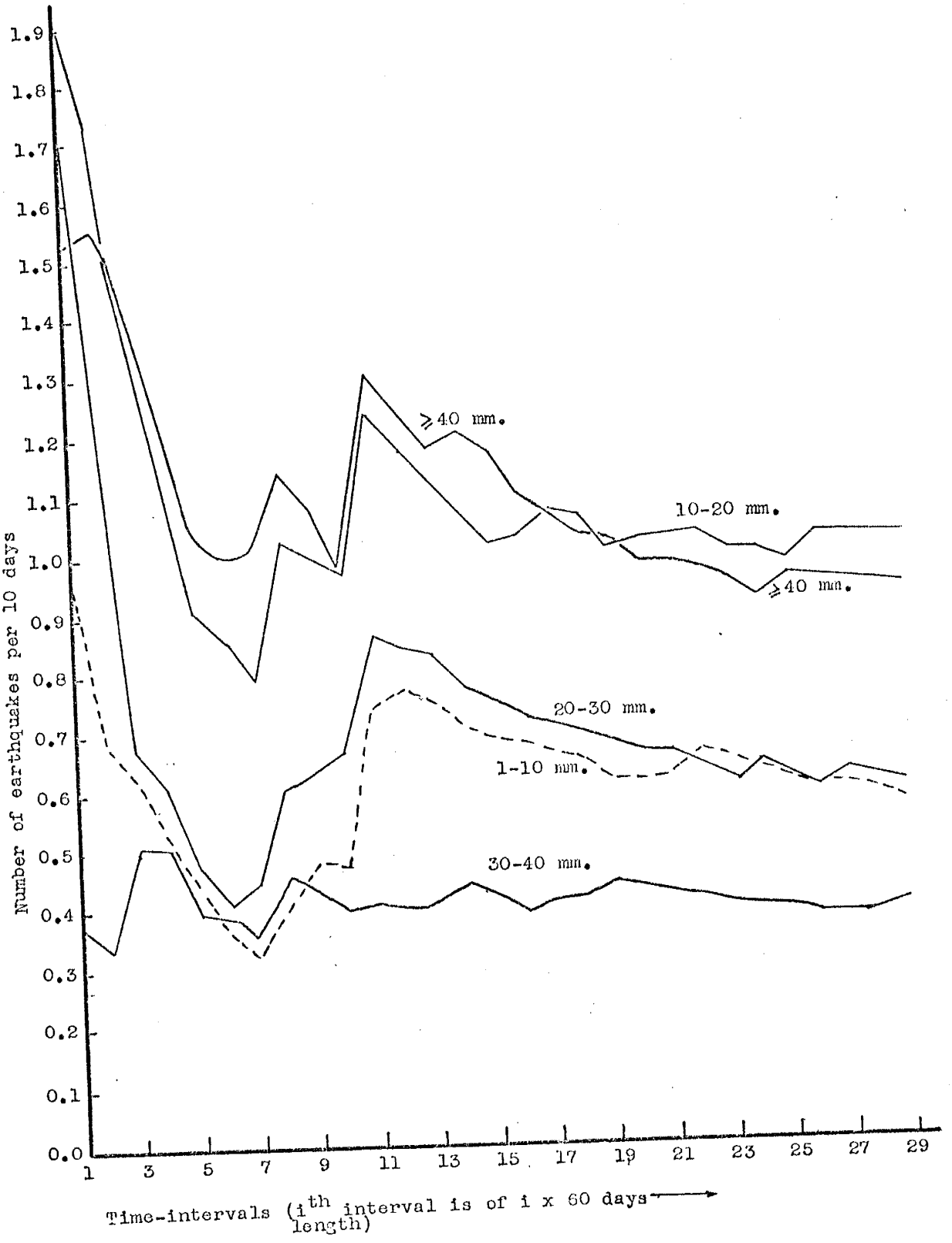

Figure 3.3. Mean number of earthquakes per 10 days over successively increasing periods, for DATA2.

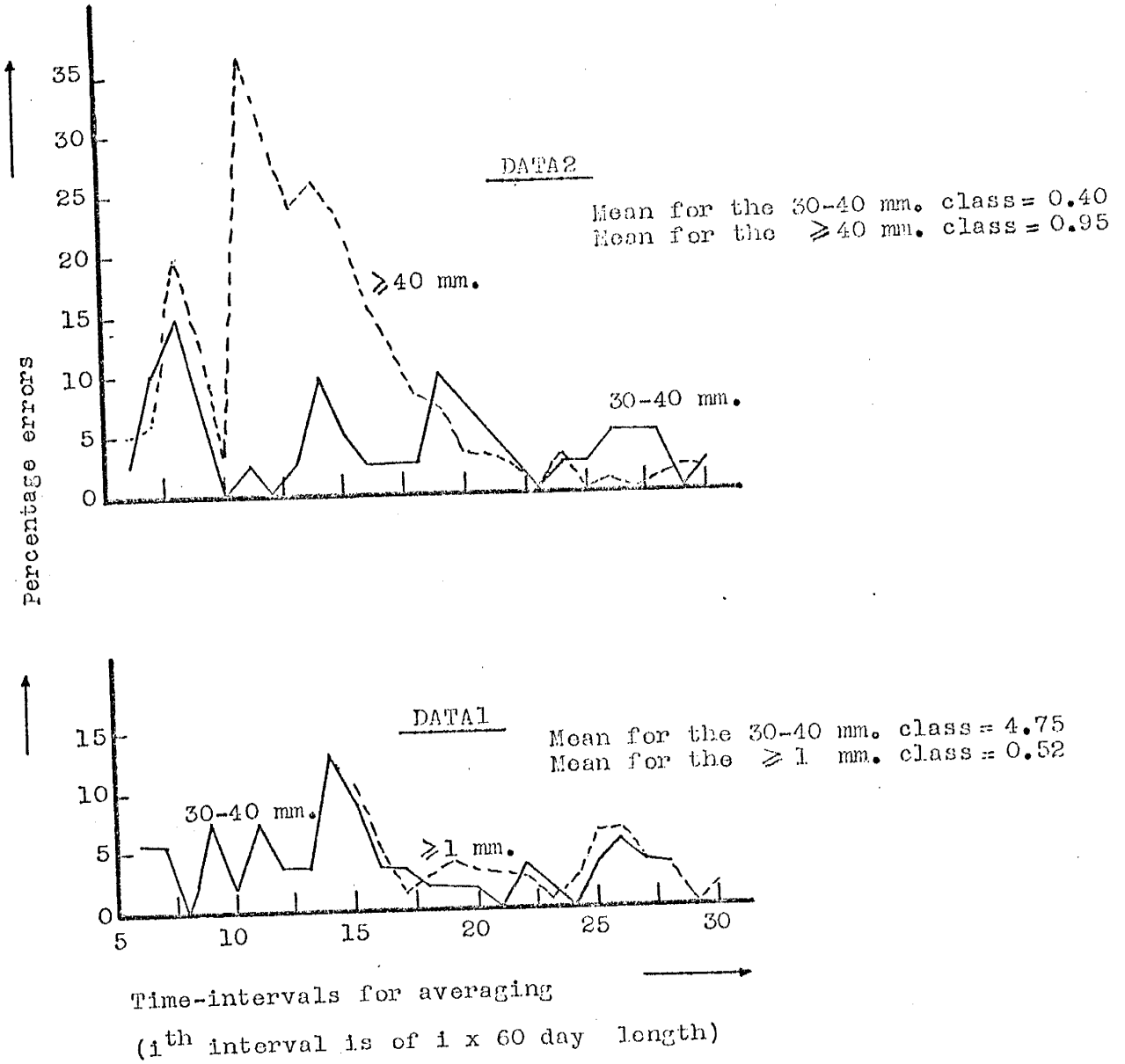

Figure 3.4. Percentage error curves.

ESTIMATION OF ENERGIES

The kinetic energy per unit volume of the seismic waves an be given as (Gutenberg and Richter, 1942)

$$E_{K.E.} = 4\pi^3 \cdot h^2 \cdot (v \cdot t_0) \cdot \rho \cdot \left(\frac{A_0}{T_0}\right)^2 \quad ,$$

here,

h = focal depth

v = wave velocity

t_0 = duration of maximum wave group on the seismogram

ρ = density = mass/volume of the propagating medium

A_0 = amplitude (ground displacement)

T_0 = period of vibration.

f the recording station is not right above the focus, the ypocentral distance D should be substituted for the quantity . Then

$$E_{K.E.} = 4\pi^3 \cdot \left[1.37 \cdot SP \cdot V_p\right]^2 \cdot v t_0 \cdot \rho \cdot \left(\frac{A_0}{T_0}\right)^2 \quad ,$$

here SP is the (S-P) interval and V_p is the compressional peed of the wave.

Assume that (1) the kinetic energy of the S-phase being used in our case) and the P-phase are equal, (2) total inetic energy equals the total potential energy, and (3) he energy in the vertical component (being recorded in our case) is qual to the energy in the North-South component and also he East-West component. Then the total energy from the ocus (ignoring the absorption of the medium) is

$$E = 48\pi^3 \cdot \rho \cdot (1.37 \cdot SP \cdot V_p)^2 \cdot vto \cdot \left(\frac{A_0}{T_0}\right)^2.$$

A_0 is peak-to-peak amplitude, then

$$E = \left(\frac{12\pi^3 \cdot \rho \cdot vto}{T_0^2}\right) (1.37 \cdot SP \cdot V_p)^2 \ (A_0^2)$$

the present study,

ρ = 2.5 gms./cm.^{3}

V = 3.5 x 10^5 cm./sec.

V_p = 6 x 10^5 cm./sec.

to = 0.5 sec. (about 5 oscillations) on the seismogram

T_0 = 0.1 sec.

en,

$$E = \frac{96\pi^3 \cdot 2.5 \cdot (3.5 \times 10^5) \cdot 0.5 \cdot (8.2)^2 \cdot 10^{10} (SP)^2 \ (\frac{1}{8} A_0^2)}{0.01}.$$

A_0 is in millimeters then,

$$E = 96\pi^3 \cdot 2.5 \cdot (3.5 \times 10^5) \cdot (0.5) \cdot (8.2)^2 \cdot 100 \cdot 10^{10} \cdot (SP)^2 \cdot \frac{1}{(1.5 \times 10^6)^2} \cdot \frac{1}{100} \cdot \left(\frac{1}{8} A_0^2\right),$$

ere (1.5 x 10^6) is the magnification of the instrument at

cycles per second.

$$E = \frac{96\pi^3 (2.5)(3.5) \cdot (SP)^2 \cdot (8.2)^2 \cdot (10^3)}{4.5} \left(\frac{1}{8} A_0^2\right)$$

$$E = 96\pi^3 \cdot (1.75) \cdot (73.8) \cdot (10^3) \cdot (SP)^2 \cdot \left(\frac{1}{8} A_0^2\right).$$

t $\quad C = 96\pi^3 \cdot (1.75) \cdot (73.8) \cdot (10^3) \cdot (SP)^2$

For SP = 1.8 seconds,

$$\log c = \log 96 + 3 \log\pi + \log 1.75 + \log 73.8 + 3 + 2 \log 1.8$$

$$\log c = 1.9823 + 3(0.4969) + 0.2430 + 1.8681 + 2(0.2553) + 3 = 9.0947$$

$$c = 12.44 \times 10^8 \ .$$

Similarly for SP = 0.9 seconds,

$$c = 6.22 \times 10^8 \ .$$

Therefore, for two (S-P) intervals,

$$E_{1.8} = (12.44 \times 10^8) \cdot (\tfrac{1}{8} A_0^2) \text{ ergs, and}$$

$$E_{0.9} = (6.22 \times 10^8) \cdot (\tfrac{1}{8} A_0^2) \text{ ergs,}$$

where A_0 is the peak-to-peak S-phase amplitude in millimeters on the seismogram.

In this section, the value of the energy is represented by the numerical value of $(\frac{1}{8} A_0^2)$ for an earthquake. To determine the energy of an earthquake in ergs, the value of $(\frac{1}{8} A_0^2)$ should be multiplied by the appropriate constant given above.

NUMBER AND ENERGY OF EARTHQUAKES FOR A UNIT TIME-INTERVAL

Results

The purpose of this analysis is to check whether there s any correlation between the number of shocks in a unit ime-interval and the seismic energy released during that articular interval. The length of the time-interval is 15 ays.

Tables (3.4), (3.5) and Figures (3.5), (3.6) list re- ults for the data DATA1 and DATA2, respectively.

Conclusions

The analysis indicates that a large number of micro- arthquakes generally means a large energy release. However, or the converse, it appears that large energy can frequently ccur when there is only a few shocks. The latter point is llustrated by points #52, 76, 80, 82 of Figure (3.5) and 3, 51 of Figure (3.6). The point #40 of Figure (3.6) has a aximum of both energy and number of shocks. There is no uch similar situation for DATA1.

It can, therefore, be concluded that the energy release rocess can be anywhere between (a) all the energy in very ew large shocks and (b) all the energy in many shocks of elatively small strength.

ble 3.4. Energy and Number of Shocks for 15 Day Intervals, for DATA1.

.	E	No. of E.Qs.	No.	E	No. of E.Qs.	No.	E	No. of E.Qs.
	172	1	39	1348	8	77	603	9
	1554	11	40	283	3	78	362	9
	370	2	41	480	4	79	6142	6
	298	2	42	375	3	80	41571	3
	1341	7	43	599	6	81	16509	8
	1763	4	44	0	0	82	17479	3
	642	7	45	293	4	83	7625	3
	2292	12	46	0	0	84	1004	3
	216	2	47	45	0	85	4961	14
0	300	3	48	0	0	86	4947	5
1	3450	13	49	0	1	87	21538	19
2	78	1	50	3055	13	88	11680	7
3	2378	17	51	72	1	89	1156	2
4	24	0	52	28435	19	90	9920	9
5	0	1	53	428	5	91	2605	3
6	0	0	54	16635	5	92	685	2
7	1218	2	55	3270	16	93	0	0
8	0	0	56	2088	6	94	0	0
9	0	0	57	830	6	95	1948	2
0	0	0	58	55	1	96	868	3
1	516	12	59	102	1	97	148	3
2	1485	12	60	0	0	98	221	1
3	0	0	61	0	0	99	177	6
4	116	3	62	36	1	100	18	0
5	2962	11	63	323	4	101	773	5
6	0	0	64	36	1	102	489	2
7	306	3	65	32	1	103	2781	17
8	707	11	66	0	1	104	0	0
9	152	3	67	15	1	105	4297	33
0	312	0	68	0	0	106	1662	13
1	49	3	69	0	0	107	656	6
2	868	8	70	5759	9	108	306	6
3	396	6	71	7101	13	109	365	2
4	436	2	72	32	1	110	0	0
5	1719	9	73	136	1	111	136	2
6	45	2	74	648	1	112	0	0
7	580	4	75	0	0	113	144	1
8	1434	8	76	22176	2	114	0	0

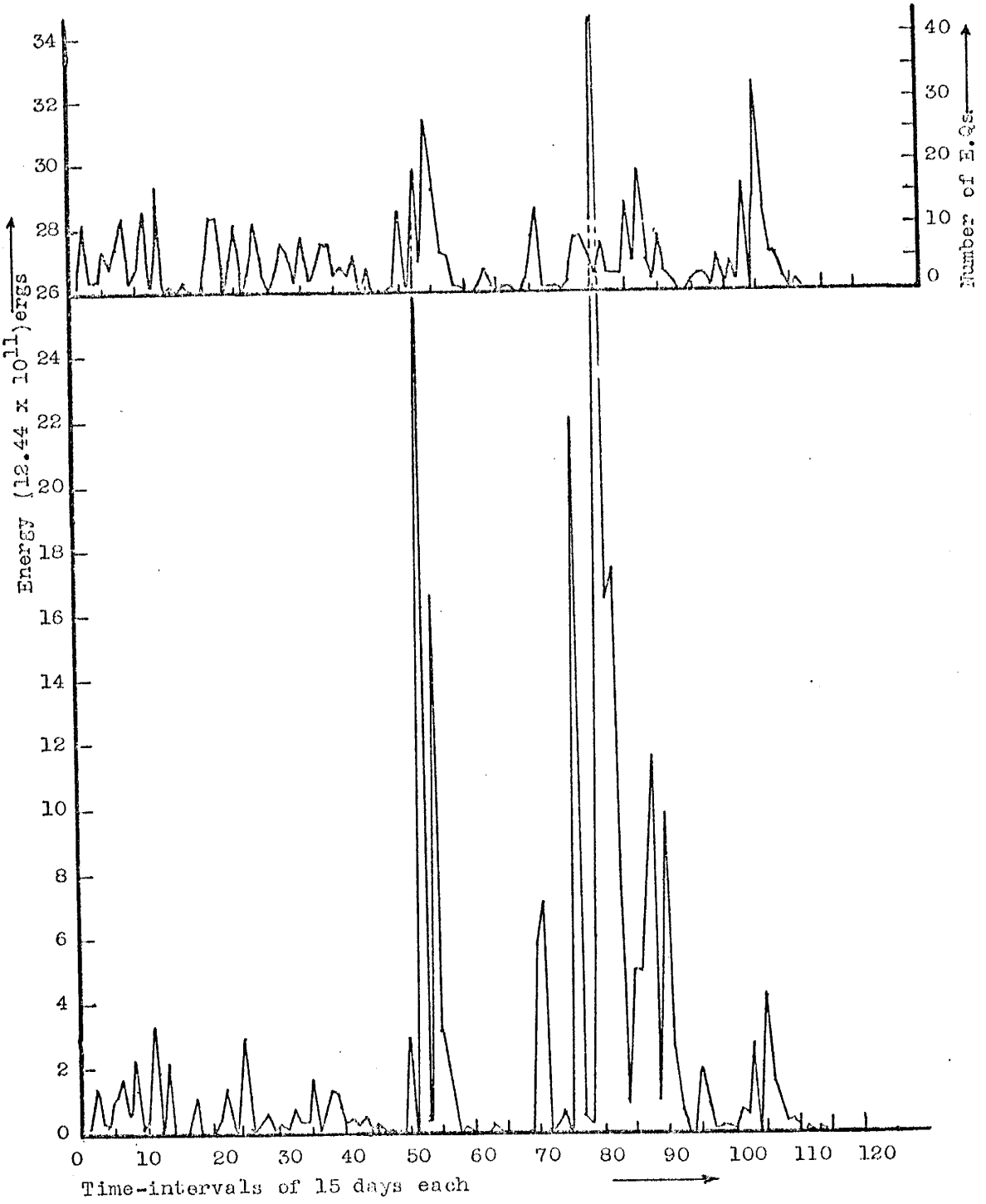

Figure 3.5. Energy and number of shocks for 15 day intervals, for DATA1.

Table 3.5. Energy and Number of Shocks for 15 Day Intervals, for DATA2.

No.	E	No. of E.Qs.	No.	E	No. of E. Qs.	No.	E	No. of E.Qs.
1	1022	5	39	7544	9	77	85	1
2	0	1	40	31979	42	78	264	2
3	13705	7	41	2310	6	79	1389	3
4	622	3	42	246	5	80	1559	5
5	328	3	43	123	2	81	1276	2
6	1203	4	44	12	1	82	71	4
7	91	2	45	288	2	83	184	2
8	933	5	46	1151	4	84	112	1
9	1195	8	47	15	2	85	1382	5
10	395	2	48	32	1	86	1106	4
11	60	1	49	434	7	87	1754	3
12	120	1	50	761	5	88	78	1
13	112	1	51	23693	10	89	0	0
14	0	0	52	212	3	90	15	2
15	21	1	53	136	1	91	141	3
16	221	2	54	450	1	92	191	3
17	5035	5	55	512	2	93	280	4
18	480	2	56	512	1	94	74	3
19	428	3	57	36	1	95	2286	5
20	1927	4	58	0	0	96	0	0
21	186	2	59	818	2	97	520	2
22	323	2	60	71	2	98	6932	9
23	162	2	61	2932	5	99	460	4
24	197	3	62	176	3	100	276	1
25	989	7	63	138	3	101	1725	11
26	224	2	64	370	8	102	33	3
27	595	5	65	404	5	103	4710	8
28	138	1	66	1152	1	104	4979	2
29	2800	25	67	164	4	105	275	4
30	1173	3	68	1294	3	106	0	1
31	223	3	69	112	1	107	508	4
32	551	3	70	0	0	108	753	5
33	1084	5	71	123	2	109	0	0
34	55	1	72	4216	13	110	28	1
35	55	2	73	512	1	111	3839	7
36	108	2	74	98	1	112	351	1
37	112	3	75	98	1	113	133	3
38	66	1	76	548	7	114	1164	1

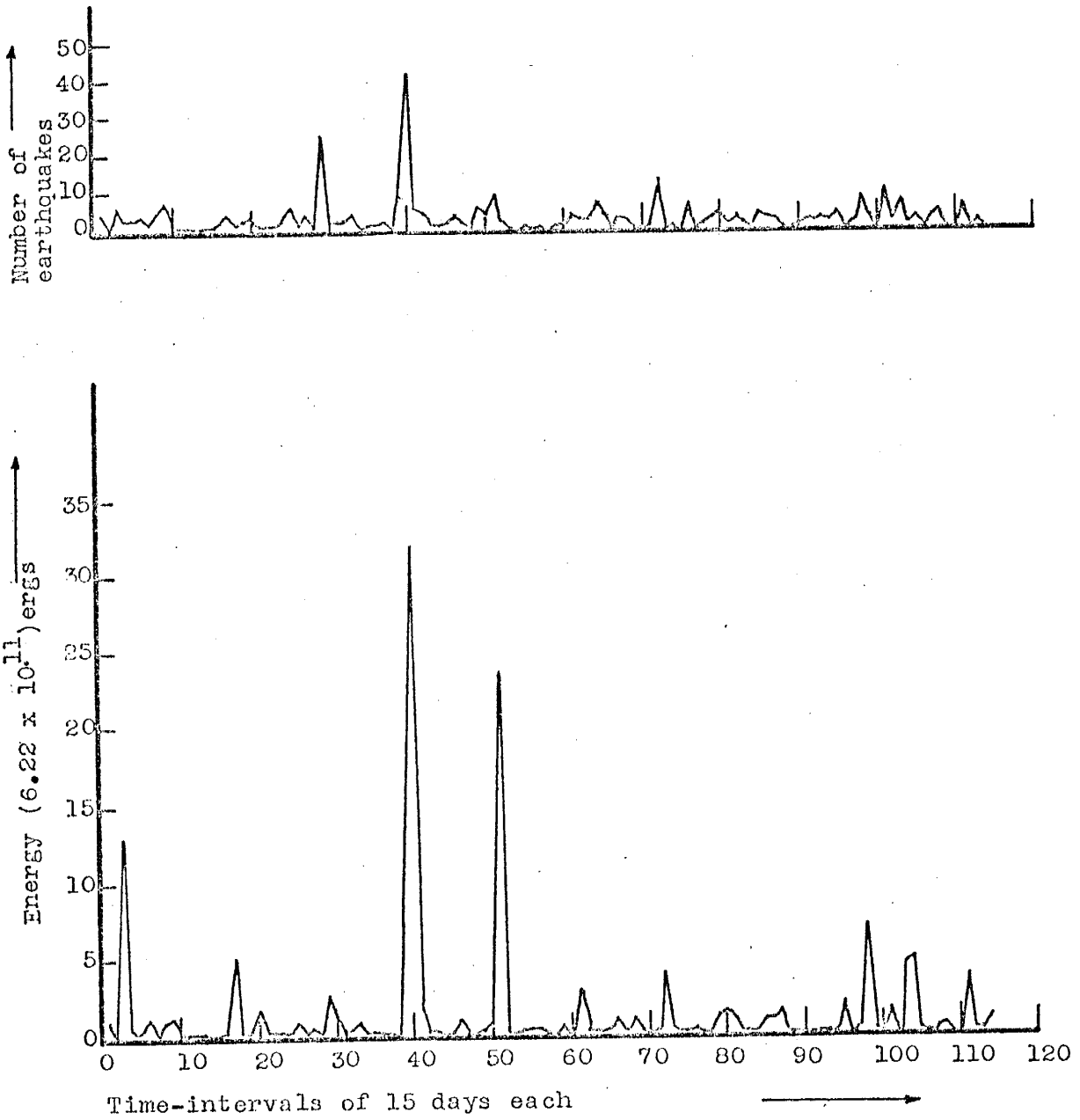

Figure 3.6. Energy and number of shocks for 15 day intervals, for DATA2.

CUMULATIVE ENERGY ANALYSIS

Results

The energies computed for individual earthquakes are grouped over 5 and 15 day intervals. These grouped energies are then successively summed to get the cumulative energies. The cumulative values for DATA1 are given in Table (3.6) and Figure (3.7) for 5 day intervals and in Table (3.7) and Figure (3.8) for 15 day intervals. Values for DATA2 are not tabulated here; however, their graphs are presented in Figures (3.9) and (3.10) for 5 and 15 day intervals, respectively.

Conclusions

(1) The total energy release for DATA1 was 3.629×10^{14} ergs and that for DATA2 was 1.039×10^{14} ergs, over a period of 5 years starting from January, 1963, to December, 1967.

(2) The largest amount of energy release for the DATA1 is about 1.119×10^{14} ergs over a period of about 2 months and in the case of DATA2 it is 0.248×10^{14} ergs over a period of 1 month.

(3) There is a lull of about 6 months between two major surges of energy release for DATA1 and it is about 9 months for DATA2.

(4) An isolated single large microearthquake rarely makes a big contribution to the energy release. Generally,

several large microearthquakes, closely spaced in time, are responsible for a large surge of energy release. This indicates that the energy stored in the focus is not released in one shock, but rather in more than one.

(5) If two enveloping parallel lines are drawn on the two sides of the curves, it is observed that the focal zone corresponding to DATA1 can store much more energy than the one corresponding to DATA2. This conclusion is drawn from the heights between the parallel lines for DATA1 and DATA2.

(6) In Figure (3.8), the slope of the lines a to b, c to d and h to i are very much the same. This indicates a nearly constant rate of the release of energy for this focal zone, except for the periods when this somewhat steady-state condition is disturbed by a large and sudden energy release, e.g., at points b and f in Figure (3.8). A similar situation exists for the focal zone of DATA2 as shown in Figure (3.10).

(7) If the slope of the two parallel lines is taken to be a measure of the average rate of the release of energy, then it is noted that there is a release of about 3.358×10^{12} ergs per 15 days for DATA1 and about 0.870×10^{12} ergs per 15 days for DATA2.

Table 3.6. Cumulative Energies of Earthquakes of DATA1, for 5 Day Successive Intervals.

Interval No.	E	Interval No.	E	Interval No.	E
1	28	46	16156	91	23599
2	28	47	16156	92	23635
3	28	48	16180	93	23635
4	112	49	16180	94	23635
5	1309	50	16180	95	23635
6	1309	51	16180	96	23947
7	1445	52	16180	97	23947
8	1481	53	16180	98	23947
9	1481	54	16180	99	23996
10	1521	55	17398	100	24862
11	2624	56	17398	101	24862
12	3034	57	17398	102	24862
13	3404	58	17398	103	24862
14	3404	59	17398	104	24862
15	3404	60	17398	105	25258
16	3404	61	17398	106	25532
17	3604	62	17398	107	25694
18	3702	63	17398	108	25694
19	5043	64	17398	109	27107
20	5043	65	17398	110	27139
21	5043	66	17398	111	27412
22	6564	67	17398	112	27412
23	6564	68	17608	113	27412
24	6806	69	17912	114	27457
25	6806	70	18010	115	27601
26	6806	71	18694	116	27601
27	7447	72	19394	117	28037
28	9567	73	19394	118	28037
29	9567	74	19394	119	28037
30	9738	75	19394	120	29471
31	9909	76	19426	121	29846
32	9909	77	19492	122	30453
33	9954	78	19510	123	30818
34	10032	79	19565	124	30923
35	10194	80	22014	125	30989
36	10254	81	22471	126	31101
37	13137	82	22471	127	31346
38	13137	83	22471	128	31418
39	13703	84	22471	129	31581
40	13781	85	22471	130	31581
41	13781	86	22777	131	31956
42	13781	87	22777	132	31956
43	13781	88	22999	133	31956
44	13905	89	23076	134	32536
45	16156	90	23483	135	32554

Table 3.6 Cont'd.

Interval No.	E	Interval No.	E	Interval No.	E
136	32554	181	87830	226	101962
137	32554	182	87830	227	101962
138	32554	183	87848	228	101962
139	32694	184	87848	229	101962
140	32847	185	87848	230	101962
141	32847	186	87848	231	101962
142	32847	187	87848	232	101962
143	32847	188	87848	233	102506
144	32847	189	87848	234	124138
145	32892	190	87848	235	124382
146	32892	191	87884	236	124486
147	32892	192	87884	237	124740
148	32892	193	87884	238	124870
149	32892	194	87996	239	124985
150	32892	195	88207	240	125101
151	32892	196	88207	241	125101
152	32892	197	88207	242	131242
153	32892	198	88243	243	131242
154	34326	199	88243	244	172729
155	35945	200	88275	245	172729
156	35945	201	88275	246	172813
154	35945	202	88275	247	173100
158	35945	203	88275	248	173121
159	36017	204	88275	249	189321
160	54990	205	88290	250	189321
161	56709	206	88290	251	205800
162	64449	207	88290	252	206800
163	64645	208	88290	253	206800
164	64876	209	88290	254	206944
165	64876	210	88290	255	214425
166	77504	211	88290	256	214425
167	81508	212	88290	257	214425
168	81508	213	88290	258	215429
169	83926	214	88320	259	216991
170	84698	215	94048	260	220204
171	84774	216	94048	261	220389
172	85074	217	100785	262	223024
173	85074	218	100913	263	223024
174	86861	219	101146	264	225336
175	87652	220	101178	265	238999
176	87673	221	101178	266	241312
177	87691	222	101178	267	246872
178	87746	223	101178	268	249519
179	87746	224	101314	269	258516
180	87746	225	101314	270	258552

Table 3.6 Cont'd.

Interval No.	E	Interval No.	E	Interval No.	E
71	258552	316	280337	361	288287
72	258552	317	280337	362	288393
73	259708	318	280337	363	288393
74	259708	319	282858	364	288635
75	265771	320	284086		
76	269627	321	284629		
77	269627	322	284878		
78	271167	323	286057		
79	272232	324	286288		
80	272232	325	286728		
81	272232	326	286783		
82	272917	327	286943		
83	272917	328	287153		
84	272917	329	287249		
85	272917	330	287249		
86	272917	331	287249		
87	272917	332	287614		
88	272917	333	287614		
89	273737	334	287614		
90	273737	335	287614		
91	274865	336	287614		
92	274865	337	287614		
93	275693	338	287614		
94	275733	339	287750		
95	275733	340	287750		
96	275733	341	287750		
97	275881	342	287750		
98	275881	343	287750		
99	275921	344	287750		
00	276101	345	287894		
01	276101	346	287894		
02	276101	347	287894		
03	276278	348	287894		
04	276296	349	287894		
05	276296	350	288022		
06	276296	351	288275		
07	276921	352	288275		
08	276921	353	288275		
09	277069	354	288275		
10	277069	355	288275		
11	277358	356	288275		
12	277558	357	288275		
13	278274	358	288287		
14	279803	359	288287		
15	280337	360	288287		

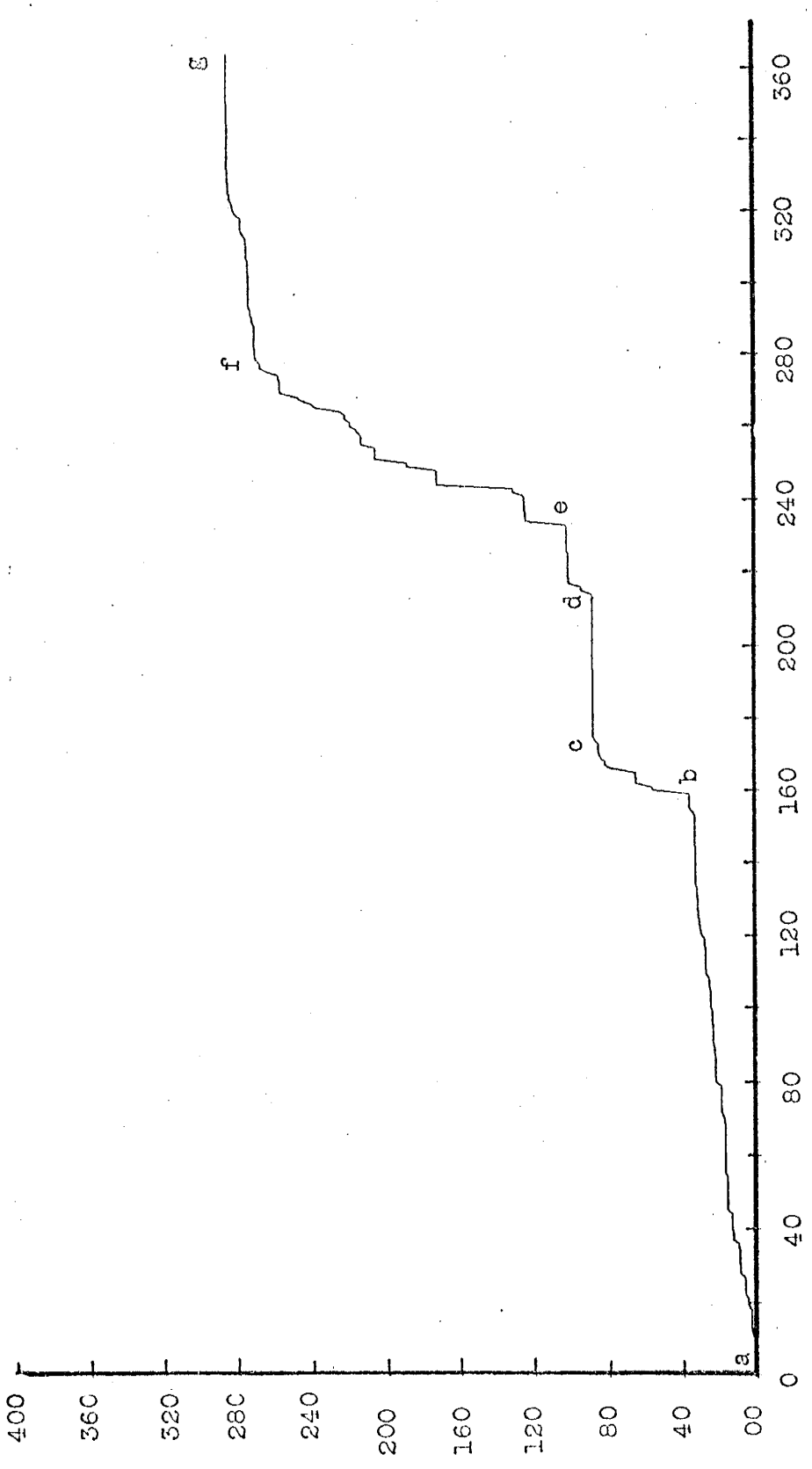

Figure 3.7. Cumulative energies for DATA1, summed over 5 day intervals.

Table 3.7. Cumulative Energies of Earthquakes of DATA1, for 15 Day Successive Intervals.

Interval No.	E	Interval No.	E	Interval No.	E
1	28	41	30818	81	131242
2	1309	42	31101	82	172813
3	1481	43	31581	83	189321
4	3034	44	31956	84	206800
5	3404	45	32554	85	214425
6	3702	46	32554	86	215429
7	5043	47	32847	87	220389
8	6806	48	32847	88	225336
9	7447	49	32892	89	246872
10	9738	50	32892	90	258552
11	9954	51	32892	91	259708
12	10254	52	35945	92	269627
13	13703	53	36017	93	272232
14	13781	54	64449	94	272917
15	16156	55	64876	95	272917
16	16180	56	81508	96	272917
17	16180	57	84774	97	274865
18	16180	58	86861	98	275733
19	17398	59	87691	99	275881
20	17398	60	87746	100	276101
21	17398	61	87848	101	276278
22	17398	62	87848	102	276296
23	17912	63	87848	103	277069
24	19394	64	87884	104	277558
25	19394	65	88207	105	280337
26	19510	66	88243	106	280337
27	22471	67	88275	107	284629
28	22471	68	88275	108	286288
29	22777	69	88290	109	286943
30	23483	70	88290	110	287249
31	23635	71	88290	111	287614
32	23947	72	94048	112	287614
33	23996	73	101146	113	287750
34	24862	74	101178	114	287750
35	25258	75	101314	115	287894
36	25694	76	101962	116	287894
37	27412	77	101962	117	288275
38	21457	78	124138	118	288275
39	28037	79	124740	119	288275
40	29471	80	125101	120	288287
				121	288393

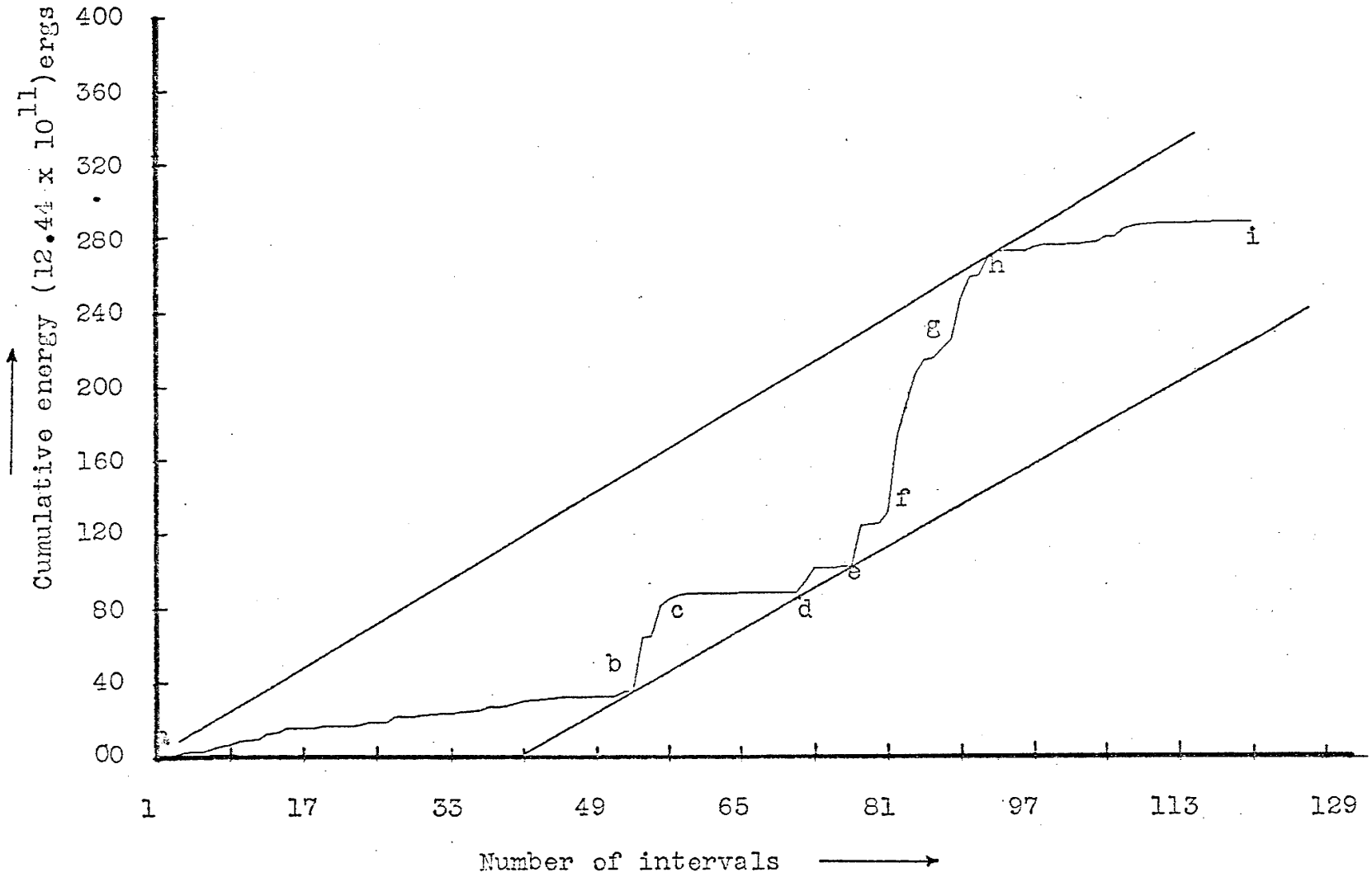

Figure 3.8. Cumulative energies for DATA1, summed over 15 day intervals.

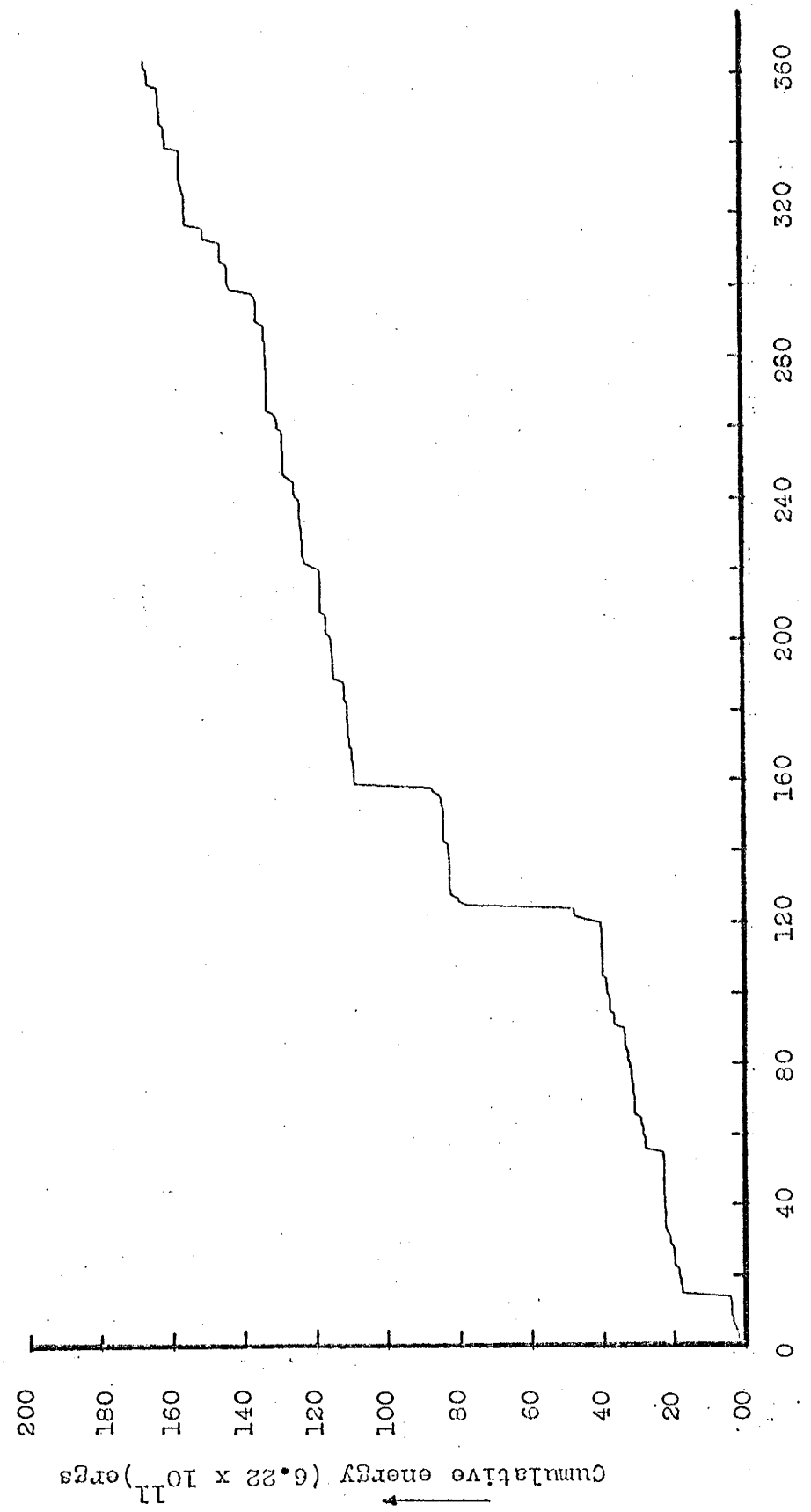

Figure 3.9. Cumulative energies for DATA2, summed over 5 day intervals.

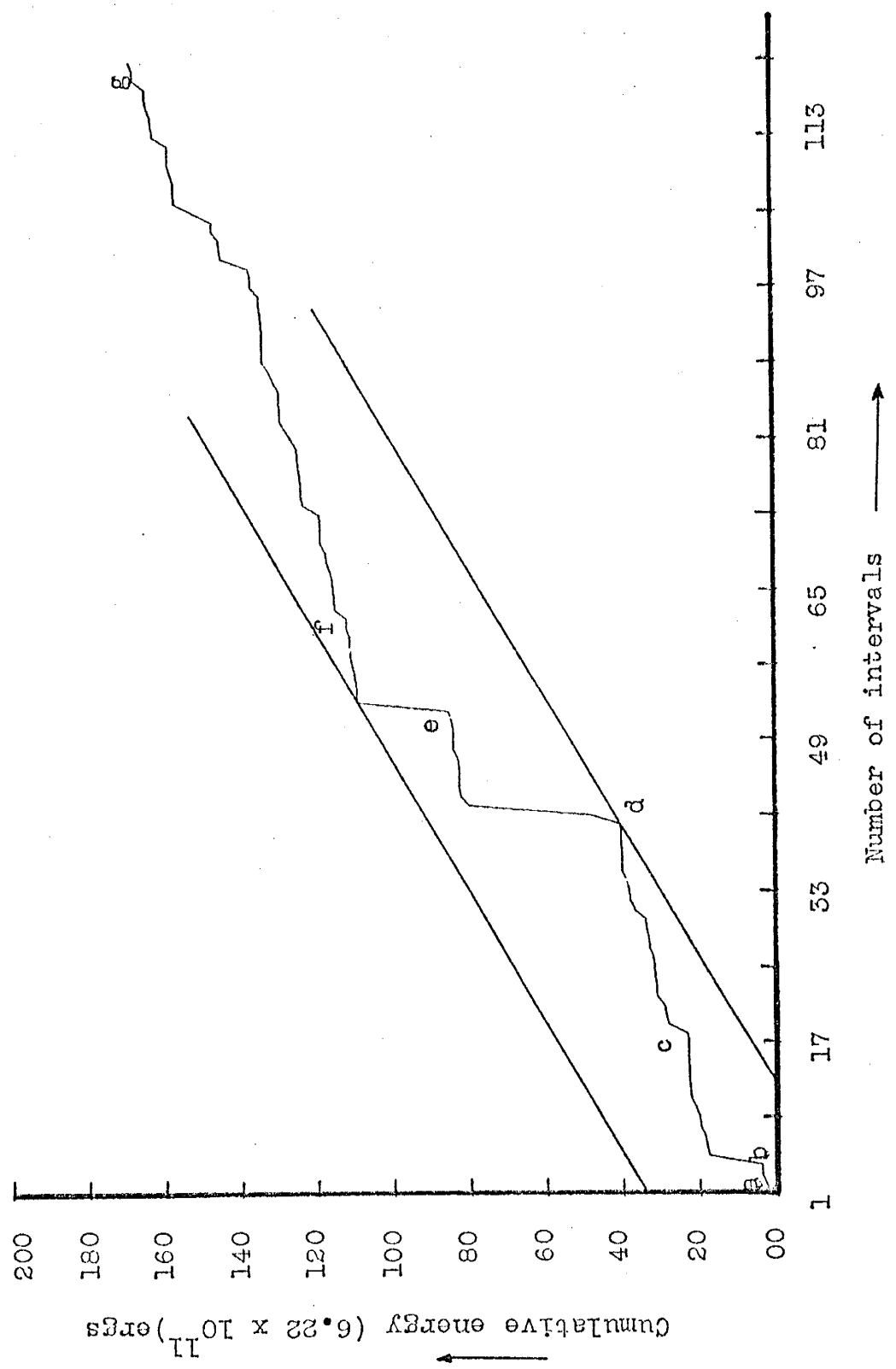

Figure 3.10. Cumulative energies for DATA2, summed over 15 day intervals.

AVERAGING FOR THE SLOPE γ

In this part, the behavior of γ as the period of observation is increased, is discussed.

The method of computing γ was the same as employed in SECTION II, i.e., by taking the arithmetic mean of three values of γ for three portions of the frequency-law curve.

Figure (3.11) shows the behavior of γ as the averaging period is increased in steps of 60 days. For a 5 year period, the slope is 1.15 for DATA1 and 1.37 for DATA2.

Figure (3.11) also shows how the value of γ fluctuates as the period of averaging is increased. Whereas it tends to stabilize with longer periods, it does so differently in different seismic zones. The value of γ is quite stable after the 15^{th} point for the curve of DATA2, but it is hard to make any such statement for DATA1. A longer period of observation is needed in order to make any positive statement about the stability of this parameter for DATA1.

Table 3.8. Values of the Slope of the Frequency-Law over Successively Increasing Period of Observation.

	DATA1		DATA2	
	Slope	Last day of the period	Slope	Last day of the period
1	2.36	603	1.55	595
2	2.32	662	1.25	658
3	2.39	721	1.54	718
4	2.05	780	1.57	755
5	1.96	817	1.48	839
6	1.96	903	1.50	902
7	1.87	946	1.64	958
8	1.96	1024	1.73	1016
9	2.06	1079	1.72	1078
10	2.08	1144	1.75	1135
11	2.16	1197	1.42	1200
12	2.20	1242	1.42	1257
13	2.11	1319	1.46	1321
14	1.45	1382	1.47	1380
15	1.43	1434	1.43	1423
16	1.43	1498	1.40	1498
17	1.44	1553	1.40	1548
18	1.39	1619	1.39	1598
19	1.38	1670	1.40	1671
20	1.37	1743	1.42	1742
21	1.32	1801	1.39	1802
22	1.23	1864	1.38	1861
23	1.05	1922	1.37	1922
24	1.04	1950	1.39	1975
25	1.03	2044	1.38	2042
26	1.05	2100	1.40	2101
27	1.12	2160	1.36	2155
28	1.13	2203	1.38	2212
29	1.14	2268	1.37	2271
30	1.15	2331	1.37	2342

Notes: The values of the logarithm of the cumulative number of microearthquakes for M = 4.0, 4.1, 4.2, ----, 6.3 for DATA1's 30^{th} point are: 2.81, 2.75, 2.70, 2.65, 2.57, 2.49, 2.39, 2.20, 2.05, 1.97, 1.74, 1.49, 1.36, 1.18, 1.08, 0.85, 0.48, 0.30, 0.0, 0.0, 0.0, 0.0, 0.0, 0.0.

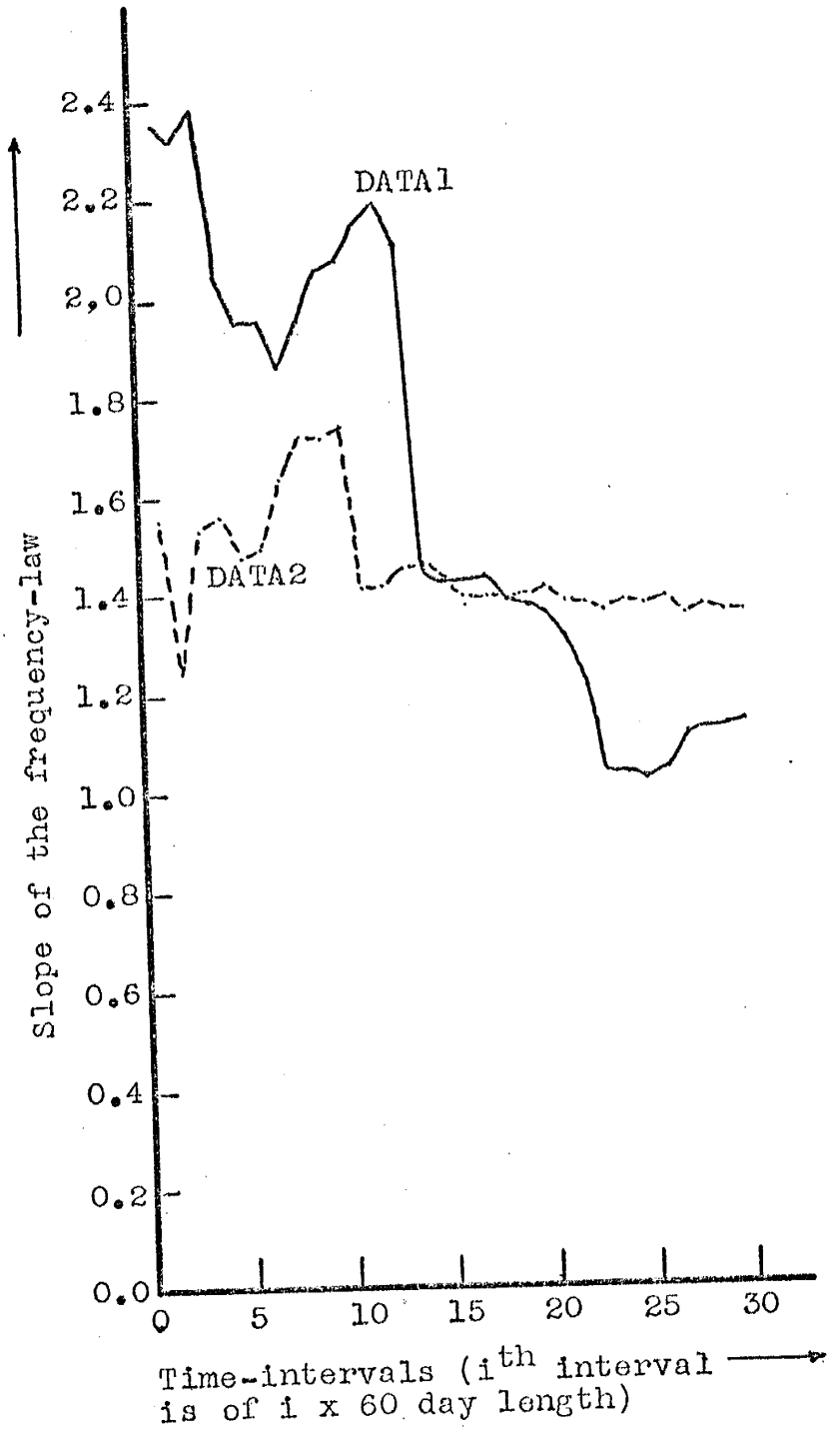

Figure 3.11. Slope of the frequency-law over increasing period of observation.

SECTION IV

STATISTICAL INDEPENDENCE OF THE INTER-ARRIVAL TIMES AND ENERGIES

A study about the statistical independence of inter-arrival times and earthquake energy is made in this section. An inter-arrival time is the time between the occurrences of two consecutive shocks. A number equal to the square of the maximum S-phase amplitude on the seismogram is used as a measure of energy release and, for convenience, is called the energy release.

The various procedures for attaching a statistical reliability to an observed value of a random variable assume that the random variable being sampled has a known distribution. However, there are some statistical tests, called the non-parametric tests, in which the knowledge of the probability distribution is not required. Tests used in this study are such non-parametric tests. A brief description of each test is given first and then the Socorro data is analysed to check the statistical independence.

THEORY

Run Test

In an ordered sequence of elements of two kinds each subsequence of like kind is called a run. Defining a criterion which will divide the sequence into two kinds depends on the problem in question. As a simple example, the arrangement of empty (E) and occupied (O) seats on a lunch counter may be EOOEEEOOOEOEEOO. Events of the kind E occur 7 times (N_1) and those of the other kind O occur 8 times (N_2), and the number of runs is 8. Next consider the arrangement EOEEOEEEOEEEOEOE. In this arrangement there are no two adjacent occupied seats. The question arises whether this can happen by chance. If, on the other hand, the lunch counter was frequented by families, there would be a tendency for occupants to sit together and the result is a smaller number of runs. An excess of runs points to intentional mixing, a paucity of runs to intentional clustering.

If N_1 is the number of observations of one kind and N_2 that of the other kind, then $N = N_1 + N_2$ is the number of total observations. Further, if all the arrangements are assumed to be equally likely, the sampling distribution for the number of runs in the sequence of N observations is a random variable, r(k), with a mean and variance as follows (Bendat and Piersol, 1966):

$$\mu_r = \left[\frac{2N_1 \cdot N_2}{N}\right] + 1 \quad , \tag{4.1}$$

$$\sigma_r^2 = \frac{2N_1 \cdot N_2 \cdot (2N_1 \cdot N_2 - N)}{N^2 \cdot (N - 1)} \quad . \tag{4.2}$$

Tables of $r(k)$ for $N_1 = N_2 = \frac{N}{2}$ are given for 100 α percentage points by Bendat and Piersol (1966) up to $\frac{N}{2} = 100$. The hypothesis of independence or randomness can then be tested at a desired level of significance α by comparing the observed number of runs to the acceptance interval, $r_{1-\frac{\alpha}{2}} < r \leq r_{\frac{\alpha}{2}}$, in the tables. If the observed value of r falls in this interval, the hypothesis of independence is accepted, otherwise it is rejected. The larger the value of α, the shorter is the acceptance interval (or the confidence interval which is equal to $1-\alpha$). Thus, the hypothesis is more likely to be rejected at $\alpha = 0.1$ than at $\alpha = 0.05$.

The criterion by which the data is divided into two kinds should be chosen carefully. Consider N observations, X_i, of inter-arrival times of microearthquakes. One kind of criterion can be their mean $\bar{x}$ such that if $X_i \geq \bar{x}$ (+) we have one kind, and if $X_i < \bar{x}$ (-) we have the other kind. However, if $X_i \geq M$ (+) or $X_i < M$ (-) where $M \geq$ maximum $(\{X_i\}_1^n)$, all of the observations will become of one kind and it will result in only one run. In the case of the inter-arrival times of microearthquakes, if only a very

few microearthquakes have very large values of the inter-arrival, e.g., 2 months, while others have values in days or hours, the mean value would not be a proper criterion owing to a major effect of those few values on the estimation of the mean. Hence, the median value of the inter-arrivals was used to separate the two kinds of events.

Trend Test

A reverse arrangement is said to exist whenever the condition $X_i > X_j$ for $i < j$ is satisfied. Then,

let $$h_{ij} = \begin{cases} 1 \text{ if } X_i > X_j \\ 0 \text{ otherwise} \end{cases} . \qquad (4.3)$$

Hence, the total number of reverse arrangements A in N observations of the random variable X(k) can be given as

$$A = \sum_{i=1}^{N-1} A_i \quad , \text{ where } A_i = \sum_{j=i}^{N} 1 \; h_{ij} \quad . \qquad (4.4)$$

If the sequence of N observations are independent observations of the random variable, then the number of the reverse arrangements is a random variable A(k) with a mean and variance as follows (Bendat and Piersol, 1966):

$$\mu_A = \frac{N \cdot (N-1)}{4} \quad , \quad \sigma_A^2 = \frac{N \cdot (2N+5) \cdot (N-1)}{72} \; . \qquad (4.5)$$

A limited tabulation of 100α percentage points for the distribution function of A(k) is given by Bendat and Piersol (1966).

The trend test is very powerful for detecting monotonic trends in the data while the run test is more suitable for fluctuating trends.

DISCUSSION OF RESULTS

Trend Test

The inter-arrival times of microearthquakes of DATA4 and DATA5 were subjected to a trend test to determine the dependence of inter-arrival times on each other in time. Similarly, the energies of microearthquakes of DATA1 and DATA2, grouped over 5 day intervals, were put to this test to check whether energies of shocks have any dependence on each other. Since the table (Bendat and Piersol) for the trend test has values available only up to N(number of observations) = 100, the total number of observations are broken into groups of 100 or less. At a given value of N and α (the level of significance), the acceptance region is determined. Then, if the number of observed reverse arrangements falls in this region, the hypothesis of independence is accepted, otherwise it is rejected.

The results of this test are given in Table (4.1) for the inter-arrival times and in Table (4.2) for the energies.

Conclusions:

(a) There are 2 Accepts and 3 Rejects for DATA5 at $\alpha = 0.1$ and 3 Accepts and 2 Rejects at $\alpha = 0.05$.

There are 2 Accepts and 2 Rejects for DATA4 at $\alpha = 0.1$ and the same at $\alpha = 0.05$.

It can be seen from equations (4.3) and (4.4) that the number of reverse arrangements is largest for a monotonically decreasing trend and smallest for a monotonically increasing trend. Therefore, a value of A smaller than the acceptance region can be taken to indicate an upward trend and a value of A larger than the acceptance region will indicate a downward trend.

The data in Table (4.1) show that some of the intervals indicate no trend, some of them indicate a downward trend and others an upward trend. It can be concluded then, that the inter-arrival times show no statistically significant time-trend.

(b) For the energies, there are 3 Accepts and 5 Rejects at $\alpha = 0.05$ and 2 Accepts and 6 Rejects at $\alpha = 0.1$. Values of A show that whenever the hypothesis of independence is rejected, there is an upward trend. However, this trend does not continue for the whole length of the period of data. Consequently, we can say that the energy values do not have any monotonic trend type dependence when they are grouped over 5 day intervals. Naturally, no trend should then be expected if the grouping interval is taken longer than 5 days.

Table 4.1. Trend Test for the Inter-arrival Times.

	DATA4					DATA5			
	100	100	100	87	100	100	100	100	62
R-	2319	2836	2403	1398	1957	2211	1352	2537	1084
					$\alpha = 0.05$				
	Acc.	Rej.	Acc.	Rej.	Rej.	Acc.	Rej.	Acc.	Acc.
					$\alpha = 0.1$				
	Acc.	Rej.	Acc.	Rej.	Rej.	Acc.	Rej.	Acc.	Rej.

Notes: R - the number of observed reverse arrangement.

For N = 100, $\alpha = 0.05$, the acceptance region is 2145 - 2804 and for N = 100, $\alpha = 0.1$, the acceptance region is 2198 - 2751.

For N = 87, $\alpha = 0.05$, the acceptance region is 1608 - 2143 and for N = 87, $\alpha = 0.1$, the acceptance region is 1651 - 2100.

For N = 62, $\alpha = 0.05$, the acceptance region is 0778 - 1100 and for N = 62, $\alpha = 0.1$, the acceptance region is 0804 - 1073.

For N = 60, $\alpha = 0.05$, the acceptance region is 0731 - 1038 and for N = 60, $\alpha = 0.1$, the acceptance region is 0756 - 1013.

Table 4.2. Trend Test for the Energies.

	DATA1				DATA2			
	100	100	100	60	100	100	100	60
R-	1965	2147	1726	0866	2271	1987	1902	0722
				$\alpha = 0.05$				
	Rej.	Acc.	Rej.	Acc.	Acc.	Rej.	Rej.	Rej.
				$\alpha = 0.1$				
	Rej.	Rej.	Rej.	Acc.	Acc.	Rej.	Rej.	Rej.

Notes: R - the number of observed reverse arrangement.

For N = 100, α = 0.05, the acceptance region is 2145 - 2804 and

for N = 100, α = 0.1, the acceptance region is 2198 - 2751.

For N = 87, α = 0.05, the acceptance region is 1608 - 2143 and

for N = 87, α = 0.1, the acceptance region is 1651 - 2100.

For N = 62, α = 0.05, the acceptance region is 0778 - 1100 and

for N = 62, α = 0.1, the acceptance region is 0804 - 1073.

For N = 60, α = 0.05, the acceptance region is 0731 - 1038 and

for N = 60, α = 0.1, the acceptance region is 0756 - 1013.

Run Test for the Inter-arrival Times

The data of the inter-arrival times were next tested by the run test. The criterion (see THEORY for details) used to divide the data into two kinds was chosen to be the median of the data. The results are as follows:

For DATA4:

Median = 629 minutes

Observations of one kind (N_1) = 195

Observations of the other kind (N_2) = 192

Theoretical mean of the run-random variable = 194.5

Theoretical standard deviation of the run-random variable = 9.8

The observed number of runs = 128

For DATA5:

Median = 1347 minutes

Observations of one kind (N_1) = 232

Observations of the other kind (N_2) = 230

Theoretical mean of the run-random variable = 232

Theoretical standard deviation of the run-random variable = 10.7

The observed number of runs = 160

Conclusions:

The tables for $N_1 = 232$, $N_2 = 230$ and $N_1 = 195$, $N_2 = 192$ are not available for 100α percentage points. However,

it is easy to see that the observed number of runs is outside the range of 6 standard deviations from the theoretical mean. Therefore, the observations of inter-arrival times of DATA4 and DATA5 are not independent.

The number of runs is significantly lower than that for the theoretical value. As mentioned in the theoretical discussion of this test, this indicates more clustering than would occur for a set of independent observations.

Run Test for Energies

Run tests of microearthquake energies for DATA1 and DATA2 are discussed here. Energy release is grouped over 5, 15, 20, 25, and 30 day intervals. The median of the energy values is the criterion for breaking up the data into 2 kinds. The table for 100 α percentage points is available only for $N_1 = N_2 = \frac{N}{2}$, where N_1 is the number of one kind and N_2 is that for the other kind. This is the main reason why the median is being used here as the criterion for dividing the data. The acceptance region at $\alpha = 0.05$ will be $R_{\frac{N}{2},0.975} < R \leq R_{\frac{N}{2},0.025}$, where R is the number of runs. N_1 is not exactly equal to N_2 in the results in Table (4.3), however, for R of the order of 100 or greater, a difference of 1 to 6 is ignored. The table of 100 α percentage points lists values only up to $\frac{N}{2} = 100$ (Bendat and Piersol, 1966).

Table 4.3. Run Test for Energies of DATA1 and DATA2.

Data	ND	Median	N_1	N_2	μ_R	σ_R	Observed Run No.	Acceptance Region	Result
	5	15	185	179	183	9.5	146	174 - 202	Reject
	10	264	93	89	92	6.7	70	79 - 106	Reject
DATA1	15	515	62	59	61	5.5	48	50 - 73	Reject
	20	854	47	44	46	4.7	40	37 - 56	Accept
	25	1275	37	35	37	4.2	33	29 - 46	Accept
	30	1657	31	29	31	3.8	26	23 - 40	Accept
	5	32	183	181	183	9.5	173	174 - 202	Reject
	10	208	92	90	92	6.7	85	79 - 106	Accept
DATA2	15	441	62	59	61	5.5	60	50 - 73	Accept
	20	734	47	44	46	4.7	48	37 - 56	Accept
	25	1136	37	35	37	4.2	41	29 - 46	Accept
	30	1636	31	29	31	3.8	38	23 - 40	Accept

Notes: Level of significance $\alpha = 0.05$

ND = number of days over which the energies are grouped.

Conclusions:

For DATA1, the grouped energies for 15 days or less do not show independence but they are independent for grouping intervals longer than 15 days.

There is also an indication of non-independence for DATA2, at 5 day grouping intervals. However, at large grouping intervals the energies are independent.

INTERPRETATION

(1) There is no statistically significant time-trend in the values of the inter-arrival times.

(2) No time-trend is found in the energies of the microearthquakes.

(3) The run test shows the inter-arrival times to be dependent. A smaller number of runs than expected means that there is more clustering than expected for random independent observations.

(4) The energies of the microearthquakes show a significant independence in the run test, when grouped over 15 day or longer intervals.

SECTION V

DISTRIBUTION FUNCTION OF INTER-ARRIVAL TIMES

In this section, the observed inter-arrival times are compared with the theoretical exponential and normal distributions. The statistical test employed in this comparison is the chi-square (χ^2) test.

THEORY

χ^2 - Test

Consider a sample of N independent observations from a random variable x(k) with a probability density function f(x). Let the observations be grouped into K intervals, called K class-intervals, which together form a frequency histogram. Let f_i be the number of observations falling in the i^{th} class and F_i be the expected number of observations within the i^{th} class-interval, if the true probability density function were $p_0(x)$. To measure the total discrepancy between the observed and expected frequency for all class-intervals, the squares of the discrepancies in each interval are summed to obtain the sample statistic,

$$\chi^2 = \sum_{i=1}^{K} \frac{(f_i - F_i)^2}{F_i} \qquad (5.1)$$

The number of degrees of freedom, n, is equal to K minus the number of different independent linear restrictions imposed on the observations. There is always at least one such restriction due to the fact that the frequency in the last class-interval is determined once the frequencies in the first (K-1) class-intervals are known.

Let it be hypothesized now that the random variable x(k) is from the population with the density function $p(x) = p_0(x)$. Any deviation of p(x) from $p_0(x)$ will cause χ^2 to increase and so a one-sided test of χ^2 is used. The region of acceptance is

$$\chi^2 \leq \chi^2_{n,\alpha} , \qquad (5.2)$$

where n is the number of degrees of freedom and α is the level of significance. The values of $\chi^2_{n,\alpha}$ at prescribed levels of significance are available in statistical tables. If the sample value of χ^2 is greater than $\chi^2_{n,\alpha}$, the hypothesis is rejected at the level of significance α; otherwise it is accepted.

The power of a chi-square test is influenced by the choice of the class-intervals. According to C. A. Williams, Jr. (1950), the minimum number of class-intervals should be given by,

$$K = 4\left[\frac{2(N-1)^2}{t^2}\right]^{\frac{1}{5}} , \qquad (5.3)$$

where K is the number of class-intervals, N is the number of observations in the sample and t is obtained from a table of areas under the normal curve such that

$$\int_{t}^{\infty} \frac{1}{\sqrt{2\pi}} \cdot e^{-\frac{y^2}{2}} \cdot dy = \alpha \quad . \tag{5.4}$$

There are two ways to select class-intervals. The most convenient way is to select classes of equal width. Another way is to select interval widths to produce equal expected frequencies in each of the class-intervals. The equal frequency procedure is more difficult to apply but will generally produce a more powerful χ^2- test.

Only the theory of the "equal expected frequency" method, as used in testing the exponential distribution hypothesis, is discussed below. A very brief description of the "equal widths of class-intervals" method will be given in the discussion of results.

χ^2-Test for the Exponential Distribution Using Equal Expected Frequency Classes

Each class will have a probability equal to $\frac{1}{K}$ where K is given by (5.3). The cumulative probability up to the end of the i^{th} class will be $F(i) = (i/K)$. For an exponential distribution, the probability density function is given by

$$\begin{aligned} f(x) &= \frac{1}{\lambda} \exp(-\tfrac{x}{\lambda}) \quad , \; x > 0 \quad , \\ &= 0 \qquad\qquad\quad , \; x \leq 0 \quad . \end{aligned} \tag{5.5}$$

λ is the mean of the random variable, x. The distribution function F(x) is then,

$$F(x) = 1 - \exp(-\frac{x}{\lambda}) \quad . \tag{5.6}$$

The value of the random variable x, from (5.6) is

$$x = -\lambda \cdot \left[\ln\left\{1 - F(x)\right\}\right] \quad .$$

Substituting the value $(\frac{i}{K})$ for F(x) and R(i) for x, where R(i) is the value of the inter-arrival time of the upper range of the i^{th} class-interval, we get,

$$R(i) = -\lambda \cdot \ln\left[1 - \frac{i}{K}\right] \quad . \tag{5.6a}$$

The relation (5.6a) gives us a means of computing the value of the random variable for the upper and lower ranges of a class. Once a class is defined, the number of observations falling in this class can be found.

It can be shown (C. A. Williams, Jr., 1950) that χ^2 statistic (5.1) becomes

$$\chi^2 = \left[(\frac{K}{N}) \cdot \sum_{i=1}^{K} O_i\right] - N \quad , \tag{5.7}$$

in the case of equal expected frequency class-intervals. O_i is the observed frequency in the i^{th} class-interval and N is the total number of observations.

DISCUSSION OF RESULTS

χ^2-Test of Observed Distribution and Exponential Distribution Using Equal Expected Frequency Classes

Procedure:

We use equation (5.6a) to compute the values of the inter-arrival times for the lower and upper ranges of the i^{th} class. The observed frequency (O_i) in each class is then determined. Substituting the values of O_i's in equation (5.7) gives us the value of the χ^2 random variable.

The value of K is computed from equation (5.3). To compute the mean (λ) used in the computations, the observations are first arranged in an ascending order of their numerical values and then the arithmetic mean is taken of the first c percent of the total N observations. This is done because the last few observations of the ascending sequence have values which greatly exceed the previous values of the sequence. Theoretically speaking, such abnormally large values are assumed here to be erratic values of the random variable of inter-arrival time. The fact that they consist of only about 5% or less of the total number of observations is taken to be the justification of this assumption. The above procedure for computing the mean is used many times in this and the next section of the study.

Results:

Table (5.1) lists the values of the chi-square random variable for the equal expected frequency classes.

Table 5.1. χ^2-Test of the Observed and Exponential Distribution Using Equal Expected Frequency Classes.

	DATA4	DATA5
No. of observations N	387	462
Arithmetic mean in minutes	6496	4233
No. of classes	40	43
Level of significance α	0.05	0.05
Fraction of N to determine the mean	0.95	0.95
Degrees of freedom	38	41
Observed χ^2 value	1807.63	1518.98
Theoretical χ^2 value	60	60

Conclusion:

For DATA4 as well as DATA5, the observed χ^2 value is much greater than the theoretical value 60. The hypothesis of exponential distribution for the inter-arrival times is, therefore, rejected according to equation (5.2).

χ^2-Test of Observed, Exponential and Normal Distribution Using Equal Width Classes

Procedure:

After arranging the inter-arrival times in an ascending order, the observation corresponding to the $(N \cdot c)^{th}$ value was divided into K equal width class-intervals. For reasons given above, $c < 1$.

The hypotheses to be tested were whether the observations followed the exponential or normal distributions. Since all the values of the inter-arrival times are non-negative, a truncated normal distribution was used which is defined as

$$F(x) = \frac{\int_{0}^{x} \frac{1}{\sqrt{2\pi}} \cdot e^{\frac{-y^2}{2}} \cdot dy}{\int_{-\infty}^{0} \frac{1}{\sqrt{2\pi}} \cdot e^{\frac{-y^2}{2}} \cdot dy}, \qquad x \geq 0,$$

$$= 0, \qquad x < 0.$$

The mean of this function is zero.

Results:

The two sets of data, DATA4 and DATA5, were tested with different values of K. The value of c was taken to be 0.98 and the level of significance α equal to 0.05.

Table (5.2) lists the results. Figure (5.1) shows graphically the three distributions -- observed, exponential and normal.

Table 5.2. χ^2-Test of the Observed, Exponential and Normal Distribution Using Equal Width Classes.

Data		Mean	Exponential χ^2	Exponential $\chi^2_{K-2,0.05}$	Exponential Result	Normal χ^2	Normal $\chi^2_{K-3,0.05}$	Normal Result
DATA4	25	3064	158.7	35	Reject	84729	34	Reject
	50	3064	324.5	65	Reject	82301	65	Reject
	75	3064	442.9	96	Reject	52756	96	Reject
DATA5	25	4152	228.8	35	Reject	331840	34	Reject
	50	4152	485	65	Reject	161346	65	Reject
	75	4152	670	96	Reject	103346	96	Reject

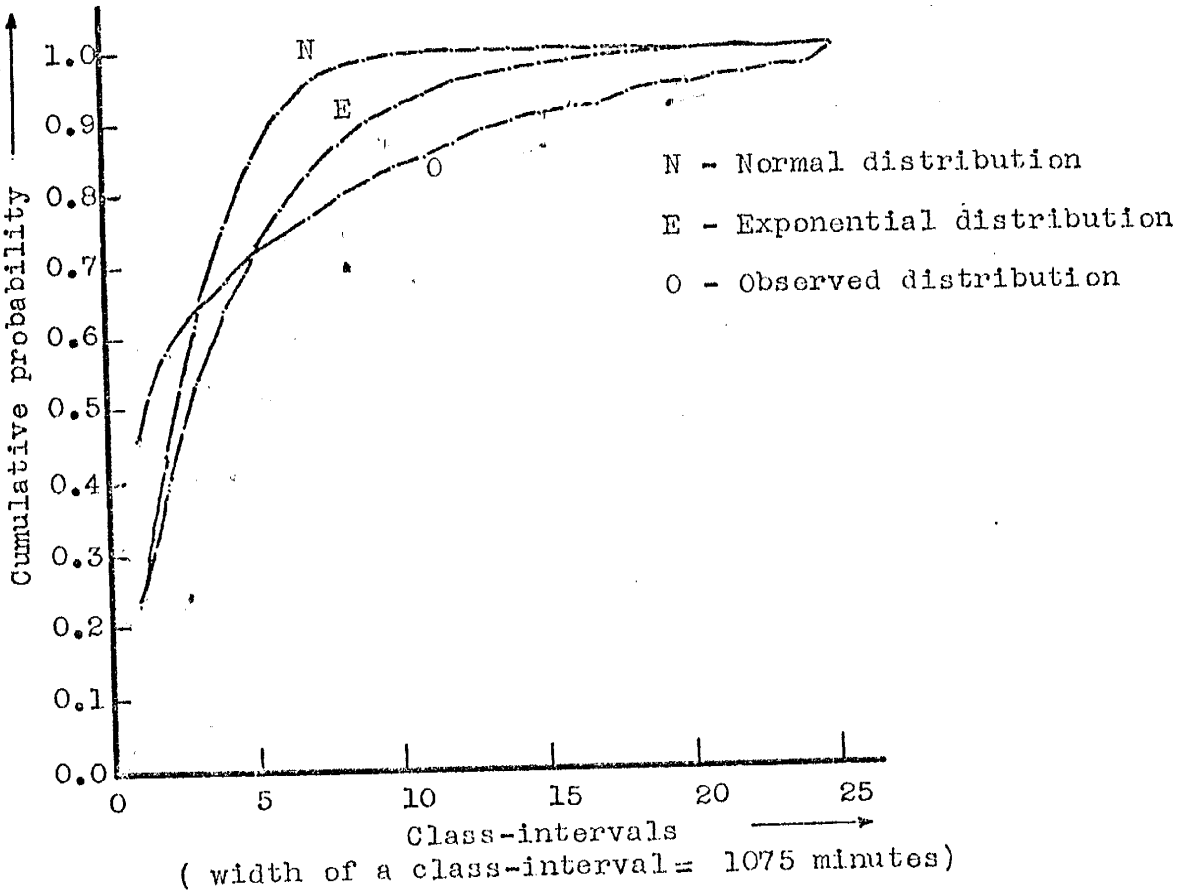

Figure 5.1. The observed, exponential and normal distributions for the inter-arrival times of DATA5.

Conclusions:

(1) The inter-arrival times are neither exponentially nor normally distributed.

(2) The distribution function values are graphed in Figure (5.1) for the theoretical exponential and normal, and the observed. The main difference between these curves is observed at small values in the first and second class-intervals. Most of the observed inter-arrival times are concentrated close to zero and after that they are spaced, more or less uniformly up to 26,884 minutes for DATA5 and 32,139 minutes for DATA4.

The normal distribution approaches the value of 1 most rapidly. The observed distribution function approaches the value of 1 most slowly.

SECTION VI

HAZARD FUNCTION FOR THE INTER-ARRIVAL TIMES

INTRODUCTION

Earthquakes can be thought of as being the mechanical failure of crustal rock which resists failure through friction and cohesion. When the failure is a rapid slippage of rock masses past each other, it is accompanied by the release of energy in the form of seismic waves. The time interval between any two consecutive failures is the interval-arrival time. These inter-arrival times will have a distribution function from which a hazard function can be computed. The hazard function will tell us, at any moment of time, the probability of the failure of the system (or the occurrence of an earthquake) in the immediate future.

THEORY

The basic assumptions of the model used here are now summarized. An earthquake, whether small or large, will be termed as a failure of the system. This point can be clarified by comparing an earthquake with a failure of a motor bus wherein the failure may be due to a loose screw in the distributor or to a broken transmission shaft. The

quantity of money or the time required to repair the system in these two types of failure will be different, but each one of them is a failure.

Let T be a random variable representing the inter-arrival time of two consecutive failures of a specified focal region. Let F(x) be its distribution function and f(x) be its probability density function. Then, Z(x), called the hazard function, is defined (Parzen, 1965) as,

$$Z(x) = \frac{f(x)}{1-F(x)} \quad . \tag{6.1}$$

$Z(x)\cdot dx$ is the probability that the system will fail between x and $x + dx$ time, given that it has survived a time $T \geq x$. Then,

$$\frac{d}{dx} \ln \left[1-F(x)\right] = -Z(x) \quad , \text{ or} \tag{6.2}$$

$$1-F(x) = \exp\left[-\int_{\epsilon}^{x} Z(u).du\right], \tag{6.3}$$

where $x > \epsilon$ and $F(\epsilon) = 0$.

Further, it can be also shown (Davis, 1952) that a constant value of the hazard function,

$$Z(x) = \lambda \quad , \tag{6.4}$$

and a lower bound $\epsilon = 0$, give rise to an exponential distribution,

$$f(x) = \lambda \cdot e^{-\lambda x} \quad , \quad x > 0.$$

DISCUSSION OF RESULTS

Procedure

Some of the procedures used here are the same as the ones for the chi-square test. The observed frequency for each class is computed and the cumulative frequency is determined. By dividing the cumulative frequency by the total number of observations, the values of the observed distribution function are found. In the analysis, the number of class-intervals was varied, and accordingly the width of the class-intervals. However, only the results obtained for 25 and 50 class-intervals are discussed. The width computations were done in the same way as in the previous section.

In order to know the value of the distribution and probability density function at any arbitrary point, the observed distribution function was fitted to a polynomial of the fifth degree with 6 coefficients. The value of the density function was found by differentiating the polynomial. To compute the conditional probability or the hazard function at any point, the value of the density function at that point was divided by the quantity (1-distribution function value at that point).

Results

Tables (6.1) and (6.2) give the results of the distribution and hazard functions for DATA5 and DATA4, respectively. The results are plotted in Figures (6.1) and (6.2).

The description of tables is given below.

Table (6.1):

Number of observations = 462

The largest value = 53,770 minutes

Values greater than 26,346 minutes are included in the last class

Number of classes = 50

Width of classes = 537.7 minutes

The coefficients of the polynomial: 0.37512, 0.05762, -0.00321, 0.00011, -0.0, 0.0.

Table (6.2):

Number of observations = 387

The largest value = 67,853 minutes

Values greater than 30,853 minutes are included in the last class

Number of classes = 25

Width of classes = 1285.6 minutes

The coefficients of the polynomial: 0.48827, 0.12777, -0.01690, 0.00119, -0.00004, 0.0.

Table 6.1. The Hazard and Distribution Functions for DATA5.

	(1)	(2)	(3)	(4)	(5)	(6)
Class	Lower range	Observed frequency	Observed distribution	Polynomially fitted distribution	Density function from (4)	Hazard function (5)/1-(4) =
1	0.0	194	0.420	0.430	0.052	0.090
2	537	19	0.461	0.478	0.046	0.088
3	1075	32	0.530	0.522	0.041	0.086
4	1613	22	0.578	0.561	0.037	0.083
5	2150	8	0.595	0.594	0.033	0.080
6	2688	21	0.641	0.625	0.029	0.078
7	3226	9	0.660	0.653	0.026	0.075
8	3763	9	0.680	0.678	0.023	0.072
9	4301	9	0.699	0.700	0.021	0.069
10	4838	9	0.719	0.719	0.019	0.066
11	5376	7	0.734	0.736	0.017	0.064
12	5914	7	0.749	0.750	0.015	0.061
13	6452	7	0.762	0.763	0.014	0.059
14	6989	6	0.775	0.776	0.013	0.057
15	7527	5	0.786	0.787	0.011	0.055
16	8065	5	0.797	0.797	0.011	0.054
17	8602	4	0.806	0.806	0.010	0.052
18	9140	4	0.815	0.814	0.009	0.050
19	9678	3	0.821	0.822	0.009	0.049
20	10215	3	0.828	0.829	0.008	0.047
21	10753	3	0.834	0.835	0.008	0.046
22	11291	3	0.841	0.841	0.008	0.044
23	11829	3	0.847	0.847	0.007	0.043
24	12366	3	0.854	0.853	0.007	0.042
25	12904	3	0.861	0.858	0.007	0.041

Table 6.1 Cont'd.

	(1)	(2)	(3)	(4)	(5)	(6)
Class	Lower range	Observed frequency	Observed distribution	Polynomially fitted distribution	Density function from (4)	Hazard function = (5)/1-(4)
26	13442	3	0.887	0.885	0.007	0.058
27	13979	4	0.895	0.892	0.006	0.059
28	14517	4	0.905	0.898	0.006	0.061
29	15055	1	0.907	0.904	0.006	0.062
30	15592	1	0.909	0.910	0.006	0.063
31	16130	2	0.913	0.915	0.005	0.064
32	16668	1	0.916	0.921	0.005	0.065
33	17205	4	0.924	0.926	0.005	0.066
34	17743	0	0.924	0.931	0.005	0.066
35	18281	5	0.935	0.935	0.004	0.065
36	18818	2	0.939	0.939	0.004	0.064
37	19356	0	0.939	0.943	0.004	0.063
38	19894	1	0.941	0.946	0.003	0.062
39	20431	3	0.947	0.950	0.003	0.062
40	20969	2	0.951	0.953	0.003	0.062
41	21507	0	0.951	0.955	0.003	0.062
42	22044	1	0.953	0.958	0.003	0.062
43	22582	1	0.955	0.961	0.003	0.062
44	23120	1	0.957	0.964	0.003	0.075
45	23657	1	0.959	0.966	0.003	0.087
46	24195	2	0.963	0.969	0.003	0.106
47	24733	1	0.965	0.973	0.004	0.138
48	25271	0	0.965	0.977	0.004	0.199
49	25808	0	0.965	0.982	0.005	0.287
50	26346	13	1.000	0.989	0.006	0.507
51				0.994	0.008	1.391

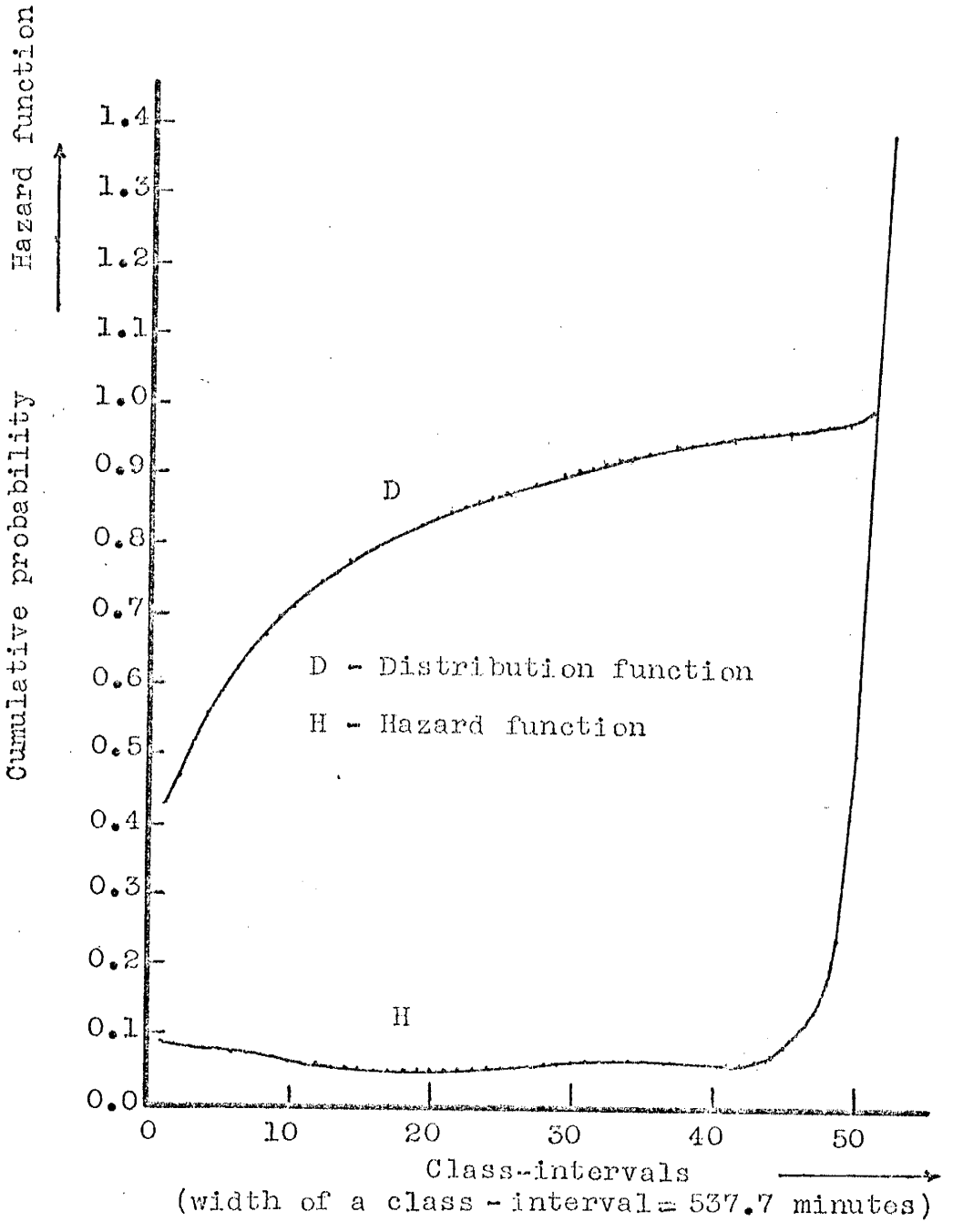

Figure 6.1. Hazard and distribution functions of DATA5.

Table 6.2. The Hazard and Distribution Functions for DATA4.

Class	(1) Lower range	(2) Observed frequency	(3) Observed distribution	(4) Polynomially fitted distribution	(5) Density function from (4)	(6) Hazard function (5)/1-(4) =
1	0.0	225	0.581	0.600	0.087	0.244
2	1285	44	0.694	0.685	0.073	0.233
3	2571	27	0.763	0.748	0.054	0.216
4	3856	15	0.802	0.795	0.040	0.195
5	5142	10	0.827	0.830	0.029	0.172
6	6427	7	0.845	0.858	0.022	0.149
7	7713	7	0.863	0.880	0.016	0.129
8	8998	5	0.876	0.896	0.013	0.114
9	10284	5	0.889	0.909	0.011	0.106
10	11570	5	0.902	0.920	0.009	0.103
11	12855	5	0.915	0.930	0.008	0.103
12	14141	4	0.925	0.939	0.008	0.111
13	15426	3	0.933	0.947	0.008	0.118
14	16712	3	0.941	0.954	0.007	0.123
15	17998	2	0.946	0.960	0.006	0.124
16	19283	2	0.951	0.965	0.005	0.119
17	20569	2	0.956	0.969	0.004	0.104
18	21854	2	0.961	0.973	0.003	0.092
19	23140	2	0.966	0.975	0.002	0.057
20	24425	1	0.969	0.977	0.001	0.040
21	25711	1	0.972	0.978	0.001	0.043
22	26996	1	0.974	0.979	0.001	0.050
23	28282	1	0.977	0.980	0.001	0.064
24	29567	0	0.977	0.982	0.002	0.084
25	30853	10	1.000	0.995	0.013	0.549
					0.018	3.704

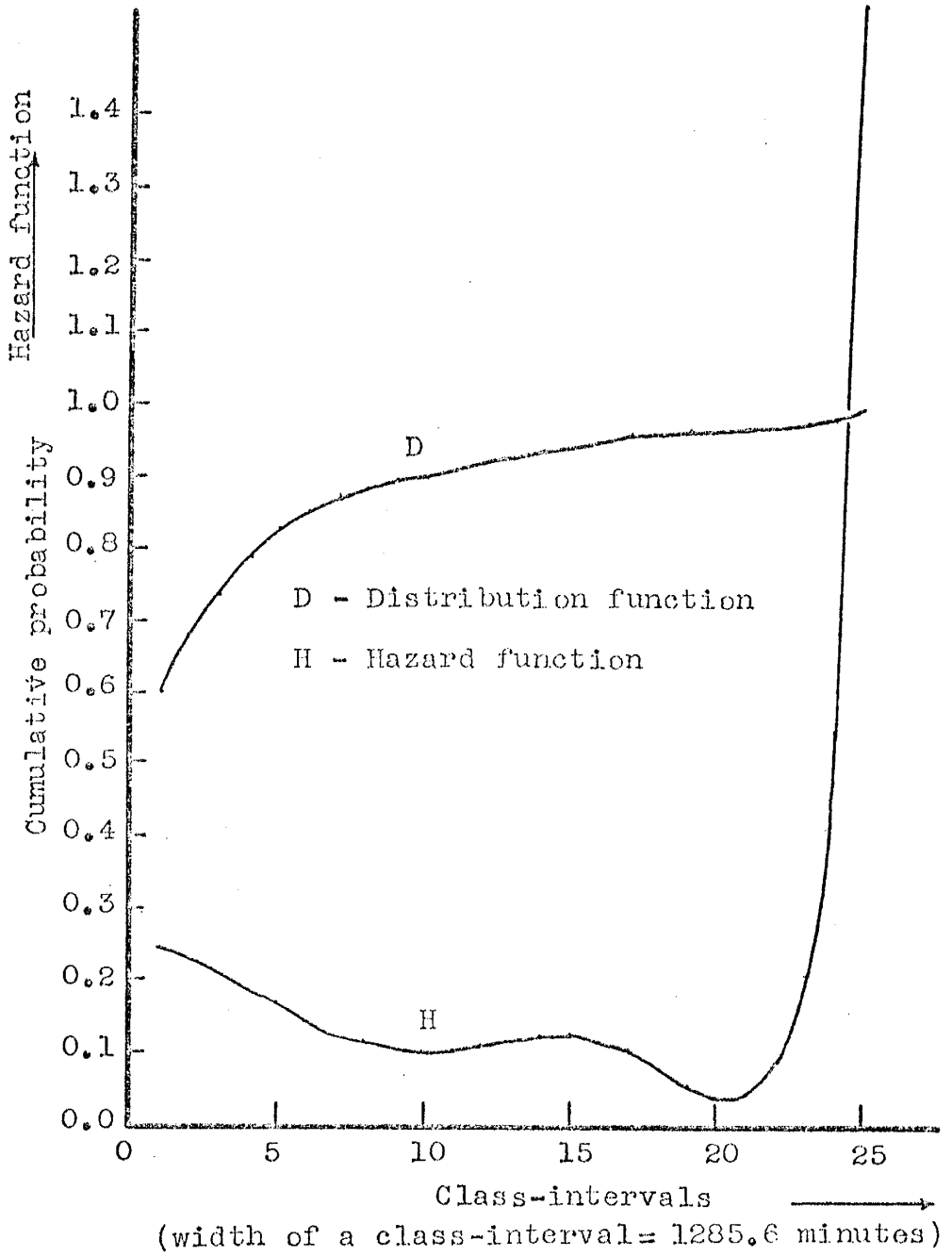

Figure 6.2. Hazard and distribution functions of DATA4.

CONCLUSIONS

(1) Values of the distribution functions in the tables show that about 46% of all the microearthquakes fall in the interval of about 18 hours for DATA5, and about 58% for DATA4 fall in the first interval of about 21 hours. After that, the inter-arrival times are spaced more or less uniformly over the whole range of 47 days and more.

(2) A comparison of the observed hazard function with those of the exponential (hazard function for the exponential should be a straight line as given in equation 6.4) and normal (Davis, 1952) indicates that the inter-arrival times are not exponentially or normally distributed. This supports our previous conclusions about the distribution function of the inter-arrival times.

(3) Figures (6.1) and (6.2) show that the curves for the hazard function can be divided mainly into two parts:

(a) The first part with an oscillating character and a slight down-hill trend continues up to about 19 days. The down-hill trend means that as the value of the inter-arrival times increases, the probability of the occurrence of a microearthquake in the immediate future decreases until the value of the inter-arrival times becomes about 19 days. After about 19 days, the probability increases very rapidly. A relatively high value of the

hazard function in the beginning is due to the fact that the probability of a shock following an earthquake will be somewhat high at the beginning and then decreases. This fact is supported by our earlier results which show that there is a tendency for shocks to group in time.

(b) The second part applies to inter-arrival times of more than about 19 days. The rise in this part is very sharp.

On the basis of the hazard functions for DATA4 and DATA5, it appears that the values of the probability of failure for the two focal zones becomes very high after about 19 days.

CONCLUSION

The results of this statistical study of the microearthquake data of the Socorro region can be summarized as follows:

(1) a. The values of the slope of the straight portion of the frequency-law graphs for microearthquake data were 1.15, 1.37 and 1.15 (for three sets of data -- DATA1, DATA2 and DATA3). Similar values have been obtained by other workers (Brazee and Stover, 1969).

b. The proposed probabilistic model for the frequency-law seems to suggest that the frequency-law may not universally be a linear relation. It can be approximated by one curve for which the slope changes continuously (not necessarily at a constant rate); depending upon the elastic properties of the medium and stress field conditions in the area.

(2) a. Whenever there is a large number of microearthquakes (small or large), they tend to be grouped. There is no consistent correlation between the number of shocks and the slope of the linear portion of the frequency-law curve.

b. There is no consistent correlation between the occurrence of a large microearthquake and the number of shocks, the slope, and the grouping behavior of shocks in the interval of time containing the large microearthquake.

(3) a. The average number of shocks per unit time-interval varies appreciably from one interval to another, indicating a non-stationary nature of the microearthquake process $\{N(t), t \geq 0\}$, where $N(t)$ is the number of shocks up to the time t.

b. The larger the value of the mean number of shocks in a particular amplitude class, the larger the variance of the number of shocks. Accordingly, the estimation of the number of shocks in a unit time-interval for a class with a large mean number of shocks is not significantly better than that for a class with a small mean number of shocks.

c. Results show that a period of much less than 5 years can be used to estimate, within 10% error, the average number of shocks for a unit interval of time.

d. The seismic energy is as likely to be released in a few large microearthquakes as in many relatively small ones. However, it is very rare that a single large shock releases a large amount of energy. A large surge of energy release is due to more than one large shock, closely spaced in time.

(4) a. Inter-arrival times of microearthquakes showed no significant time trend. Furthermore, they were not found independent, and they showed a tendency of clustering.

b. The energies of microearthquakes did not

show any significant time trend. For energies of shocks summed over intervals larger than 15 days, there is a statistically significant independence, while energies summed over intervals smaller than 15 days were not found independent.

(5) The distribution functions of the inter-arrival times were found to be significantly different from the exponential and normal types of distributions. About 50% of all the inter-arrival times have values less than about 20 hours. Values greater than 20 hours are distributed more or less uniformly.

(6) The hazard function for the inter-arrival times of microearthquakes show that the probability of a shock is relatively high immediately after the preceding shock, and then it decreases and remains more or less constant up to about 19 days. After that, the probability increases very rapidly.

(7) The microearthquakes studied do not follow a Poisson process. According to some workers (Lomnitz, 1966), earthquakes follow a Poisson process, but do not seem to do so because of inhomogeneity of the data (i.e., due to mixing of data from two different regions). However, the microearthquake data used in this study is spatially homogeneous, and for this reason, as well as other results about dependence, stationarity, grouping, distribution and hazard function of the inter-arrival

times, etc., we can say that the disagreement of the micro-earthquake data studied with a Poisson process is not due to any kind of inhomogeneity.

(8) a. Concerning the probability of a very large earthquake in the future, this writer would first like to quote Gubin (1964):

> ". . . that is, are the basic assumptions true - namely, that shocks of intensity [magnitude] 9 may occur wherever there have been weak shocks and that the numerical ratio between weak and strong shocks [slope of the frequency-law] is in general the same everywhere and invariable, irrespective of the size of the observation area or of the period covered by the observations?"

Based on some scanty results of this study (cumulative energy analysis, temporal behavior of the seismic activity, analysis of the slope parameter with increasing period of observation, etc.), this writer's personal feeling is that a large earthquake of magnitude 8 or 9 may never occur in this area. That is, the answer to Gubin's question seems to be "no". It may be, for example, that the mechanical properties of the focus and the conditions of the stress field in the area may never allow a large accumulation of energy in the focus, thus ruling out the possibility of

any major earthquake. However, 5 or 6 year data is not sufficient for making any positive statement about this point.

b. Evidences such as grouping of shocks, dependence of inter-arrival times, dependence of energies of shocks closely spaced in time and others indicate that individual microearthquakes are not independent random phenomena. Further investigation into the degree and kind of dependence between various seismic quantities, and the statistical distribution followed by the microearthquake process $\{N(t)\ ,\ t \geq 0\}$, is required for making any reliable and quantitative forecasting of the seismic behavior of this area.

APPENDIX

CONVERGENCE AND VARIANCE OF A VARIABLE

Let X be a random variable with finite mean m and variance σ^2. Then, the Chebyshev's Inequality states that,

$$Q(h) = P\left[|X-m| \leq h\sigma\right] \geq 1-\frac{1}{h^2} \quad \text{for any } h>0, \quad \text{(II.1)}$$

or in other words, that $Q(h)$ which is equal to the probability that an observed value of a numerically valued random phenomenon, will lie in an interval centered at the mean and of length 2h standard deviation, is equal to or greater than the quantity $(1-\frac{1}{h^2})$.

The sample mean of n observations of X can be given by

$$M_n = \frac{(X_1 \quad X_2 \quad \text{----------} \quad X_n)}{n} \quad . \qquad \text{(II.2)}$$

If these n observations are independent and identically distributed, then, M_n which is the average of n values of X, will itself be a random variable with

$$E\left[M_n\right] = E\left[X\right] = m \text{ and } \text{Var}\left[M_n\right] = \frac{\text{Var}\left[X\right]}{n} \qquad \text{(II.3)}$$

where E and Var stand for the Expectation and Variance, respectively.

To rewrite (II.1), for an $\epsilon > 0$,

$$P\left[\left|M_n - m\right| > \epsilon\right] \leq \frac{\sigma_{M_n}^2}{\epsilon^2} \qquad \text{(II.4)}$$

or $$P\left[\left|M_n - m\right| \leq \epsilon\right] \geq 1 - \frac{\sigma_X^2}{n \cdot \epsilon^2}$$

using (II.3).

Let the probability that the sample mean be within a pre-assigned distance ϵ from the true mean m, be desired to be equal or greater than α. Then,

$$P\left[\left|M_n - m\right| \leq \epsilon \mid m\right] \geq \alpha \quad . \qquad \text{(II.5)}$$

$P[\cdot \mid m]$ means that the probability is being computed under the assumption that the true mean is m. Since

$$P\left[\left|M_n - m\right| \leq \epsilon\right] \geq 1 - \frac{\sigma_X^2}{n \cdot \epsilon^2} \quad ,$$

it follows that (II.5) is satisfied if n is chosen (Parzen, 1963, p. 230) so that

$$n \geq \frac{\sigma_X^2}{\epsilon^2 \cdot (1-\alpha)} \quad . \qquad \text{(II.6)}$$

Notice that α is fixed and is equal to $\left(1 - \frac{\sigma_X^2}{n_0 \cdot \epsilon^2}\right)$ for some $n = n_0$ and is less than $\left(1 - \frac{\sigma_X^2}{n_0 \cdot \epsilon^2}\right)$ for $n > n_0$.

Let us now define the random variable in the case of microearthquakes here. Consider a time period T which is

divided into intervals T_1, T_2, -----, T_n of equal length where T_i is positioned in time right after T_{i-1}. If the number of earthquakes in the T_i^{th} interval is designated by X_i, then, X_i's will represent the values of the random variable X. There will be n values of X in n intervals of equal length. If M_n of (II.2) is the estimate of m, then from (II.6), with a fixed arbitrary ϵ and α, there is an $n = n_0$.

The purpose is, then, to show that the larger the value of m, the smaller the value of n_0.

Consider that X is identically distributed for two earthquake sequences and has the mean m_1 and m_2 and variances σ_{1X}^2 and σ_{2X}^2, respectively. The two sequences have intervals of equal length.

Suppose $m_2 < m_1$. Increase, then, the length of a T_i for the second sequence such that

$$E[{}_1X] = E[{}_2X] \text{ and also } \sigma_{1X}^2 = \sigma_{2X}^2 \quad . \qquad \text{(II.7)}$$

Therefore, the T_i for the first sequence will become shorter than that for the second sequence. Under the modification (II.7), $n = n_0$ for both the sequences, from (II.6).

After increasing the length of an interval for the second sequence, we can relate the two intervals as

$$T_{1i} = T_{2i} \cdot b \qquad \text{where } b > 1 \quad . \qquad \text{(II.8)}$$

Thus, in order to have the same value of n_0, the time period required for the first sequence is $(T_{11} + T_{12} + \cdots\cdots + T_{1n})$ while for the second sequence it is $(T_{21} + T_{22} + \cdots\cdots + T_{2n})$ which is equal to $b \times [(T_{11} \quad T_{12} \cdots\cdots \quad T_{1n})]$, $b > 1$.

Hence, a shorter time period is needed to estimate the mean parameter within a preassigned error, if there is a larger number of earthquakes in the sequence. However, this is true only under the condition that their variances are equal, as seen from (II.6). If σ_{1X}^2 and σ_{2X}^2 are not equal, the value of n_0 will not be the same for the two sequences. Let $\sigma_{1X}^2 > \sigma_{2X}^2$. Then n_0 for the first sequence $> n_0$ for the second sequence, as seen from (II.6). Since n_0 represents the number of intervals required to estimate the value of the true mean within some fixed error, a greater value of n_0 will mean a relatively slow rate of convergence of the sample mean to the true mean.

REFERENCES CITED

Bendat, J. S., and Piersol, A. G., 1966, Measurement and analysis of random data: John Wiley & Sons, Inc., New York.

Biles, N. E., 1967, Vertical ground motion showing the free surface effect: M. S. Thesis, New Mexico Institute of Mining & Technology.

Brazee, R. J., and Stover, C. W., 1969, The distribution of earthquakes with respect to magnitude (mB): Bull. Seis, Soc. Am., v. 59, no. 2, p. 1015-1017.

Davis, D. J., 1952, An analysis of some failure data: J. Am. Stat. Ass., v. 47, no. 258, June, p. 113-150.

Gubin, I. E., 1964, Earthquake forecasting: Geophys. Ser. (Izv.), no. 8, p. 702-707.

Gutenberg, B., and Richter, C. F., 1942, Earthquake magnitude, intensity, energy and acceleration: Bull. Seis. Soc. Am., v. 32, no. 2, p. 163-191.

Gutenberg, B., and Richter, C. F., 1949, Seismicity of the earth and associated phenomena: Princeton University Press, Princeton, New Jersey.

Housner, G. W., 1955, Properties of strong ground motion earthquakes: Bull. Seis. Soc. Am., v. 45, no. 3, p. 197-218.

Katok, A. P., 1966, Some features of the seismic regime after Khait earthquake: Phys. of the Solid Earth (Izv.), v. 2, no. 7, p. 419-423.

Lomnitz, C., 1966, Statistical prediction of earthquakes: Reviews of Geophys., v. 4, no. 3, p. 377-393.

Mogi, K., 1962, Study of elastic shocks caused by the fracture of heterogeneous materials and its relations to earthquake phenomenon: Bull. Earthquake Res. Inst., v. 40, p. 125-173.

Parzen, E., 1963, Modern probability and its applications: John Wiley & Sons, Inc., New York.

Parzen, E., 1965, Stochastic processes: Holden-day, Inc., San Francisco.

Richter, C. F., 1957, Elementary seismology: W. H. Freeman and Company, San Francisco.

Riznichenko, Yu. V., 1958, The study of seismic conditions: Geophys. Scr. (Izv.), no. 9, p. 615-622.

Riznichenko, Yu. V., 1965, Interpretation of the earthquake frequency law in terms of energy: Phys. of the Solid Earth (Izv.), v. 1, no. 10, p. 661-666.

Riznichenko, Yu. V., 1966, Problems of earthquake physics: Phys. of the Solid Earth (Izv.), v. 2, no. 2, p. 73-86.

Sanford, A. R., and Holmes, C. R., 1962, Microearthquakes near Socorro, New Mexico: J. Geoph. Res., v. 67, no. 11, p. 4449-4459.

Sanford, A. R., and Long, L. T., 1965, Microearthquake crustal reflections, Socorro, New Mexico: Bull. Seis. Soc. Am., v. 55, no. 3, p. 579-586.

Sanford A. R., and Singh, S., 1968, Minimum recording times for determining short-term seismicity from microearthquake activity: Bull. Seis. Soc. Am., v. 58, no. 2, p. 639-644.

Vinogradov, S. D., 1959, On the distribution of the number of fractures in dependence on the energy liberated by the destruction of rocks: Geophys. Ser. (Izv.), no. 12, p. 1292-1293.

Vinogradov, S. D., 1963, Accoustic observations of rock bursts in the Ann lead mine (Czechoslovakia): Geophys. Ser. (Izv.), no. 4, p. 313-319.

Willard, M., June 1969, Personal communication: New Mexico Bureau of Mines, Socorro, New Mexico.

Williams, C. A., Jr., 1950, on the choice of the number and width of classes for the chi-square test of goodness-of-fit: J. Am. Stat. Ass., v. 45, p. 77-86.

This thesis is accepted on behalf of the faculty of the Institute by the following committee:

Allan R. Langford

Martin S. Fairbrother

A. T. Bradley

Charles R. Holmes

Date: June 25, 1969